



Department of Mechanical and Aerospace Engineering

## **The Thermal Analysis of a Flooded Absorber Type Solar Collector for Low Temperature Application**

Author: Chris Thom

Supervisor: Dr. Daniel Cóstola

A Thesis submitted for the partial fulfilment for the requirement of the degree

Master of Science

Sustainable Engineering: Renewable Energy Systems and the Environment

2018

## Abstract

In this study, the design and simulation of a flooded absorber type solar collector is developed and analysed for the production of low temperature water for domestic use. Design objectives include water production bounds of 40°C – 60°C and simplicity of design. Through the literature, a base model is formed, using the design principles of a parallel tube FPC. The performance characteristics are determined within simulation environment software ESP-r. In the simulation software, various aspects of the FAC are altered to ensure optimal design. The final model FAC design results are produced. An overall system efficiency is found at 37.5% which is deemed acceptable within the simplicity of design.

## Acknowledgments

I would like to thank Dr Daniel Cóstola for seeing me at very short notice on several occasions after my initial topic change and for giving me guidance throughout the three months. I would also like to thank Dr Jon Hand who provided guidance in installing ESP-r software onto my Mac, which proved to be very important. I would also like to thank Graeme Flett who answered to many of my emails about my ESP-r model that should have been sent to my supervisor. Last but not least, to Strathclyde Business School where I worked and to the security team who always kept me company late into the night.

## Table of Contents

<b>Abstract</b> .....	<b>2</b>
<b>Acknowledgments</b> .....	<b>3</b>
<b>List of Figures</b> .....	<b>6</b>
<b>List of Tables</b> .....	<b>7</b>
<b>Nomenclature</b> .....	<b>8</b>
<b>Acronyms</b> .....	<b>9</b>
<b>1. Introduction</b> .....	<b>10</b>
<b>1.1 Solar Resource</b> .....	<b>10</b>
1.1.1 System Types - Background.....	11
<b>1.2 Project Motivation</b> .....	<b>13</b>
<b>1.3 Project Aim</b> .....	<b>14</b>
<b>1.4 Project Methodology</b> .....	<b>15</b>
<b>1.5 Scope</b> .....	<b>15</b>
<b>1.6 ESP-r</b> .....	<b>15</b>
<b>2. Literature Review</b> .....	<b>16</b>
<b>2.1 Introduction</b> .....	<b>16</b>
<b>2.2 Solar Collector System</b> .....	<b>16</b>
2.2.1 Previous Solar Thermal Systems.....	16
<b>2.3 The Flat Plate Collector</b> .....	<b>19</b>
2.3.1 Absorber Modifications.....	21
2.3.2 Absorber Efficiencies.....	24
2.3.3 Alternate Designs.....	25
2.3.4 Enhancement Devices.....	25
2.3.5 Glazing.....	26
2.3.6 Optimum Tilt.....	28
2.3.7 Heat Loss Reduction.....	31
<b>2.4 Application of Flat Plate Collectors</b> .....	<b>33</b>
2.4.1 Desalination.....	33
2.4.2 Domestic Hot Water.....	34
<b>2.5 Calculation</b> .....	<b>35</b>
2.5.1 Efficiency Calculation.....	35
<b>2.6 Conclusion</b> .....	<b>37</b>
<b>3. Design Considerations</b> .....	<b>37</b>
<b>3.1 Orientation &amp; Inclination</b> .....	<b>37</b>
<b>3.2 Collector Materials</b> .....	<b>39</b>
<b>3.3 Thermal Expansion</b> .....	<b>40</b>
<b>3.4 Stagnation Temperature</b> .....	<b>40</b>
<b>4. FAC Design</b> .....	<b>41</b>

<b>5.</b>	<b><i>Model Description</i></b> .....	<b>42</b>
5.1	<b>Introduction</b> .....	<b>42</b>
5.2	<b>Base Model</b> .....	<b>42</b>
5.3	<b>Surface Attributes</b> .....	<b>44</b>
5.3.1	Insulation.....	44
5.3.2	Absorption.....	45
5.3.3	Glazing.....	45
5.3.4	Thermal Storage.....	45
5.4	<b>Thermal Zones</b> .....	<b>47</b>
5.4.1	Casing .....	47
5.4.2	Absorber Plates.....	48
5.4.3	Environment.....	49
5.5	<b>Network Flow</b> .....	<b>49</b>
5.5.1	Water Network.....	50
5.5.2	Air Network .....	51
5.5.3	Control System.....	52
5.5.4	Connections.....	53
<b>6.</b>	<b><i>Results</i></b> .....	<b>54</b>
6.1	<b>Climate</b> .....	<b>54</b>
6.1.1	Seasonal Performance.....	54
6.2	<b>Modifications to Base Model</b> .....	<b>58</b>
6.3	<b>Design Objective</b> .....	<b>58</b>
6.4	<b>Base Model</b> .....	<b>58</b>
6.4.1	Temperature Distribution.....	58
6.4.2	Stagnation Temperature .....	59
6.5	<b>Modifications to Base Model</b> .....	<b>60</b>
6.5.1	Flowrate and Tank Size.....	60
6.5.2	Glazing.....	64
6.5.3	Absorber Plate Spacing.....	67
6.5.4	Insulation.....	69
6.6	<b>Final Model</b> .....	<b>71</b>
6.7	<b>System Efficiency Model</b> .....	<b>72</b>
6.7.1	Calculation.....	74
<b>7.</b>	<b><i>Final Discussion</i></b> .....	<b>77</b>
<b>8.</b>	<b><i>Conclusion</i></b> .....	<b>79</b>
<b>9.</b>	<b><i>Future Work</i></b> .....	<b>80</b>
<b>10.</b>	<b><i>References</i></b> .....	<b>80</b>
<b>11.</b>	<b><i>Appendices</i></b> .....	<b>86</b>
	<b>Appendix A: Base Model Supplementary Data</b> .....	<b>86</b>
	<b>Appendix B: Final Model Supplementary Data</b> .....	<b>88</b>

## List of Figures

FIGURE 1 - EXISTING SOLAR HOT WATER HEATING CAPACITY. TOP 10 REGIONS/COUNTRIES (2010) (RAISUL ISLAM, SUMATHY, & ULLAH KHAN, 2013)	10
FIGURE 2 – LAYOUT OF A CONVENTIONAL SOLAR HOT WATER SYSTEM (JAMAR, MAJID, AZMI, NORHAFANA, & RAZAK, 2016)	11
FIGURE 3 – LAYOUT OF A "THERMOSIPHON" SWH SYSTEM (JAMAR ET AL., 2016)	12
FIGURE 4 - THE CLIMAX SOLAR WATER HEATER ADVERTISEMENT	17
FIGURE 5 - CONFIGURATION OF A FLAT PLATE SOLAR COLLECTOR: (A) CROSS-SECTIONAL (B) ISOMETRIC	20
FIGURE 6 - DESIGNS OF VARIOUS FLUID PASSAGEWAYS WITHIN ABSORBERS (LENEL, 1984)	22
FIGURE 7 - SOLAR ANGLES	29
FIGURE 8 - INCLINATION AND ORIENTATION ANGLES (FIREBIRD,2011)	38
FIGURE 9 - OPTIMUM TILT ANGLE	38
FIGURE 10 - EXPLODED VIEW, FLOODED ABSORBER SOLAR COLLECTOR WITH MAJOR DIMENSIONS	41
FIGURE 11 - FULL ESP-R MODEL LAYOUT	43
FIGURE 12 - CONTROL ACTION OF COLLECTOR – TANK PUMP	53
FIGURE 13 - ARBITRARY 5-DAY PERIOD IN WINTER (GLASGOW)	55
FIGURE 14 - ARBITRARY 5-DAY PERIOD IN SPRING (GLASGOW)	55
FIGURE 15 - ARBITRARY 5-DAY PERIOD IN SUMMER (GLASGOW)	56
FIGURE 16 - ARBITRARY 5 DAY PERIOD IN AUTUMN (GLASGOW)	56
FIGURE 17 - TEMPERATURE DISTRIBUTION ACROSS ABSORBER PLATE WITH VARYING SURFACE CONVECTION	59
FIGURE 18 - STAGNATION TEMPERATURE OF MID ABSORBER	60
FIGURE 19 - WATER TEMPERATURE GAIN FOR VARIOUS FLOWRATES (152L)	61
FIGURE 20 - WATER TEMPERATURE GAIN FOR VARIOUS FLOWRATES (206L)	61
FIGURE 21 - WATER TEMPERATURE GAIN FOR VARIOUS FLOWRATES (369L)	62
FIGURE 22 - MASS FLOW: 0.1KG/S TANK VOLUME: 369L	64
FIGURE 23 - EFFECTS OF GLAZING LAYERS ON TANK & ABSORBER TEMPERATURE - SUMMER	65
FIGURE 24 - EFFECTS OF GLAZING LAYERS ON TANK & ABSORBER TEMPERATURE – WINTER	67
FIGURE 25 - EFFECTS OF PLATE SPACING WITH ABSORBER TEMPERATURE	68
FIGURE 26 - EFFECTS OF WATER TEMPERATURE GAIN WITH PLATE SPACING	68
FIGURE 27 - EFFECTS OF INSULATION ON WATER TEMPERATURE ACHIEVED	71
FIGURE 28 - ABSORBER TEMPERATURE & INCIDENT SOLAR RADIATION (SIMULATION PERIOD - DAY 1)	72
FIGURE 29 - ABSORBER TEMPERATURE & INCIDENT SOLAR RADIATION (SIMULATION PERIOD - DAY 2)	73
FIGURE 30 - ABSORBER TEMPERATURE & INCIDENT SOLAR RADIATION (SIMULATION PERIOD - DAY 5)	73
FIGURE 32 - ABSORBED CONVECTION IN GLAZING SURFACE (WINTER)	86
FIGURE 33 - ABSORBED CONVECTION IN GLAZING SURFACE (SPRING)	87
FIGURE 34 - ABSORBED CONVECTION IN GLAZING SURFACE (SUMMER)	87
FIGURE 35 - ABSORBED CONVECTION IN GLAZING SURFACE (AUTUMN)	88
FIGURE 36 - AMBIENT TEMPERATURE AND WATER TANK TEMPERATURE GAIN FOR FINAL MODEL	88
FIGURE 37 - TOTAL DIRECT NORMAL SOLAR FLUX ON COLLECTOR CASING FOR FINAL MODEL	89

## List of Tables

TABLE 1 - COMMONLY USED SELECTIVE COATINGS (G. D., 1987)	23
TABLE 2 - BASE MODEL INSULATION	44
TABLE 3 - BASE MODEL ABSORBER MATERIAL	45
TABLE 4 - BASE MODEL GLAZING	45
TABLE 5 - BASE MODEL TANK INSULATION	46
TABLE 6 - THERMAL ZONES	47
TABLE 7 - CASING ZONE CONSTRUCTION	48
TABLE 8 - ABSORBER PLATE CONSTRUCTION	49
TABLE 9 - ESP-R MODEL CONNECTIONS	54
TABLE 10 - CONSTRUCTION DETAILS OF GLAZING MATERIALS	65
TABLE 11 - INSULATION LAYERS FOR TESTING	70
TABLE 12 - VARIABLES FOR EFFICIENCY CALCULATION	76
TABLE 13 - CALCULATED SYSTEM ENERGY & EFFICIENCY	76

## Nomenclature

$Q_{net}$  = Daily total net energy absorbtion  $\left(\frac{MJ}{day}\right)$

$Q_c$  = Daily total energy absorbtion  $\left(\frac{MJ}{day}\right)$

$Q_{loss}$  = Daily total energy loss  $\left(\frac{MJ}{day}\right)$

$M$  = Total mass of water in system (kg)

$C_p$  = Heat capacity of water  $\left(\frac{MJ}{kg^{\circ}C}\right)$

$T_f$  = Final tank temperature ( $^{\circ}C$ )

$T_i$  = Initial tank temperature ( $^{\circ}C$ )

$\alpha_e$  = Effective solar absorbnce (dimensionless)

$A_c$  = Total collector area ( $m^2$ )

$H_t$  = Daily total solar irradiation incident upon collector surface  $\left(\frac{MJ}{m^2}\right)$

$t_f$  = Final time of energy collecting phase (hour)

$t_i$  = Initial time of energy collecting phase (hour)

$I_T$  = Incident solar radiation on collector surface  $\left(\frac{W}{m^2}\right)$

$U_t$  = Overall heat loss coefficent ( $MJ/^{\circ}C$ )

$T'$  = Daily average tank temperature ( $^{\circ}C$ )

$T_a'$  = Daily average ambient temperature ( $^{\circ}C$ )

$q_{net}$  = Daily total net energy absorbtion per collector area  $\left(\frac{MJ}{m^2 day}\right)$

$U_s$  = Overall system loss rate  $\left(\frac{MJ}{m^2^{\circ}C}\right)$

$\eta_s$  = Daily System efficiency (%)

$\eta_T$  = Overall System efficiency (%)

## Acronyms

FAC – Flooded Absorber Solar Collector

FPC – Flat Plate Solar Collector

STC – Solar Thermal Collector

EU – European Union

DHW – Domestic Hot Water

ST – Solar Thermal

PV – Photovoltaic

SWH – Solar Water Heater

ETFE – Ethylene Tetra Fluro Ethylene

CLTE – Coefficient of Linear Thermal Expansion

GW<sub>th</sub> – GigaWatt thermal

# 1. Introduction

## 1.1 Solar Resource

Solar Energy is the primary light and heat resource of the earth. In the modern day, there are two major ways in which to utilise solar resource, for heat and for electricity. The most common is for electricity production. Photovoltaic materials convert radiation from the sun into electricity due to a phenomenon known as the photoelectric effect. These materials have the ability to absorb photons of light and release electrons, creating an electrical current. Big players in the market include China, USA, Japan and Italy.

The other major resource is the sun's thermal energy. One of the most widely recognised solar thermal application is solar water heating. Solar water heaters are typical devices that absorb the solar thermal energy and use it to directly heat a transfer fluid (Chong, Chay, & Chin, 2012). Technological viability of solar thermal systems has long been recognised and is employed in many domestic and commercial sectors worldwide.

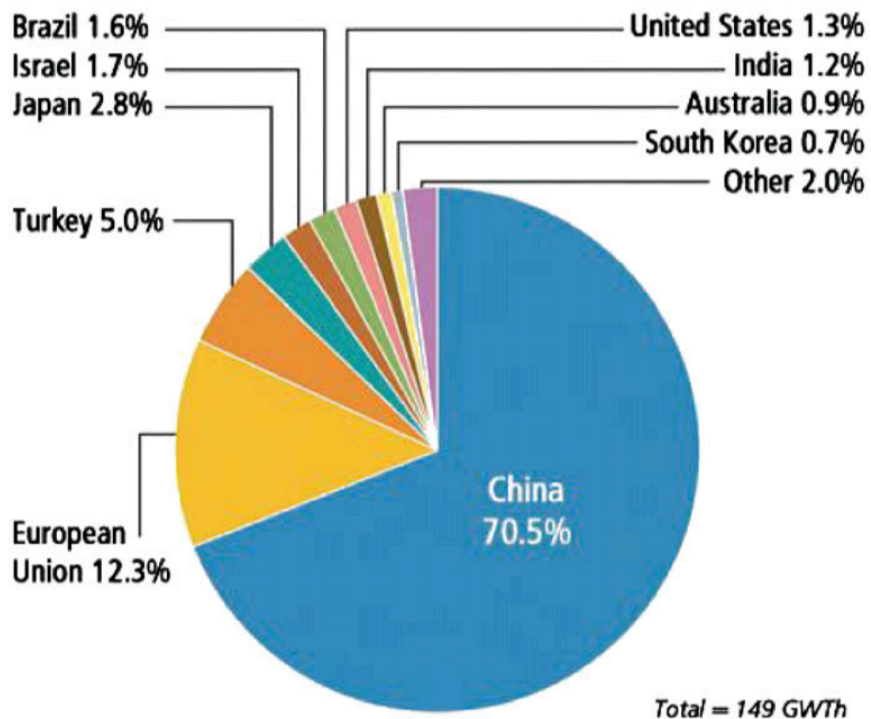


Figure 1 - Existing Solar Hot Water Heating Capacity. Top 10 regions/countries (2010) (Raisul Islam, Sumathy, & Ullah Khan, 2013)

In Figure 1 above, the share of the thermal market in 2010 was owned by China at 70.5%, followed by Europe at 12.35. Four years later in 2014, the installed capacity of thermal collectors worldwide was at 410.2GW<sub>th</sub>. (Mauthner, Weiss, & Spörk-Dür, 2014). This figure corresponds to roughly 586 million square meters of collector area in operation across the globe. In the present thermal energy market, China leads, with 289.5GW<sub>th</sub>. Europe is still a large distance behind at 47.5GW<sub>th</sub>. Together, this makes up 82.1% of the worldwide market. Countries in areas such as Sub-Saharan Africa and MENA which have ample solar resource, have a total installed capacity of less than 10GW<sub>th</sub> between them. This could be blamed on the fact that current solar collectors are relatively expensive to design and require complex procedures to build them.

In 2014, the breakdown of cumulated capacity in operation was 71.2% evacuated tube collectors, 22.1% glazed flat plate collectors and 6.3% unglazed water collectors. These systems are classed as “Active” or “Passive” systems. (Mordor Intelligence, 2017) Of these systems, they are classed as high temperature or low temperature. High temperature systems tend to be associated with industrial applications. Low temperature thermal solar collectors are those which produce heat, mainly for domestic use, from 40°C – 60°C (Solar Energy, 2015)

### 1.1.1 System Types - Background

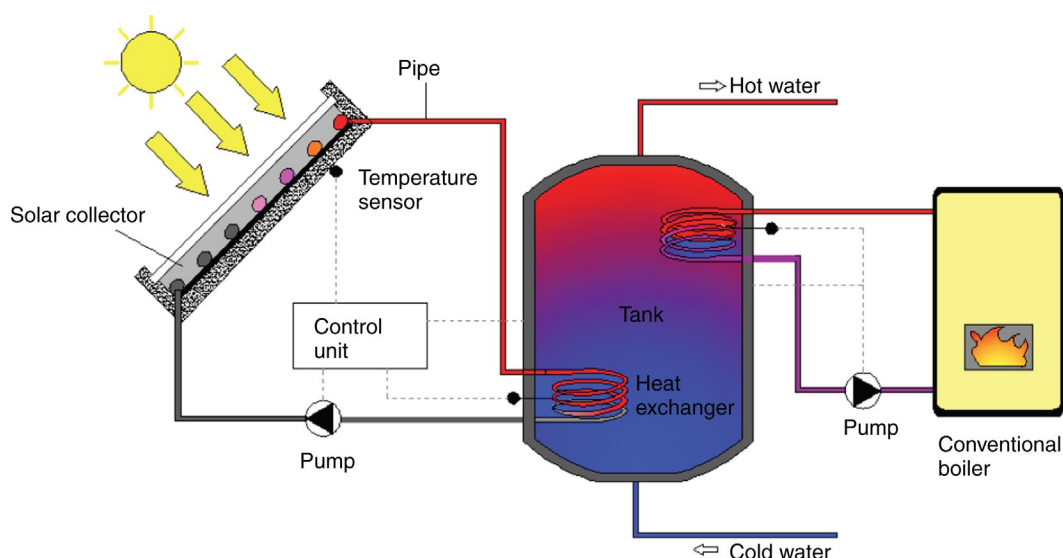


Figure 2 – Layout of a conventional solar hot water system (Jamar, Majid, Azmi, Norhafana, & Razak, 2016)

A conventional “Active” or Forced Circulation SWH system is shown in Figure 2. The major components of the system are the pump, the Solar Collector and the Tank. Often, in

conventional systems, the collectors are backed up with an externally powered boiler to ensure hot water can be supplied in times when solar energy is not available. The active system uses electrical pumps, valves and controllers to circulate water through the collector (Jamar et al., 2016). Preferably, in these systems, the storage tank is located below the collector to reduce the pump work, although this is not essential (Yeh & Chen, 1985). Active systems can be open or closed loop forced circulation type. In the case of domestic water, open loop (direct) active systems transfer thermal energy directly to the actual water the household will be using. The water is heated and then pumped into storage for use in the home. A closed loop (indirect) active system heats a separate heat transfer medium from the household water. This heat transfer fluid (sometimes anti-freeze) is heated in the collector and then pumped into a storage tank where a heat exchanger transfers heat from the fluid to the household water (Patel, Pragna Patel, & Patel, 2012)

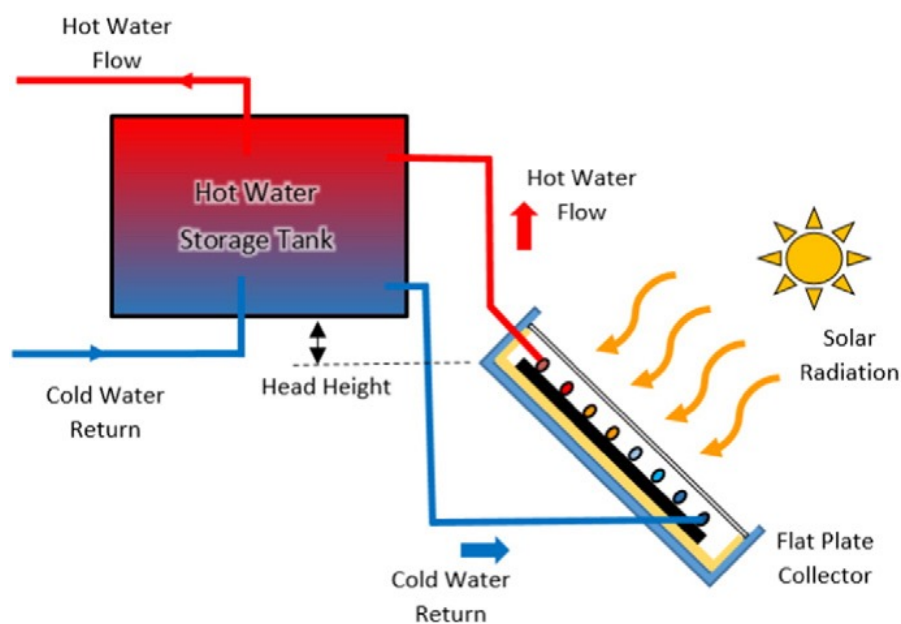


Figure 3 – Layout of a "thermosiphon" SWH system (Jamar et al., 2016)

The Passive system or "Thermosiphon" system uses the method of natural convection heat transfer without the necessity of mechanical devices to circulate water or to transfer fluid from the solar collector to an elevated storage tank as can be seen in Figure 3 (Jamar et al., 2016). The storage tank is elevated due to the fact, when the collector is at a lower temperature than the storage tank temperature, the thermosiphon effect will be reversed, cooling the stored water. In this system, as the fluids temperature increases, the density will decrease. This will cause the fluid to upsurge to the collector header and flow to the storage

tank. The cold fluid in the storage tank sinks to the bottom, causing it to flow back down into the collector. This is a continuous process until there is no sun to supply energy (Patel et al., 2012). The Thermosiphon system design is cheap and simple due to the fact no instrumentation or control system is needed. It is the most common type of solar water heating system on the market and most commercially available (Drosou, Tsekouras, Oikonomou, Kosmopoulos, & Karytsas, 2013).

The efficiency of this configuration of system is related to the difference in ambient temperature and collector temperature and is inversely proportional to solar radiation intensity (Patel et al., 2012). Despite the advantages of the thermosiphon system, there are various drawbacks to the design. Connecting lines must be well insulated to prevent heat losses and be sloped to ensure air pockets are not formed that would stop circulation (Jamar et al., 2016). They also must be designed with no bends in the tubing to ensure liquid cannot pool. The system must also be completely air tight; if not, the thermosiphon process will fail and only cause water to evaporate over a short period of time.

## 1.2 Project Motivation

One of the main challenges facing solar thermal applications, is the drop in total capital of PV plants since 2005. Between the years 2001 – 2013 the price of Solar Thermal systems remained level, although there was a drop in price of roughly 70% in Photovoltaic systems (Streicher, 2016). It is therefore essential that solar thermal technology is cheap and easy to construct to remain in competition with solar electrical technology. As previously mentioned, major countries like Sub Saharan Africa which have an abundance of solar resource, have a total installed capacity of less than  $10\text{GW}_{\text{th}}$  (Mordor Intelligence, 2017). It bares questioning why in such solar rich climates, the solar energy is not utilised to its full potential.

In the latest developments of Solar hot water systems, researchers are mainly focusing on improving system performance and reducing total cost (Chong et al., 2012). The conventional design of flat plate collectors is known as harp or parallel tube type and is a complex procedure including welding pipes to an absorber plate with millimetre exact spacing (Kalidasan & Srinivas, 2014).

Despite the harp type configuration being the most prominent design on the flat plate collector markets, as well as complexity of design, there are some disadvantages to its thermal performance. Initially, the pipes are usually separated by 3", meaning the plate temperature must be several degrees higher than the temperature of the pipes (Khanna+, 1968). Also, the distribution of thermal fluid (usually water) through the absorber pipes is rarely uniform, therefore leads to variations in plate temperature. Another reason for this temperature distribution, is that a small amount of thermal energy is wasted via conduction through redundant areas of plate to the areas where the risers lay. This results in the temperature, half way along the tubes, being higher than the temperature throughout the length of the tubes.

The serpentine configuration can partially solve these problems, most prominently in low flow rates. The serpentine configuration increases the heat transfer coefficient by being arranged in a zig-zag fashion across the absorber plate which allows an extensive volume of fluid to contact the absorber at once. The temperature distribution, however, is still similar to that of the parallel tube configuration.

A FPC configuration that has been given little attention is the Flooded Absorber or "Twin Parallel Plate" design (Nikogosian, 2017). The Flooded absorber configuration would involve having two sheets of metal separated by a small distance for fluid flow in between. This would mean the design would be simplified, removing the need for tube welding and complex measurements.

Through this thesis, the design of a flooded absorber solar collector is produced and simulated, basing the design from current parallel tube configurations were possible.

### 1.3 Project Aim

The aim of this project is to assess the feasibility of a flooded absorber type solar collector for domestic water heating. The design of the system will be based heavily on the design of a parallel tube solar collector. Through virtual software ESP-r (Section 1.5), the design will be inputted and tested for validation. Then, various system attributes will be modified to ensure correct operation. The main aim for the project is to produce a flooded absorber solar collector system suitable for use in low temperature application. This means producing water in the ranges of 40°C – 60°C. A secondary goal of the project will be to simplify the design

due to the complexity of current collector types. With a simpler design, the technology could be far more feasible in less developed parts of the globe due to ease of system construction.

#### 1.4 Project Methodology

In order to successfully meet the aims of this project, the full design specification for a flooded absorber type solar collector must be produced. In order to do this, a wide range of literature must be reviewed in order to base the design. To assess the best possible design of the system, various systematic aspects must be researched in order to make good judgement. After a good understanding of solar thermal collectors has been accomplished through research a full design will be presented. This design will then be inputted into simulation software ESP-r (Section 1.6). In the simulation environment the FAC will be assessed on various aspects of design. These aspects will include thermal insulation, absorber plate spacing and various other aspects affecting complexity of design and thermal performance. Once a suitable model has been obtained the thermal efficiency will be calculated and compared to current collectors.

#### 1.5 Scope

The main limitation to this thesis will be that the FAC will not be physically designed. This means certain aspects of the design produced may not be feasible to a real-life system. ESP-r is a mathematically based software so therefore cuts corners by making assumptions. For example, the heat transfer coefficient of such a system will be constantly changing. In ESP-r, the software assumes a constant value depending on the surface attribute used. However, ESP-r has been developed for many decades therefore gives a largely accurate result. The findings will produce a framework in order to base a real-life system. However, a more rigorous method of design would be essential in order to physically model the thermal system

#### 1.6 ESP-r

ESP-r is a virtual environment simulation software that is employed in this project in order to assess the technical potential of the flooded absorber solar collector. ESP-r is developed and licenced by the Energy Systems Research Unit (ESRU, n.d.) at the University of Strathclyde and

Natural Resources Canada (NRC, n.d.). ESP-r was developed to assess building energy performance although can be used as a simulation software for any thermal device. The software is designed to simulate thermal energy networks, power flows and atmospheric factors. More specifically, it is equipped to model surface heat transfer, 2D and 3D conduction between surfaces, short and long wave radiation exchange and various other thermophysical interactions.

In light of this, ESP-r was chosen as the simulation software to simulate and assess the performance of a flooded absorber solar collector (FAC).

## 2. Literature Review

### 2.1 Introduction

Solar thermal systems have a variety of uses through domestic and industrial applications. Solar thermal systems have been analysed by researchers based primarily on economical, environment and energy benefits of their installation. (Karagiorgas, Botzios, & Tsoutsos, 2001) evaluated industrial solar thermal technologies in terms of economic potential by comparing against energy equivalent systems like diesel, LPG and natural gas. (Soteris A. Kalogirou, 2004) presented a number of the most common configurations of solar thermal collectors along with their main purposes. It was also highlighted in the report that for low temperature applications, solar water heating is preferred. (S A Kalogirou, 2009) focused more on flat plate solar water heaters and the potential environmental benefits that came with the design. The main focus of research in the field of solar thermal systems has been aimed at increasing efficiency of the systems by varying operation variables along with design.

### 2.2 Solar Collector System

#### 2.2.1 Previous Solar Thermal Systems

The first solar water heater commercially manufactured was termed “The Climax Solar Water Heater” and patented in 1881 (Kemp, 1891). The system was of ICS type, meaning the storage and collector were integrated together. The simple system was made up of a metal tank inside

a wooden box which was covered by a glass glazing. The device was used to produce water hotter than 38.8°C on “warm days”. Kemp used the scientific principle of the “hot box” to capture and retain solar heat. The device was marketed to simplify household duties as at the time hot water mains had not been introduced. An advertisement from the time can be seen below (Kemp, 1891). One of the claims on the devices was that it could produce hot water for “3 to 8 baths”.

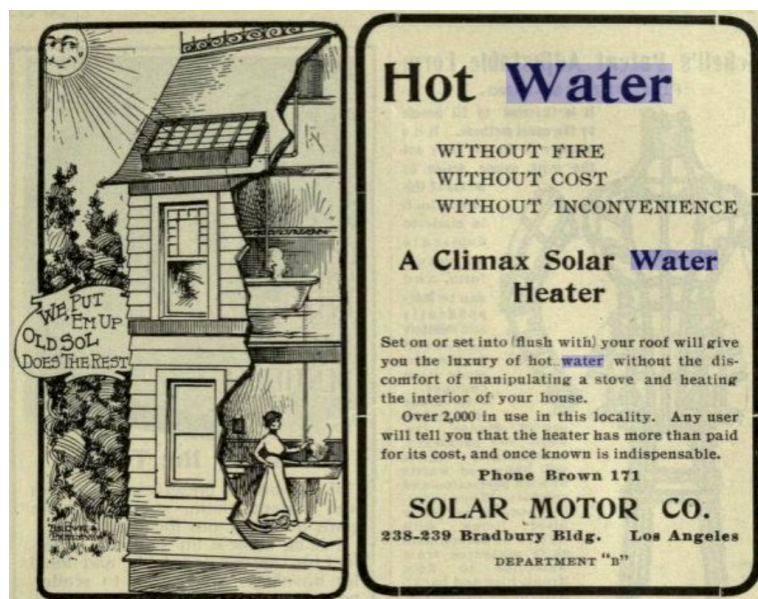


Figure 4 - The Climax Solar Water Heater Advertisement

From then on various advancements were made to the Climax solar water heater by inventors. The breakthrough came in 1909 when William J. Bailey created a more ergonomic design by separating the system into a heating element that was exposed to solar radiation and a thermal tank that was well insulated. (U.S Department of Energy, 2002) The system was called the “Day and Night”. The heating element was made up of pipes connected to a black metal sheet which was contained inside a glass-covered box. The tank was placed on the roof and the collector beneath. The advancement in separating the heating element and storage tank meant that hot water was available at night, one of the problems of the Climax Solar Water Heater.

Just a few years previous, in 1905, a paper on the photoelectric effect had been published by Albert Einstein. As a result, focus in solar technology was heavily motivated towards photovoltaic devices, instead of thermal devices. Although, solar thermal devices were still being sold on the market. From 1923 a large percentage of the housing in the Florida regions used solar water heaters to heat domestic water as it was a cheaper alternative to coal or wood. The system used was made up of a Flat Plate Collector and galvanized steel storage tank, which operated on the thermosiphon principle. These systems however, were all replaced by conventional hot water electric systems by 1951 (Scott, 1976)

New Installations of solar water heaters fell sharply from the early 1950's due to three principles. The first principle was the economic advantage that the solar thermal systems had possessed was lost due to electric conventional systems being far cheaper to build. The second principle was that the design problems were becoming more and more apparent and the public were becoming aware. And the last principle was that a shift in building development meant that large-scale building developers now had control over how houses were built. The homeowner had little decision on what appliances would be implemented into his/her dwelling. These building developers looked for the cheapest technologies on the market and at the time electricity prices had been decreasing since the 1930's. (Scott, 1976)

Throughout the next few decades, fossil fuels dominated the energy markets. As a result, the spotlight drew from solar water heaters. However, basic solar water heaters were still used around the world in countries such as Japan and Australia. Rice farmers used solar water heaters in living quarters in order to bath. In Australia, through the late 1960's and 1970's, solar devices were used to heat domestic water in thousands of homes. This spiked drastically in due to the increase in oil price in 1972 and 1979. (California Solar Center, 2015)

Although in the 1980's, the Solar Water Heater market in Australia began to stagnate again with the introduction of pipelines that brought natural gas to places previously out of reach. The need for solar heating devices became scarce. Solar water heaters were left largely untouched by researchers in this decade. Although, some countries, such as Israel, did not turn to conventional methods for water heating – worried by the fact the oil prices would

again spike. In 1983, 60% of the population used solar water heaters to heat water and currently around 90% of Israeli households own solar water heaters (Scott, 1976)

In current times, with oil prices staying high and global warming being a pressing issue, renewable energy such as solar water heating has come back into focus. New designs are being produced for high efficiency, and various components are being studied in detail in order to gain maximum performance.

### 2.3 The Flat Plate Collector

The two main configurations on the market for stationary SWH are:

- Evacuated Tube Solar Collector (ETC)
- Flat Plate Solar Collector (FPC)

(Chong et al., 2012)

The ETC design consists of a header and heat pipe, manifold and evacuated tube. Although efficiencies can be extremely high, they are the most expensive design of SWH (TheGreenAge, 2018). Flat plate solar collectors are the most common device used for domestic solar water heating (Sö zen & Menlik, 2008). FPC's are usually designed for working with temperatures ranging between 40°C - 60°C which is generally the case with domestic hot water. FPCs are advantageous over ETCs as they as they collect radiation coming from all angles (direct and diffuse) which means they can be stationary at all times. Various investigations over the past two decades have been aimed at reducing the FPCs thermal loss to the ambient environment (Jeena & Nidhi, 2015).

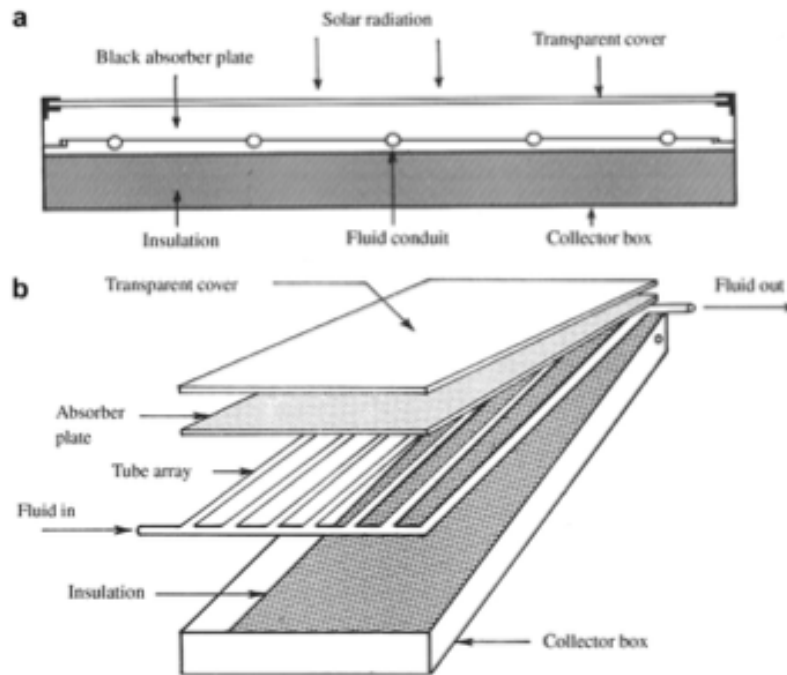


Figure 5 - Configuration of a Flat Plate Solar Collector: (a) cross-sectional (b) isometric

As can be seen in Figure 4, a typical FPC will consist of an insulated metal box with a plastic or glass glazing and a dark coloured absorber plate. Glass is preferred as glazing material due to its enhanced properties: it will, on average, transmit up to 90% of harmful incoming radiation and absorb nearly 100% of the infrared radiation emitted by the absorber plate (Gunjo, Mahanta, & Robi, 2017). This glazing will also protect the absorber, situated inside, from harmful environmental effects such as hail, wind and snow. Additionally, the glazing will prevent the absorber from cooling down due to wind exposure and contain heat. The conventional design of the absorber is known as “harp design” or “parallel tube” and consists of multiple finned tubes as can be seen in Figure 4, arranged in parallel. These tubes are usually made of thermally conductive metal and are connected conductively to the absorber plate. The absorber consists of a heat conducting metal sheet made of copper or aluminium, in strips or in a continuous surface. The absorber plate is given a dark “selective coating”, usually black chrome or black Nickel, in order to increase radiant absorption and reduce emission (Gammon, 1978). Commonly, in designs coupled to heat exchangers, the thermal fluid flowing through the tubes is water as it is inexpensive and non-toxic. With a low viscosity and high specific heat, it makes an ideal heat absorber (Jeena & Nidhi, 2015). In areas

where there is an average availability of solar radiation, flat plate collectors are sized approximately one half to one square foot per gallon of one days hot water (Moss et al., 2017)

The main idea behind a flat plate solar collector is that solar energy is converted into heat energy when sunlight passes through the glazing and strikes the absorber plate. This heat is then convectively transferred to the heat transfer medium inside the finned tubes. In an active system, the flowrate circulates at a constant rate. In the case of a passive system, as the flow medium heats up, the density drops and the “hotter part” flows up and out of the header tubes. These tubes are often of a larger diameter to encourage this process. (S. Kalogirou, 2014).

### 2.3.1 Absorber Modifications

One of the most important features of the solar water heater is the absorber. The absorber is responsible for taking the solar radiation and passing in into the heating medium. Absorber plates have undergone many modifications with the aid of better techniques in manufacturing and material science (Pandey & Chaurasiya, 2016).

Within the design of the solar absorption plate, the primary construction materials tend to be either Steel, Copper or Aluminium. Steel is a lesser choice although it is a truly sustainable material. Once steel is made, it can be used as steel forever. Copper is the most common material choice due to its high thermal performance over the other absorber materials. Copper is also very resistant to corrosion, adding to its lifetime. Aluminium has a slightly lower thermal conductivity than Copper however its low weight makes up for this. When solar absorber systems increase in size, a light weight construction material is desirable if the collector is going to be placed on top of roofing. Since these materials are not strongly absorbing, especially Aluminium, a coating must be provided which absorbs solar radiation (Lenel, 1984).

Plastics can also be used for the absorber material. Materials such as Polypropylene and acrylic can be pigmented with black and used as highly conductive absorber plates. Plastics can also be produced to be transparent and formed in such a way that liquid can pass in

between. The coloured liquid contained inside the plastic is picked so that high thermal conductance can be achieved (Lenel, 1984).

The heat transferred to the fluid depends not only on the thermal conductivity of the material but also on the distance between fluid passageways. (Lenel, 1984) looked at the different materials and configurations of fluid passageways to lower cost of solar thermal heaters. In the study he found that different configurations of absorber allow for lower thermally conductive materials to be used in the design.

**(a) High thermal conductivity materials**

---

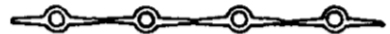
1. Plate and tube



2. Profiled plate and tube



3. Tube and fin extruded



**(b) High to medium thermal conductivity materials**

---

1. Quilted plate, profiled and selectively welded



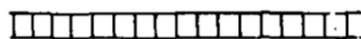
2. "Rollbond" selectively welded and expanded



**(C) Low thermal conductivity materials**

---

1. Sandwich e.g. extruded plastic



2. Tubes e.g. rubber



Figure 6 - Designs of various fluid passageways within absorbers (Lenel, 1984)

Shown in Figure 6 are several different typical absorber configurations. Plate & tube and Tube & Fin designs are commonly used with high thermally conductive materials like Copper and Aluminium. In these designs, heat is transferred through the plate or fin to the fluid carrying tubes. The quilted or roll bond design consists of selectively welded plates that can be spaced accordingly, depending on the thermal conductivity of absorber material. Materials with the lowest thermal conductivity tend to be arranged in sandwich form or close tubing (Figure 6c). When the thermal conductivity of the material used is very low, the heat transfer path must be very short. It is possible to use plastics in configurations such as plate & tube, however most of the absorber surface must be in contact with the fluid and the contact walls must be extremely thin (Blaga, 1978)

Table 1 - Commonly used selective coatings (G. D., 1987)

Type of coating	$\alpha$	$\epsilon$	Temperature °C Air/Vacuum	Life (year) Air/Vacuum
Interference	0.94	0.10	175/200	5/30
Black Chrome	0.96	0.12	175/200	15/30
Black Nickel	0.90	0.07	-	-
CuO	0.88	0.15	100	-
Enamels	0.95	0.8-0.9	250/250	$\infty$
PbO <sub>2</sub>	0.98	0.30	100/150	20
Stainless steel	0.90	0.40	75	30/30
Anodic aluminium	0.95	0.80	250	50
Aluminium conversation	0.93	0.85	100/100	10-20
Paints	0.97	0.91	70/80	5-20

The popular metals chosen for design often have low absorbance characteristics. This is because metals tend to be reflective and therefore reflect most of the useful shortwave radiation. To counter this problem an absorbent coating is required. (Lenel, 1984) discusses the different types of coatings that can be applied. Either a selective or non-selective coating is used. Non-selective coatings are not specifically designed to absorb a "select range" from the electromagnetic spectrum whereas selective coatings are. The typical nonselective coating of choice is matte black paint although can be a hinderance to performance above

40°C and has relatively high infrared emittance. Selective coatings consist of two layers. An upper layer to absorb shortwave radiation, while transmitting long wave radiation and a lower layer to absorb long wave radiation. Selective surfaces are particularly useful in colder climates where the exterior environment is colder than that of the surface of the solar collector (Lampert, 1979). Table 1 summarise the details of the most commonly used selective surfaces.

(Madhukeshwara & Prakash, 2012) also presented a study concerning the selective surface coatings added to the absorber. It was reported that a good selective surface consists of a material that enables only a small fraction of solar radiation to be lost due to reflection and radiation. The selectivity of the surface is defined as the ratio of the solar radiation absorbed to the thermal radiation emitted. Characteristics of a good selective surface combine a low emittance in the relative temperature range with a high absorbance for radiation. If the selectivity of a surface is low, it may be enhanced by the addition of filters. In the study, it was found that black chrome had the best selectivity and so achieved the highest water temperatures. In their findings, the absorptivity of black chrome was found to be 0.93 and the emissivity was 0.11 giving a selectivity result of 9.3.

### 2.3.2 Absorber Efficiencies

(Karim, Nakoa, Mahmood, & Akhanda, 2012) reported on the effects different absorber colours may have on the performance of flat plate solar water heaters. On an average basis, blue and black absorbers performed better than colourless and red-brown absorbers. The highest monthly efficiencies for the blue and black absorbers were 53% and 57% respectively, fixed at a 23.5° angle to the horizontal. The maximum temperature achieved for each absorber colour was: 41°C for colourless, 43°C for red-brown, 50°C for blue and 54°C with black.

(Amrutkar, Ghodke, & Patil, 2012) conducted a study under laboratory conditions evaluating the performance of an FPC with different absorber geometries. Collector area was varied from 1.9m<sup>2</sup> – 2.5m<sup>2</sup> and systems from Sunbeam Solar, Tata BP solar system, Jain Solar, Avin

Solar, along with many others were used in the study. The maximum storage temperature ranged from 50°C to 70°C and efficiencies of collector from 55% to 71%. The aim of their study was to prove that there was a significant drop in capital with the increase in efficiency of collector.

### 2.3.3 Alternate Designs

Attempts have been made over the years to change the design of the collector from most common configurations like the Evacuated Tube Solar Collector (ETC) and Flat Plate Solar Collector (FPC) (Chong et al., 2012). It has been reported that collector arrangement has the biggest influence on thermal performance (Van Niekerk, du Toit, & Scheffler, 1996)

(Rommel et al., 1997) experimented with various different absorber geometries, contrary to the norm used with metal absorbers. This was possible due to the polymer material, which was used, being easily shaped. Their main aim was to create a corrosion free collector system by creating a selectively coated plastic absorber. In result of their research, they found that an absorber geometry of heating fluid contacting rectangular channels had performance characteristics of that of fin and tube absorbers.

### 2.3.4 Enhancement Devices

(Hobbi & Siddiqui, 2009) reported on an experimental study to investigate what impact heat enhancement devices had on flat plate solar collectors. Various passive heat enhancement devices were studied including twisted strip, coil spring wire and conical ridges although none of the devices showed appreciable difference in heat flux to the collector fluid. It was also indicated that the main heat transfer mechanism in solar collectors were of mixed convection type with free convection as the dominant heat transfer mode.

(Z. Chen, Furbo, Perers, Fan, & Andersen, 2012) carried out a study of the potential efficiency increase of using Ethylene Tetra Fluoro Ethylene (ETFE) foil in a flat plate solar collector. They compared the result of the ETFE foil collector with that of copper collector. Different flow rates of heating medium were trialled and efficiencies of each collector estimated. It was

established that the collector with the ETFE foil had a higher yearly thermal performance when average temperatures were above 30°C. It was also found that when the volumetric flowrate of the fluid through the collector was increased, the efficiency of the system also increased while the heat loss coefficient decreased.

Nanoparticles and Nanofluids have been in the spotlight for research and development of Solar thermal systems in recent years. (Meibodi, Kianifar, Niazmand, Mahian, & Wongwises, 2015) evaluated the role of nanofluids on heat transfer enhancement within flat plate solar collectors. Tests were taken using SiO<sub>2</sub>/ethylene glycol water nanofluid with volume fractions up to 1%. It was found that the effects of particle loading on thermal efficiency was more defined at lower values of heat loss coefficient. The potential of SiO<sub>2</sub> nanoparticles is highlighted in this study for thermal enhancement despite the lower thermal conductivity of other similar nanoparticles.

(Jouybari, Saedodin, Zamzamin, Nimvari, & Wongwises, 2017) studied the effects of nanofluid particle size on thermal efficiency of flat plate collectors. It was found that the efficiency of system decreases with diminishing particle size. (Kumar Verma, Kumar Tiwari, & Singh Chauhan, 2017) tested different nanoparticles mixed into the water heating medium. Of all nanoparticles tested, the exergy efficiency of system was increased by 29.32% by a graphene/water mixture showing graphene's potential in thermal systems.

### 2.3.5 Glazing

The glazing of the solar collector primarily reduces convective losses to the environment from the upward facing side of the absorber while still allowing solar radiation to pass through. The glazing's secondary function is absorber protection.

The most widely used material for the glazing of the collector is tempered glass. Tempered glass can achieve a 90% transmittance due to the low iron content. Iron is often found in glass and can be detrimental to transmittance even at very low concentrations. When performing energy calculations for glass standards, roughly 2% of the radiative energy is absorbed by the glass therefore it is often disregarded. However, tempered glass can be fragile and is very

heavy compared to its polymer competitors. The glass is prone to breaking when bonded to the frame of the collector (Köhl, 2012).

Using multiple layers of glazing is a topic that has been discussed thoroughly in research (Kalidasan & Srinivas, 2014; Köhl, 2012; Singh, Sarviya, & Bhagoria, 2010). (Kalidasan & Srinivas, 2014) also looked into the benefits of more than one layer of collector glazing. It was found that on colder days, when the absorber temperature was lower, a single layer of glazing was superior to a double layer as the single layer transmitted larger amounts of useful energy. However, when the general exterior temperature was higher, meaning the absorber temperature was higher – more than one layer was advantageous due to the increased trapping potential of extra layers of glazing. A compromise must be taken depending on the environment the solar collector is being placed in. (Singh et al., 2010)

reported that there was a 10% - 15% decrease in heat loss coefficient with a double layer compared to that of a single layer of glazing.

(Kalidasan & Srinivas, 2014) studied the effects of different numbers of covers (glazing) and refractive index to improve optical and thermal efficiencies of collectors. It found that a reliable cover should have low transmissivity for long wave radiation and high transmissivity for shortwave radiation. These two attributes together are commonly known as the “greenhouse effect”. Having low emittance in the long wave spectrum means that radiation will be trapped inside the collector, giving the absorber more opportunity to heat up and therefore increase efficiency. The shortwave radiation contains most of the useful energy therefore it is important that this energy can easily make its way to the absorber plate, hence high transmittivity for short wave desirable.

(Bakari, Minja, & Njau, 2014) looked into how glazing thickness effected the performance of a flat plate collector. A glass glazing was used to ensure reflection and absorption was as low as possible and transmission was as high as possible. Glazing of 3,4,5 and 6mm were used (low iron content glass) and it was found 4mm thickness attained the best increase in performance of 7.6%. The downside to a thinner sheet of glass, however, is that risk of breakage during construction is increased.

Polymers can also be used for glazing material. (S A Kalogirou, 2009) looked at the potential of such polymer materials. It was found that the biggest downfall of using polymers, such as plastic, for the glazing layer is that they have high transmittance in the longwave spectrum. This means energy can escape more readily from the absorber than with tempered glass. The longwave transmittance of plastics can reach up to 0.4 which, considering tempered glass is as low as 0.02, proves to be a big problem with deployment. In the shortwave spectrum, plastics compare better with glass, however still fall short. The transmittance absorbance ratio for polymers averages around 0.7 while for glass its 0.8 (higher value desirable for shortwave transmittance). Despite this, polymers such as Polycarbonate are on the market for other reasons such as their low weight and cost and the possibility of being made into almost any shape or structure.

A study was undertaken by (Köhl, 2012) to look into the performance characteristics of 58 different polymer materials for use as solar glazing. Out of all the polymers tested, only two were selected to rival tempered glass. One was PMMA (acrylic) and the other was Polycarbonate (PC). However, the materials were only tested for short periods of time. It was found that after a reasonable number of working hours, degrading due to UV exposure started to affect the PC glazing so much that it changed in dimensions. PMMA also experienced some of these changes although to a much lesser extent.

### 2.3.6 Optimum Tilt

The level of solar radiation that is absorbed by a solar collector depends on many variables including azimuth angle, location altitude, declination angle, etc (Figure 8). Out of all the variables, most are controlled by nature although the azimuth angle (horizontal measured clockwise) and tilt angle (inclination) are set manually.

It is well established that the optimum azimuth angle for FPCs is zero when south facing, although tilt angle has not been as well defined. Tracking can be done with solar collectors although it is an expensive technology and cannot be installed with many solar devices.

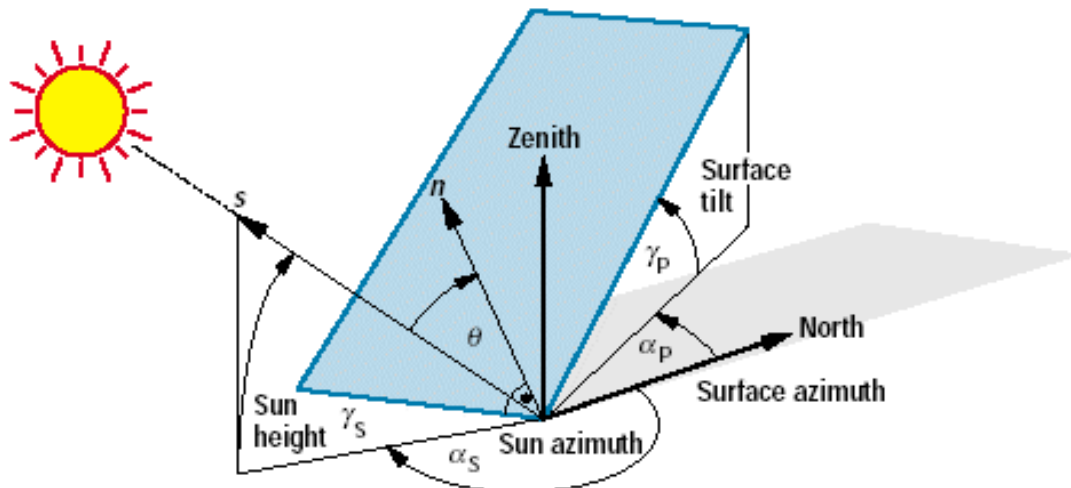


Figure 7 - Solar Angles

(Ulgen, 2006) realised that the ability of a solar collector to absorb solar radiation is largely down to the geometric and optical properties. The amount of solar radiation absorbed is dependent on the collector tilt with the horizontal. In their study, a mathematical model was used to determine the optimum tilt angle on a flat plate collector in Turkey. The main findings were that the collector tilt varies from  $0^\circ$  in June to  $61^\circ$  in December. In Winter, the collector tilt should be  $55.7^\circ$ , in Spring the collector tilt should be  $18.3^\circ$  in Summer  $4.3^\circ$  and in Autumn  $43^\circ$ . The trend shows that the colder the season, the lower the collector tilt to the horizontal. The yearly average of these results was found to be  $30.3^\circ$  therefore this would be the optimum tilt for a fixed (non-tracking) solar collector through the year.

(Chang, 2008) studied the optimum tilt angle for three main types of solar radiation: empirically correlated data for global radiation, ten-year observation data (1990-1999) and extra-terrestrial data. For collectors in Taiwan, optimum monthly averaged tilt angle in summer was  $-10^\circ$  and approximately  $+50^\circ$  in winter. The yearly average of this tilt would be a  $20^\circ$  tilt. It was found that the angles concerning the correlated and extra-terrestrial radiation could be well defined due to the simple fact they were latitude dependant. The radiation concerning the observation data however would vary continuously due to changing location. It was also found that the optimum tilt for observation data radiation was flatter presenting the outcome of flatter tilt angle for collectors in cloudy locations.

(Al-Rawahi, Zurigat, & Al-Azri, 2011) presented a comparison of predicted hourly terrestrial solar radiation on a horizontal surface. The predicted results were based on isotropic reflection on diffuse radiation and showed that in Muscat, the optimum tilt angle for January is  $40^\circ$  for an azimuth of  $0^\circ$  (South facing). In Winter, it is found that a horizontal angle tilt is best suited to maximum solar absorption.

(Eke, 2011) experimented with a flat plate collector of area  $0.5\text{m}^2$ . The FPC was hinged on a support for quick tilt angle adjustment from  $0^\circ$ - $90^\circ$ . Measurements were taken for clear sky hours from 12:00 to 14:30 in Zaria, Nigeria. A solar radiometer took averaged measurements over each degree of tilt. The study showed that the optimum tilt angles were  $26.5^\circ$ ,  $24.5^\circ$ ,  $10.0^\circ$ ,  $19.5^\circ$ ,  $26.0^\circ$ ,  $30.0^\circ$ ,  $24.0^\circ$ ,  $21.0^\circ$ ,  $11.5^\circ$ ,  $19.5^\circ$ ,  $27.0^\circ$ ,  $30.0^\circ$  from January – December, respectively. The averaged angle of inclination for Zaria was found to be  $22.5^\circ$  and this was found to have a small increase of 4.23% in solar intensity of that of a horizontally orientated FPC. The observation was made that the calculated and measured solar energy intensities incident on the collector surface increased in intensity from an angle of  $25^\circ$  –  $30^\circ$  and thereafter fell in intensity.

(Nnamchi, 2012) focused on optimum tilt angles for areas of low latitude in Nigeria. They developed expressions for monthly optimum tilt based on latitude in monthly increments for a year. The main finding of the study was that tilt angle for maximum insolation was different for various locations based on the area latitude. Polynomial expressions linking insolation with latitude were developed. The results obtained compared favourably with the literature.

(Keshavarz, Talebizadeh, Adalati, Mehrabian, & Abdolzadeh, 2012) determined values of optimum tilt for every day of a year in 30 different Iranian cities in order to create a map of maximum insolation locations. These values were averaged weekly, monthly and yearly and then an atlas of optimum slope angle and maximum energy gain was developed. The Geographic Information System (GIS) was used to outline the maps. The radiation predicted in all locations were compared with that of real data from 1983 – 2005 that was recorded by IMO (Iranian Meteorological Organization). The optimum tilt angle through January was

found to vary from  $46^{\circ}$  –  $56^{\circ}$ . The angle changed to negative tilt angles of  $-5.3^{\circ}$  –  $2.3^{\circ}$  through Summer month June.

### 2.3.7 Heat Loss Reduction

One of the main factors to solar collector performance is the amount of heat the system can contain from the environment. The insulation layer must completely encapsulate the collector, just leaving the glazing area uninsulated for solar radiation. Although no insulation can completely remove thermal losses, a number of attempts have been made to find the best suitable material for the task.

Vacuum insulation has been looked into by various different researchers. (El-Sherbiny, Hollands, & Raithby, 1978) conducted one of the first experiments for free convective heat transfer across inclined air layers, heated from below and bounded by one flat plate and one corrugated plate. The results showed that the solar collector's efficiency was not majorly effected by an air gap of 20mm between the casing and rear absorber plate. (Monterrey, 2008) realised a potential problem with vacuum sealing was the fact that due to the different expansion coefficients between metal and glass, the vacuum seal would usually fail if rapid temperature changes occurred. In order to sustain the vacuum seal, a pump, powered by solar panels was inserted in line with the FPC. This protection method was only needed with high temperature applications.

(Al-Beaini, Benhabib, Engelage, & Langton, 2007) described the most commonly used materials for insulation in solar collectors as mineral wool, glass wool, fibreglass and polyurethane. However, the use of fiberglass (Glass wool) can be detrimental if high temperatures occur. If temperatures are higher than the particulates melting point, they can evaporate into the absorber area and condensate on the glazing, reducing transmittivity. However, as glass wool was extremely cheap, it is highly suitable for use below temperatures with low temperature application.

(Beikircher, Berger, Osgyan, Reuß, & Streib, 2014) looked into alternatives to mineral wool for insulation. Flat plate collectors are usually insulated by a 40-60mm layer of mineral wool. The reason for the research was the fact wool can absorb humidity through the collector's

lifetime which greatly decreases the insulation properties. Mineral wool has a thermal conductivity between 0.035 and 0.06 W/mK but it was show that if the wool was removed, the air chamber remaining (assuming adequately confined), has acceptable insulation properties. The study showed that absorber rear side losses with mineral wool are around 1 W/m<sup>2</sup>K when empty while a well confined chambers losses are in the region of 1.5-2W/m<sup>2</sup>K. It was also found that Aluminium foil, positioned parallel between absorber and rear casing showed similar properties to mineral wool, but had no affinity to absorb humidity. Thicknesses of foil between 30-50mm showed comparable and even slightly better performance than mineral wool.

(Beikircher, Möckl, Osgyan, & Streib, 2015), the year later, looked at advanced methods of insulation. TIM or Transparent Insulating Material can be used to actually insulate the front cover of the collector. TIM is made up of a honeycomb network and has transmittance rating of up to 98% for direct radiation. This high transmittance means that it is suitable to insulate the glazing. On the other hand, for diffuse radiation, the transmittance is dependent on the thickness of the TIM layer. A compromise must be made to be thick enough to scatter infrared radiation while also thin enough to transmit diffuse radiation. Using a 40mm thick honeycomb layer, a heat loss coefficient of 2W/m<sup>2</sup> was found, which is double that of fibreglass (lower value desirable for low heat conduction). However, it was found with TIM that degradation occurs at high temperatures which causes softening.

(Hirasawa, Tsubota, Kawanami, & Shirai, 2013) looked at reducing radial heat loss from the collector by placing a porous medium on top of the absorption system. The shading effect on the copper tubing absorption system had to be minimised in order to maximise solar radiation gains. In their experiment, they used a series of offset wire screens made of fine nylon fishing lines to create a string net layer. This layer was situated between the absorber and glass plate. The result of their experiment found that the net reduction of heat loss by natural convection was 7% when the porous medium was placed above the absorber. However, total losses from the shading effect caused were not discussed.

## 2.4 Application of Flat Plate Collectors

### 2.4.1 Desalination

Water Desalination in simple terms means to remove salt from water. Over the past two decades, low temperature desalination has not progressed passed the demonstration stage. International standards report that a minimum of 5l/day per person and 10l/day per person is need in average and hot climates for consumption respectively (Ayoub & Alward, 1996).

(Schwarzer, Vieira, Müller, Lehmann, & Coutinho, 2003) produced a simple desalination system consisting of simply a flat plate collector and a desalination tower with heat recovery. The system was aimed at purifying either sea or salty ground water for human consumption. The flat plate collector implemented could either be used in direct or indirect heating mode. In the indirect configuration, an additional thermal oil is needed for heat transport. The desalination tower has six stages and incorporates a water circulation system in each stage to ensure salt doesn't build up. The water was rendered drinkable when the laboratory tests showed that the Coliform group bacteria was eliminated.

(Sengar, 2004) studied the performance of an FPC when coupled to a small scale distillation system. Hot water production was also investigated. 100 litres of water was heated using a FPC system of area 2m<sup>2</sup> and tilt angle of 45° facing south. Tests were conducted seasonally, and maximum water temperature was found at 58.3°C and 48.7°C in summer and winter respectively. It was found that the collector system obtained efficiencies ranging from 27.48% to 35.7%.

(S. Kalogirou, 2005) presented various techniques of salt water desalination using renewable energy technologies. The need for water desalination technologies were highlighted in this paper due to the energy crisis. The current systems in place like MED, MSF, vapor compression and many others were analysed and discussed with focus on energy usage. A review of current renewable energy desalination technologies included solar ponds, photovoltaic and wind energy systems. It was found that one of the most promising renewable energy technologies for water desalination, was solar energy.

(Joseph, Saravanan, & Renganarayanan, 2005) used a solar collector of 5m<sup>2</sup> in order to obtain a 10:1 yield of potable water (drinkable). A maximum distillate of 8.5 l/day was achieved with a maximum efficiency of 26%. The efficiency ranged from 15%-26% over the insolation fluxes of 400 – 900 W/m<sup>2</sup>. Using this technology, not only was the purity well above limits but the capital of such water was low compared to that of conventional cleaning systems.

(Wessley & Mathews, 2014) conducted an experiment to test the performance of FPCs for small scale desalination applications in India. The study presented that a maximum water temperature of 64°C was found on a solar rich day of 932.2 W/m<sup>2</sup>. The efficiency of the 2m<sup>2</sup> collector was recorded at 43.4%. The study also comments on the fact the maximum water temperature obtained is directly related to the availability of solar radiation. Losses via convection were also found around the collector due to wind velocity – highlighting the importance of insulation.

#### 2.4.2 Domestic Hot Water

Large amounts of energy are expended in obtaining hot water for domestic use. Shortages of supplies, harmful carbon emissions and expensive utility bills are all consequences of producing hot water in the home via conventional methods. In a typical UK household, more than half the money spent on fuel bills goes towards providing hot water and heating (Energy Saving Trust, 2018). In terms of developing nations, hot water for bathing and cooking is often the most expensive and time-consuming process in the household energy budget. If the upfront prices of solar water systems was competitive with current methods, they could produce a sustainable solution for poor households. (Al-Beaini et al., 2007)

(Al-Beaini et al., 2007) discussed in detail the potential of solar water heating to replace current methods of water heating in less developed nations. In communities in poorer parts of the world, obtaining enough hot water to live on is a problem. Households that do not have electricity rely on either biomass or wood to burn to produce hot water. In many areas, demand for wood has been the major cause of deforestation.

Household water usage varies enormously depending on how many occupants are living in a house, alongside their personal needs. According to the DEFRA, the average person in the UK uses around 142 litres of water each day (DEFRA, 2013). The average household uses 349 litres of water each day. The hot water used contributes to £228 to the average combined energy bill annually and emits 875kg of CO<sub>2</sub> per year when produced by natural gas boiler.

## 2.5 Calculation

### 2.5.1 Efficiency Calculation

(Huang & Du, 1991) developed a mathematical method to calculate the thermal performance of a solar collector. The method developed takes real data from experimental and applies this in the method. They found that the hot water load pattern was a complicated factor that effected the system performance during load phase. It was found that if the hot water load pattern was standardized, this problem could be solved. For accurate results, the variation of daily loads should be small. For the test method the assumptions made were:

- The temperature of the whole system can be represented by a system mean temperature
- The system mean temperature equals the mean water temperature of the tank
- Neglect the heat capacity effect of the construction material of the system

The instantaneous system performance must be integrated over the total energy collecting period per day (e.g. from sunrise to sun set). Therefore, an energy balance over the whole system and integrating over a full day (ignoring heat capacity effects) gives:

$$Q_{net} = Q_c - Q_{loss}$$

*Eqn. 1*

$Q_{net}$  is the total energy absorbed daily and can be expressed as:

$$Q_{net} = MC_p(T_f - T_i)$$

*Eqn. 2*

$Q_c$  is the total daily radiation absorbed by the collector which is assumed to be proportional to the daily irradiation total, incident on the collector surface ( $H_t$ ) and collector area ( $A_c$ ) where  $\alpha_e$  is a proportionality constant:

$$Q_c = \alpha_e A_c H_t \tag{Eqn. 3}$$

The total daily irradiation incident upon the collector surface can be expressed via the integral:

$$H_t = \int_{t_i}^{t_f} I_t dt \tag{Eqn. 4}$$

Where the initial and final time bounds are represented by  $t_i$  and  $t_f$ . The total daily heat loss is assumed to be proportional to the difference of the average tank temperature and average ambient dry bulb temperature:

$$Q_{loss} = U_t (T' - T'_a) \tag{Eqn. 5}$$

Where  $U_t$  is the total heat loss coefficient, which acts as another proportionality constant. To further simplify the equation, it is further assumed that the daily mean system temperature  $T'$  can be taken as the average between the initial and final temperatures of the water achieved;

$$T' = \frac{(T_i + T_f)}{2} \tag{Eqn. 6}$$

The energy balance (Eqn. 1) can be written in terms of equation 2, equation 3 and equation 5. The result, per unit collector area, is written as:

$$q_{net} = \frac{Q_{net}}{A_c} = \alpha_e H_t - U_s (T' - T'_a) \tag{Eqn. 7}$$

$U_s$  in the developed energy balance is simply the overall heat loss coefficient per unit area. Then to calculate the *daily system efficiency relation*, the energy balance is divided by the incident total solar radiation upon the collector surface ( $H_t$ ) giving:

$$\eta_s = \frac{q_{net}}{H_t} = \alpha_e - \frac{U_s(T' - T'_a)}{H_t}$$

Eqn. 8

## 2.6 Conclusion

It is apparent that there has been in-depth research into the design and upgrade of solar thermal collectors. Experiments and computer aided models have been developed in order to precisely obtain performance data to further improve the design of solar collectors. In general, flat plate solar collectors have received the most attention.

Research has shown the effects of variables such as inclination angle, water inlet temperature, total solar flux, ambient conditions and design. Within the broad scope of research, there has been little attention towards the flooded absorber type solar collector.

Throughout the rest of this report, the design considerations, design and thermal analysis of design shall be conducted in order to assess the performance of such an absorber design.

## 3. Design Considerations

### 3.1 Orientation & Inclination

The angle of orientation of a solar thermal collector is also known as the azimuth angle. The azimuth angle is that of the angular distance between due South and the horizontal point below where the sun is located. Reports show that the optimum performance of collectors is found when the azimuth is either 0°, 40° West or 40° East. When collectors are installed outside of these bounds, compensation factors must be considered. Figure 8 below shows the performance of solar thermal systems at various inclinations and orientations (Firebird, 2011).

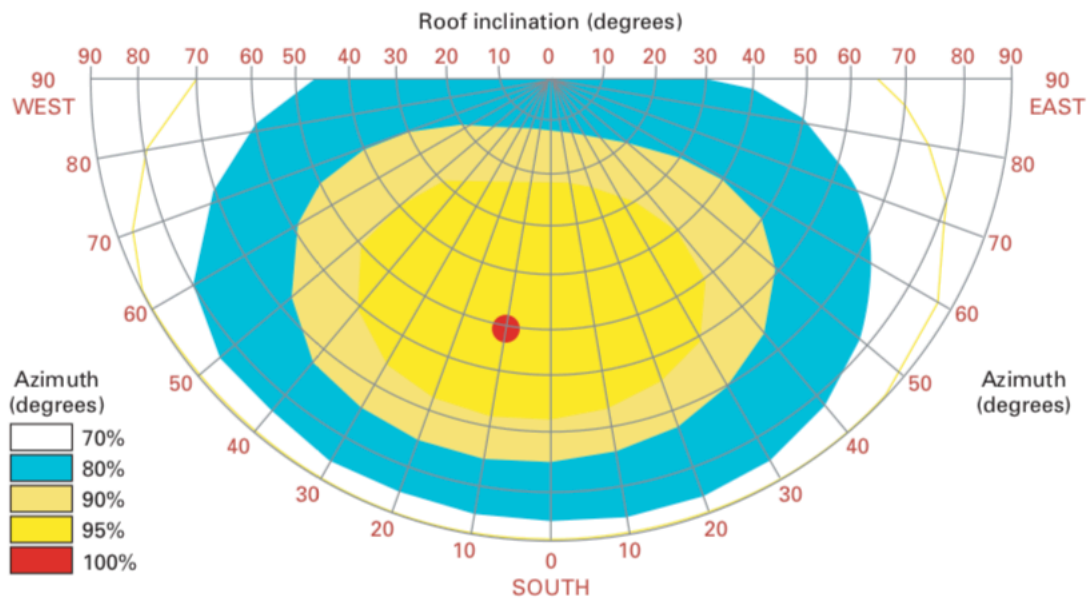


Figure 8 - Inclination and Orientation Angles (Firebird,2011)

The angle of inclination of a solar collector system is that of the angle between the collector and the roof (or ground if positioned horizontally). The exact position of the sun varies seasonally relative to the horizon, so in winter an inclination angle of minimum  $20^\circ$  and in summer  $45^\circ$  is essential to maximise solar performance (Figure 9). A  $0^\circ$  tilt angle, meaning the face of the collector is aimed directly overhead, has the advantage of leaving the azimuth angle redundant, therefore making the solar collector easier to install. (Elminir et al., 2006) ran a study in 2006 highlighting the year-round benefits of positioning a solar collector flat.

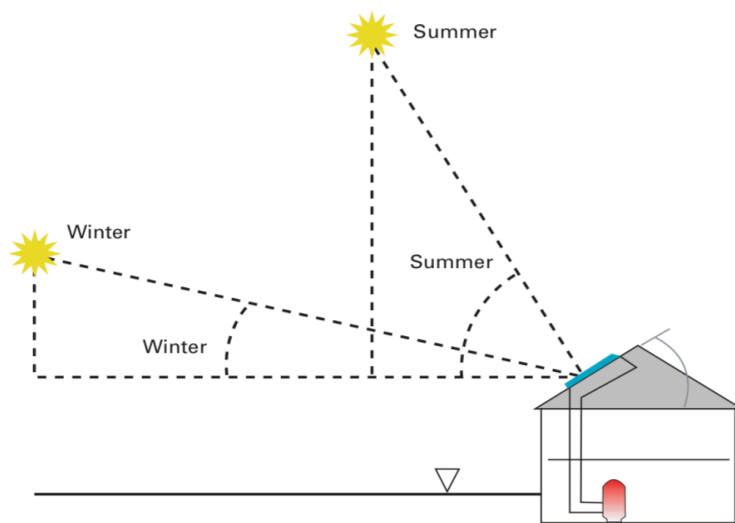


Figure 9 - Optimum Tilt Angle

Some solar panels used for heating concentrate radiation and some do not. For low to medium temperature requirements, panels do not and for high heating requirements solar panels do. Hot water heating comes under low temperature technology and technologies heating up water tend not to be solar concentrating.

### 3.2 Collector Materials

Materials selected for design need to meet major design objectives: high temperature stability, low cost, weatherability and durability. An important design aspect of a surface used for exchanging heat is selecting an appropriate material in order to transfer heat efficiently and quickly.

Copper is generally chosen for collector surface as it is an excellent conductor of heat as it has a high thermal conductivity (Amrutkar et al., 2012) (Hirasawa et al., 2013). Copper also has high corrosion resistance, high maximum allowable stress and pressure and high specific heat (Table 3). It also has cost benefits due to ease of joining and ease of fabrication.

For basic surface enhancement of the absorber, a layer of black “paint” is applied to the top surface. This “paint” can be made of a range of materials although Titanium Dioxide is a popular choice (X. Chen, Liu, Yu, & Mao, 2011). Although Titanium is an expensive metal, it is applied in such a small amount this doesn’t affect collector price significantly (X. Chen et al., 2011)

Insulation of the collector can be done in a number of ways. Vacuum sealing the collector has been reported to work well in reducing thermal losses (Joseph et al., 2005). The problem with vacuum sealing in the lifetime of a collector, is that air can make its way in through very small ruptures in the sealing and completely remove insulation properties. Glass wool is a cheap and abundant insulation material. With thermal conductivities of 0.04W/mK, it has excellent heat containing properties (Sengar, 2004)

### 3.3 Thermal Expansion

The major areas where thermal stresses affect an FPC is where the absorber joins the frame. The stresses are increased further if the absorber and headers are only connected at each end of the solar collector. This is due to the fact large temperature differences between the frame and absorber can cause differential thermal expansion of the absorber and the frame. (Russell, 2015). This problem can be solved by using expansion joints or slots in the enclosure frame to allow relative motion between the frame and the header connectors. Although, this option will add to an increased complexity with design. A simpler answer to this problem is presented by ensuring the frame and absorber/headers are made from materials with the same CLTE numbers.

If materials that are connected within the solar collector have significantly different coefficients of linear thermal expansion (CLTE), large thermal stresses occur through the changing of temperature. Therefore, the manifold, connecting absorber and connector pieces in a flat plate collector all must be of the same CLTE, or very similar. The back cover, top cover and Frame all have the same CTLE as the manifold, absorber and connector (Firebird, 2011).

However, using a flooded absorber, mean that the two plates can be left relatively freely inside the casing of the collector. Using sheet material has the added benefit of being very easy to stabilise inside a case, meaning that joins in the manifold can be loose. This means CTLE's can be of relative difference, giving the possibility of a cheaper casing material.

### 3.4 Stagnation Temperature

Another potential problem that could be detrimental to a solar collector is stagnation temperature of the absorber surface. This is the surface temperature when there is no heating medium flowing through the absorber. It is noted in literature that stagnation temperatures of average base design FPCs can reach around 140°C – 150°C in extreme cases (Russell, 2015).

As the FACs design is slightly different to the FPCs design, it is important to ensure the materials employed can withstand higher stagnation temperatures with the change in

absorber design. However, this is generally only a problem when polymers with lower thermal properties are used. The materials selected for design can safely withstand temperatures over 150°C.

In a flooded absorber design, the surface contact area of absorber to water is extremely large due to the fact the whole absorber surface is in contact with the fluid. This means the heat transfer mechanism will be extremely large and temperatures could rise dramatically past 100°C. In the event of a pump failure, if fluid flow rate is lost, water in the absorber could quickly heat up and turn into steam causing a steam explosion. In light of this, it is extremely important to ensure water cannot stagnate inside the absorber plates.

#### 4. FAC Design

The technology being investigated is a FLOODED ABSORBER SOLAR COLLECTOR (FAC). Design of the system is very similar to the design of a FLAT PLATE SOLAR COLLECTOR (FPC) although instead of using copper tubing for heating medium flow in the absorber, two parallel metal sheets will be used separated by a small distance (Figure 10 (3)). An exploded view of the FAC is shown below. Major dimensions have been included.

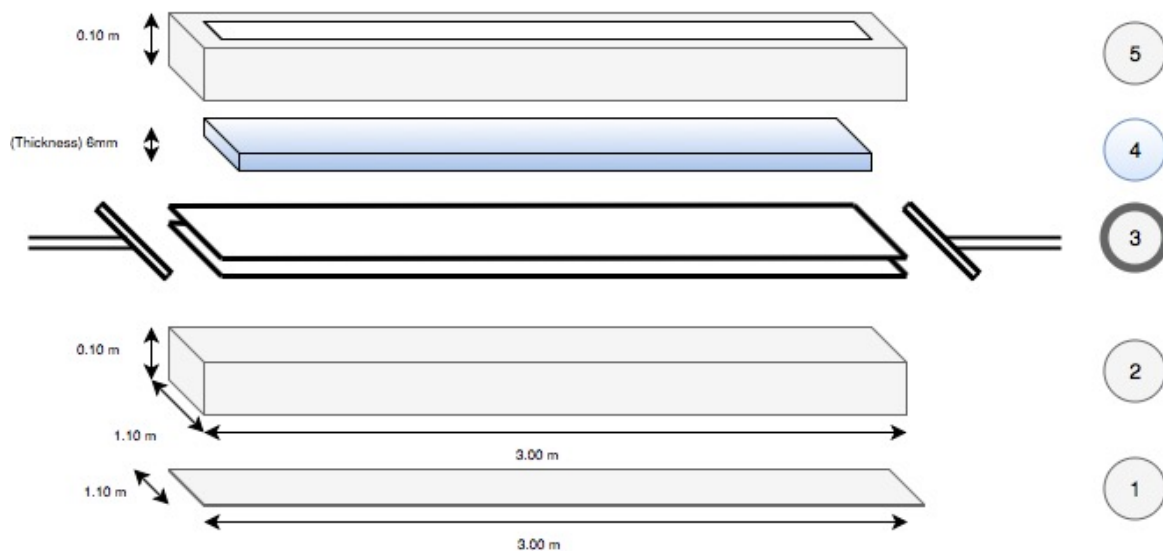


Figure 10 - Exploded view, Flooded Absorber Solar Collector with major dimensions

Numbers from Figure 10:

1. Base plate of exterior Casing
2. Main exterior casing
3. Flooded Absorber with inlet & outlet manifolds
4. Single glazed, clear float glass
5. Upper exterior frame

## 5. Model Description

### 5.1 Introduction

When attempting to assess the performance characteristics of a Flooded Absorber type solar collector, it was important to use a tool that would accurately simulate the outdoor environment that the collector would perform in. ESP-r provides a virtual, natural atmosphere in which almost any climate data can be simulated so was assumed as the ideal software. A general model of a Flooded Absorber type solar collector was created in ESP-r.

### 5.2 Base Model

Due to the fact the design of a Flooded absorber type solar collector has not been attempted, the design of the system was based on a typical Flat Plate solar collector (Kalidasan & Srinivas, 2014). An exploded view of the model can be seen in Figure 10.

The main components of a typical flat plate solar collector are as follows:

- Black surface – incident solar radiation absorption system.
- Glazing cover – prevents radiant and heat losses from absorber surface, while allowing radiation to contact the absorber.
- Manifold – to carry fluid in order to transfer thermal energy from the absorber.
- Support structure – to hold the system together and protect components from the external.
- Insulation – covering sides and lower surfaces to reduce heat losses.

These points were taken into consideration in the design process of the Flooded Absorber solar collector. The initial model incorporates a solar collector of total area 3.318m<sup>2</sup> (each absorber plate is made up of an opaque surface area of 1.106 m<sup>2</sup>) and is at a tilt angle of 0° from horizontal. The Average U value is 7.1W/m<sup>2</sup>K and a UA value of 7.86 W/K per absorber plate.

The system modelled in ESP-r consisted of a simple thermal storage tank and an upstream flooded absorber solar collector (FAC) (Figure 11).

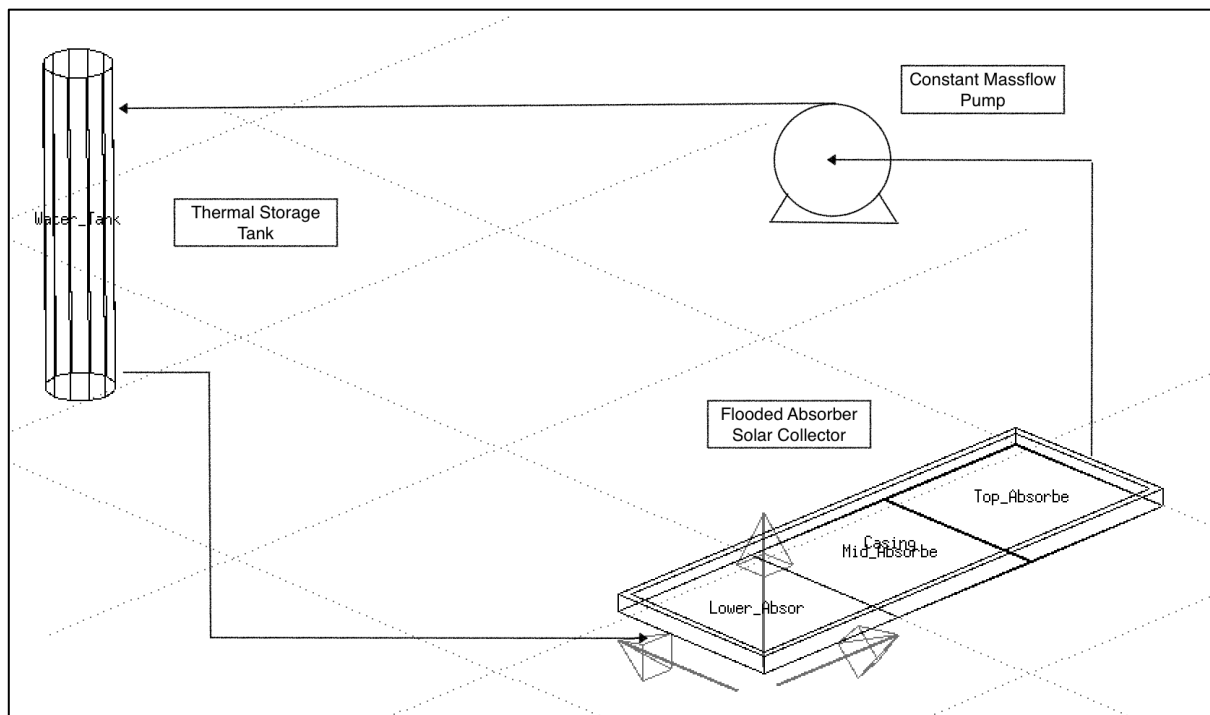


Figure 11 - Full ESP-r model layout

The FAC consists of 4 distinct thermal zones:

- Casing – main protection layer and thermal housing
- Lower Absorber – initial flow solar thermal plate
- Mid Absorber – mid flow solar thermal plate
- Upper Absorber – Upper flow solar thermal plate

The thermal tank is positioned roughly 2m away from the system to ensure shading doesn't cause a loss in efficiency to the solar collector. Also, due to the storage tanks sole purpose to

store energy, only one thermal zone was needed. To ensure contact flowrate, a pump is connected up stream between the upper section of the FAC and water tank.

Within the base design of the model, 4 main materials for construction were used:

- Opaque construction: insul\_frame
- Opaque construction: collector\_pl
- Opaque construction: tank\_i\_35mmi
- Transparent construction: single\_glaz

### 5.3 Surface Attributes

In order to create the correct surface attribution, the material database had to be updated. The main factors implemented in to the software was composition, opacity, boundary conditions and use.

#### 5.3.1 Insulation

Material “insul\_frame” was created to be used as a base insulation layer. The layer is composed of two thin layers of grey coated aluminium as the internal and external layers, with a thicker layer of non-hygroscopic glass fibre quilt with low thermal conductivity in between. Table 2 below gives a description of the “insul\_frame” material:

Table 2 - Base model insulation

Construction	Layer	Description	Thickness	Conductivity	Density	Specific Heat	Emmissivity	Absorptivity	R
			(mm)	(W/mK)	(kg/m <sup>3</sup> )	(J/kgK)			(m <sup>2</sup> K/W)
insul_frame	External	Grey Coated Aliminium	4	210	2700	880	0.82	0.72	0
	2	Glass Fibre Quilt	80	0.04	12	840	0.9	0.65	2
	Internal	Grey Coated Aliminium	4	210	2700	880	0.82	0.72	0

### 5.3.2 Absorption

Material “collector\_pl” was created to be used as the base primary absorption material. Previous research, detailed in the literature review has shown that black coated copper has the highest thermal capabilities of absorption materials (Karim et al., 2012; Madhukeshwara & Prakash, 2012; Pandey & Chaurasiya, 2016). Black coated Copper was used on each upper face of the absorption plates and also on the internal walls connecting each absorption plate zone. Table 3 below gives a description of the “collector\_pl” material:

Table 3 - Base model absorber material

Construction	Layer	Description	Thickness	Conductivity	Density	Specific Heat	Emmissivity	Absorptivity	R
			(mm)	(W/mK)	(kg/m <sup>3</sup> )	(J/kgK)			(m <sup>2</sup> K/W)
collector_pl	1	Black coated Copper	3	200	8900	418	0.72	0.85	0

### 5.3.3 Glazing

Material “single\_glaz” was the base material created to be used as the cover that contains the absorber plates inside the casing. As a glazing material it was important that the material created was transparent to ensure solar radiation was able to pass through to contact the absorption plates. The glazing chosen was clear float glass with optics from National method database. Float glass is cheap and widely available. Table 4 below gibes a description of the “single\_glaz” material:

Table 4 - Base model glazing

Construction	Layer	Description	Thickness	Conductivity	Density	Specific	Emmissivity	Absorptivity	R
			(mm)	(W/mK)	(kg/m <sup>3</sup> )	(J/kgK)			(m <sup>2</sup> K/W)
single_glaz	1	Clear Float Glass	6	1.05	2500	750	0.83	0.05	0.01

### 5.3.4 Thermal Storage

The material used for the construction of the water tank consisted of a three-layer insulation mechanism. The exterior layer of insulation consisted of a 3mm thick section of white painted steel. The colour white reflects cold convective energy at night time when the temperature

falls. A 3mm layer of copper coats the inside of the tank, the shiny finish helping reflect thermal energy. A layer of Urea-Formaldehyde foam of thickness 35mm is the main heat containment layer, situated in between these metals. The low thermal conductivity of UF foam (0.03W/mK) ensures minimal heat is lost from the water. Table 5 gives the construction attributes:

Table 5 - Base model tank insulation

Construction	Layer	Description	Thickness	Conductivity	Density	Specific Heat	Emmissivity	Absorptivity	R
			(mm)	(W/mK)	(kg/m <sup>3</sup> )	(J/kgK)			(m <sup>2</sup> K/W)
Tank_i_35mmi	External	White painted steel	3	40	7800	502	0.82	0.3	0
	2	UF - foam	35	0.03	30	1764	0.9	0.5	1.17
	Internal	Copper	3	200	8900	418	0.72	0.65	0

## 5.4 Thermal Zones

The model is made up of 4 main zones. Each zone, or thermal zone, is implemented with geometry, construction and operational details prior to simulation. The model created for the simulation of a FAC was made up of 4 zones:

- Casing
- Lower Absorber
- Mid Absorber
- Upper Absorber

Table 6 - Thermal zones

Zone	Fluid	Dimensions (mm)		
		Length	Width	Height
Casing	Air	3000	1100	100
Lower Absorber	Water	1000	1100	2
Mid Absorber	Water	1000	1100	2
Upper Absorber	Water	1000	1100	2

### 5.4.1 Casing

The Casing of the collector was made up of 9 main surfaces. These were the 4 walls encasing the inner absorber, the glazing and the parent upper frame and the 3 lower insulation plates for the bottom of the collector. The dimensions of the casing were based off that of a typical FPC. Table 7 below shows the various surfaces that make up the Casing zone along with dimensions:

Table 7 - Casing zone construction

Zone	Surface	Description	Material
<b>Casing</b>	Wall_C_East	External East facing wall	insul_frame
	Wall_C_North	External North facing wall	insul_frame
	Wall_C_West	External West facing wall	insul_frame
	Wall_C_South	External South facing wall	insul_frame
	Glazing	Transparent glazing cover	single_glaz
	Upper_Frame	Parent of glazing cover	insul_frame
	Lower_Plate	Lower absorber insulation plate	insul_frame
	Mid_Plate	Mid absorber insulation plate	insul_frame
	Top_Plate	Upper absorber insulation plate	insul_frame

#### 5.4.2 Absorber Plates

The model was also made up of an inner solar absorption system. This absorption system was split into three main zones, a lower absorber, a mid absorber and an upper absorber. The reason for creating 3 zones is that each zone within ESP-r accounts for one thermal environment. This means that it is associated with one temperature. From previous research (Soteris A. Kalogirou, 2004; Michaelides & Eleftheriou, 2011; Sengar, 2004) it is proven that thermal stratification occurs through the absorber from inlet to outlet. In simple terms, the longer time that the water is inside the collector, the more solar flux it is exposed too, creating a temperature increase along the length of the collector. In order for the ESP-r to simulate this, 3 zones were created to create the effect of the temperature increase flowing along the absorption plates.

Each absorber plate was situated above the lower insulation plates and below the collector glazing. Table 8 below gives a description of the various surfaces and material used in the

absorber plates (due to the fact 3 absorber plates are designed the same way, only Lower\_Absor is shown)

Table 8 - Absorber plate construction

Zone	Surface	Description	Material
Lower Absorber	Wall_L_East	East facing sidewall	insul_frame
	Wall_L_North	Mid absorber connection	collector_pl
	Wall_L_West	West facing sidewall	insul_frame
	Wall_L_South	South facing sidewall	insul_frame
	Top_L_Absorb	Radiation absorbing surface	collector_pl
	Base_L_Absorb	Absorber base	insul_frame

### 5.4.3 Environment

Each surface related to each zone in the model needs to be linked to the correct simulation environment in order to properly perform. In this case most of the surfaces created are inputted to be in boundary with exterior environment. However, various surfaces in the absorption system are thermodynamically linked. These surfaces are primarily between the absorption plates, in line with fluid flow.

### 5.5 Network Flow

ESP-r simulates one dimensional fluid flow within the model zones. This involves the calculation of fluid flow through branches and nodes in a network which represents the collector network. The nodes and branches define boundary pressure points, internal node characteristics and flow restrictions. ESP-r uses an iterative mass balance approach in which nodal pressures are adjusted until the mass residual of internal nodes satisfies some criterion.

The main features of a flow network are Nodes and Components. Nodes can either be internal or boundary conditions. Internal nodes represent either water or air and have specific data relating to thermophysical properties. Boundary nodes use an azimuth angle to derive the angular dependant pressure, from the pressure coefficient database and the wind speed and

direction at a certain point in time within the simulation. Additional internal nodes can be implemented to give control e.g. an extra node in order to connect a component in series. Components are related to the flow regime, for example a pump.

Within the design of the FAC, there are two flow networks relating to water and air.

### 5.5.1 Water Network

The water network is the main flow network within the ESP-r model. It simulates the water flowing through the absorber plates and is the main focus of investigation.

#### 5.5.1.1 Nodes

In the model created there are three main nodes situated in each of the absorber plates (Lower, mid and top absorber plates). This is so the change in temperature can be accurately measured as the water passes through the collector. The temperature associated with each node is the temperature assumed at the start of the simulation. As these internal nodes are part of the thermal model, the temperature is updated with calculated values as the simulation progresses. Having three zones accurately models the increase in temperature. If there was just one zone there would be no temperature change through the absorber as zones are associated with just one temperature only. To increase the accuracy of the simulation, more zones could be created in order to have a smoother increase in temperature as the water flows from zone to zone. For this simulation, however, 3 zones were deemed satisfactory.

Each node also has a height attribute above some arbitrary datum which is used to support buoyancy calculations. Due to the collector angle tilt being  $0^\circ$ , each node is at 0.001m (middle of the absorber plate, where water flows).

#### 5.5.1.2 Components

Within the water network there are two main components:

- Absorber Pump (Abs\_Pump)

- Nodal Linkage (Abs\_Link)

The pump is implemented as a constant mass flowrate inducer and follows the simple mass flowrate equation:

$$m = A$$

Where:

- $A = x - \text{sectional area (m}^2\text{)}$

The nodal linkage is simply used to connect nodes within the absorber and to the pump. Abs\_link is a general flow conduit (pipe) which accounts for frictional and dynamic losses assuming the following: no pressure gain from a pump, a uniform cross-section and steady state conditions. The mass flowrate equation takes the form:

$$m = \rho * f(D, A, L, SCi)$$

Where:

- $\rho = \text{density } \left(\frac{\text{kg}}{\text{m}^3}\right)$
- $D = \text{diameter (m)}$
- $A = x - \text{sectional area (m}^2\text{)}$
- $L = \text{length (m)}$
- $SCi = \text{sum of local dynamic loss factors (n/a)}$

### 5.5.2 Air Network

The airflow network is primarily included to induce external losses due to wind effects. If there was no air flow to the system, the simulation would be largely redundant as would not accurately model the outdoor environment.

#### 5.5.2.1 Nodes

The air network consists of only 2 nodes, an internal node and a boundary node. The internal node represents the casing thermal zone (casing, glazing, under panels), while the boundary node represents the wind pressure. The pressure of the node is generated by wind impinging upon a surface. The pressure is a function of wind velocity, wind direction and pressure coefficient ( $C_p$  – assigned based on the orientation and geometry of the surface). In the FAC model, the pressure coefficient is set to that of a semi exposed wall.

#### 5.5.2.2 Components

The only component related to the air flow network is the Frame Crack. This emulates the fact that the collector is not 100% air tight. The simple mass flowrate equation is as follows:

$$m = \rho * f(W, L, dP)$$

Where:

- $\rho = \text{density} \left( \frac{kg}{m^3} \right)$
- $W = \text{width} (m)$
- $dP = \text{pressure difference} (Pa)$

When inputting the Length of the airflow crack, a length roughly the perimeter of the collector casing was chosen to consider the fact there could be leakages all the way around the model.

#### 5.5.3 Control System

In order to ensure energy was not wasted when external temperatures cooled through the simulation period, a control system was implemented. The simple, direct control system is connected to thermal storage tank and the upper absorption plate. When the temperature of the absorber plate surface rises greater than 3°C compared to the water tank, the pumped connected between the upper absorber and water tank is actuated. When the temperature of the absorber plate falls within 3°C, the pump is turned off and the storage tank holds the heated water. The idea behind this control system is to ensure when the collector area starts

to cool, the water flow is stopped, storing the captured thermal energy. The control system is described in Figure 12, through an arbitrary 3 day period in June.

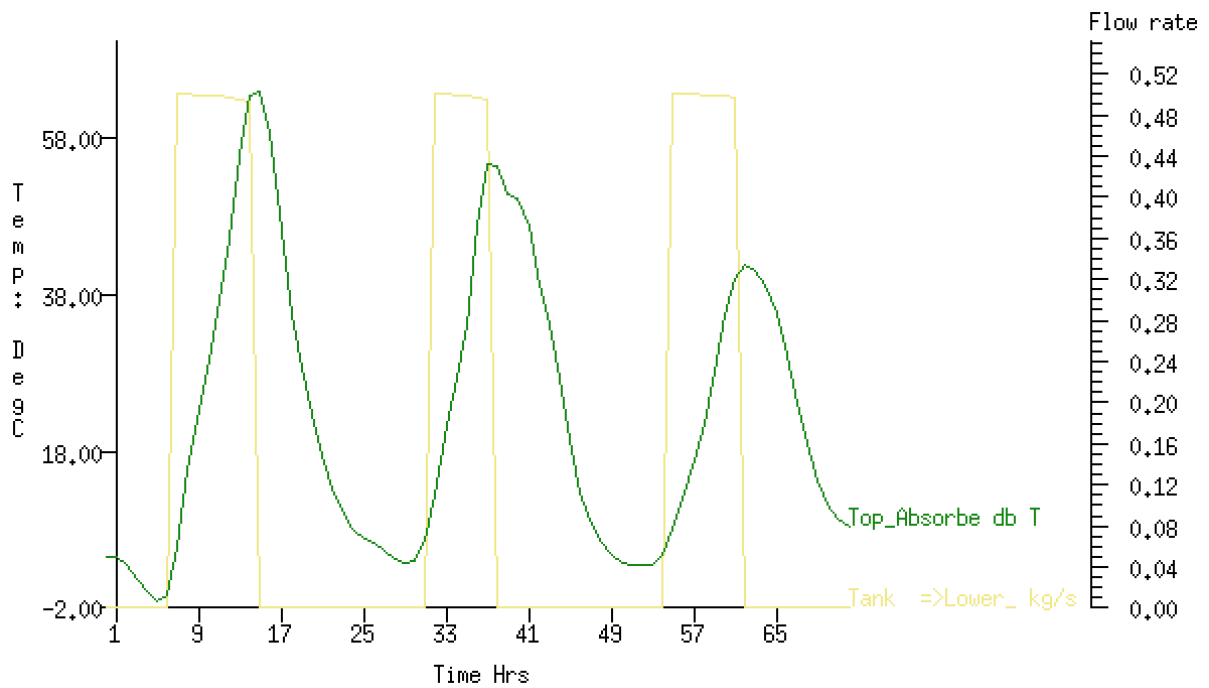


Figure 12 - Control action of collector – tank pump

The green line shows the absorber temperature rising and falling relating to the day and night time. The yellow line shows the flowrate of the water tank to the absorber system. The flowrate from the pump can be observed to reach 0.5kg/s intermittently, in relation to the increase and decrease in absorber temperature.

#### 5.5.4 Connections

The below table shows the layout of each node and connection type. Connection a,b,c and f are all part of the flow network, while d and e represent the air flow network.

Table 9 - ESP-r model connections

Node +ve	IdHght tol	Node -ve	IdHght via	Component
a Lower_Absor	0.0	--> Mid_Absorbe	0.0	Abs_Link
b Mid_Absorbe	0.0	--> Top_Absorbe	0.0	Abs_Link
c Top_Absorbe	0.0	--> Water_Tank	0.0	Pump
d Casing	-0.0	--> Wind_Adj	0.0	Frame_crack
e Wind_Adj	0.0	--> Casing	-0.0	Frame_crack
f Water_Tank	-0.5	--> Lower_Absor	0.5	Abs_Link

## 6. Results and Discussion

### 6.1 Climate

#### 6.1.1 Seasonal Performance

Glasgow was chosen as the Scottish test location and the climate file was inputted into ESP-r. Initially, it was hypothesised that the thermal collector would not perform very well unless in temperate climates. Although, after assessing performance, it was concluded that the FAC could perform well for low temperature application in Scottish climates.

Below are graphical representations of ambient temperature and water temperature against a 5-day period through 4 different seasons in Glasgow. The horizontal red and blue dashed lines across figures 13 – 16 represent the upper and lower bound of water temperatures suitable for low temperature application, as recommended by (Sö zen & Menlik, 2008). A start up period of 3 days was issued to normalise the initial water tank temperature. The time period picked for each season are as follows:

- Winter: Jan 23<sup>rd</sup> – Jan 28<sup>th</sup>
- Spring: Apr 15<sup>th</sup> – Apr 20<sup>th</sup>
- Summer: Jun 8<sup>th</sup> – Jun 13<sup>th</sup>
- Autumn: Oct 2<sup>nd</sup> – Oct 7<sup>th</sup>

Periods were picked that show large variations in temperature to ensure the month was best described by the days simulated. It is then assumed if the model can perform well in the simulation period, it can perform well in the month/season.

Winter

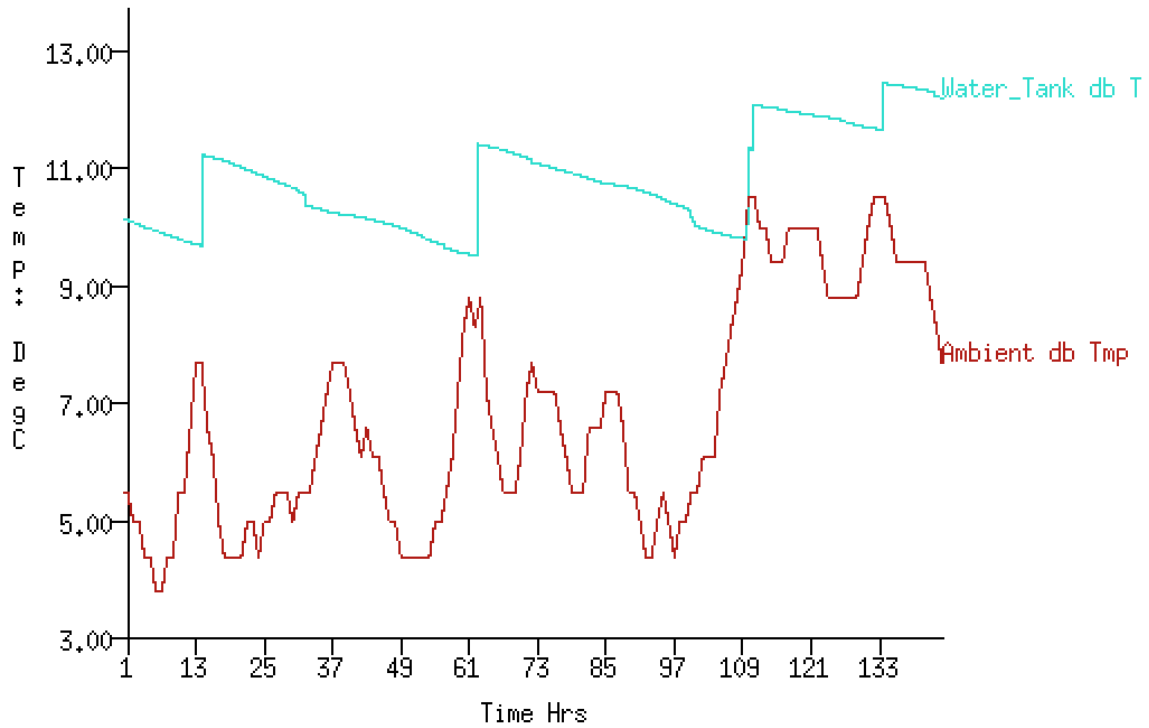


Figure 13 - Arbitrary 5-day period in Winter (Glasgow)

Spring

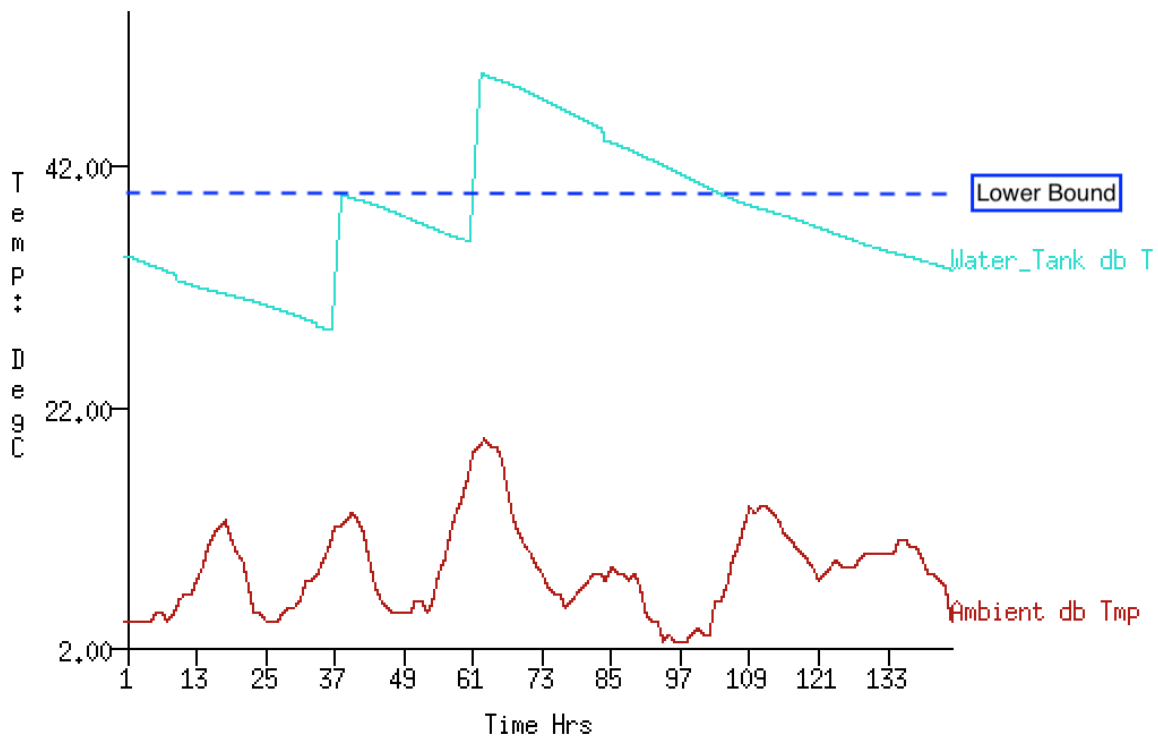


Figure 14 - Arbitrary 5-day period in Spring (Glasgow)

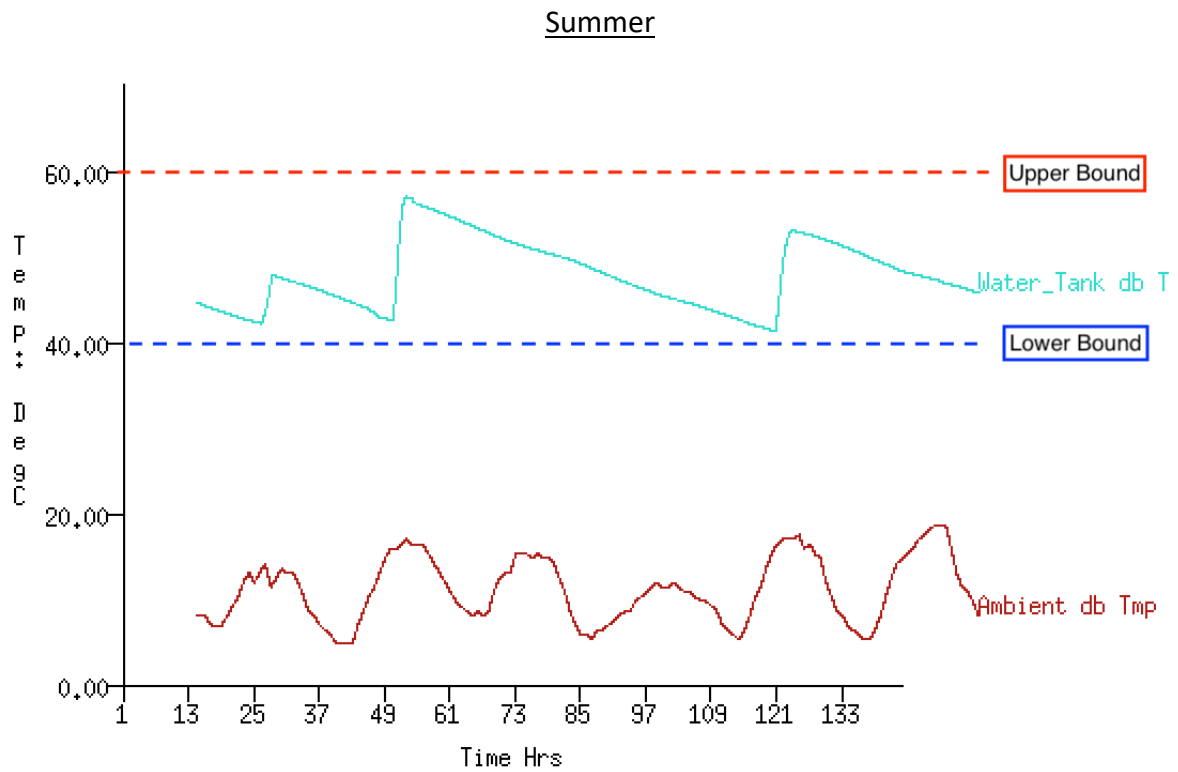


Figure 15 - Arbitrary 5-day period in Summer (Glasgow)

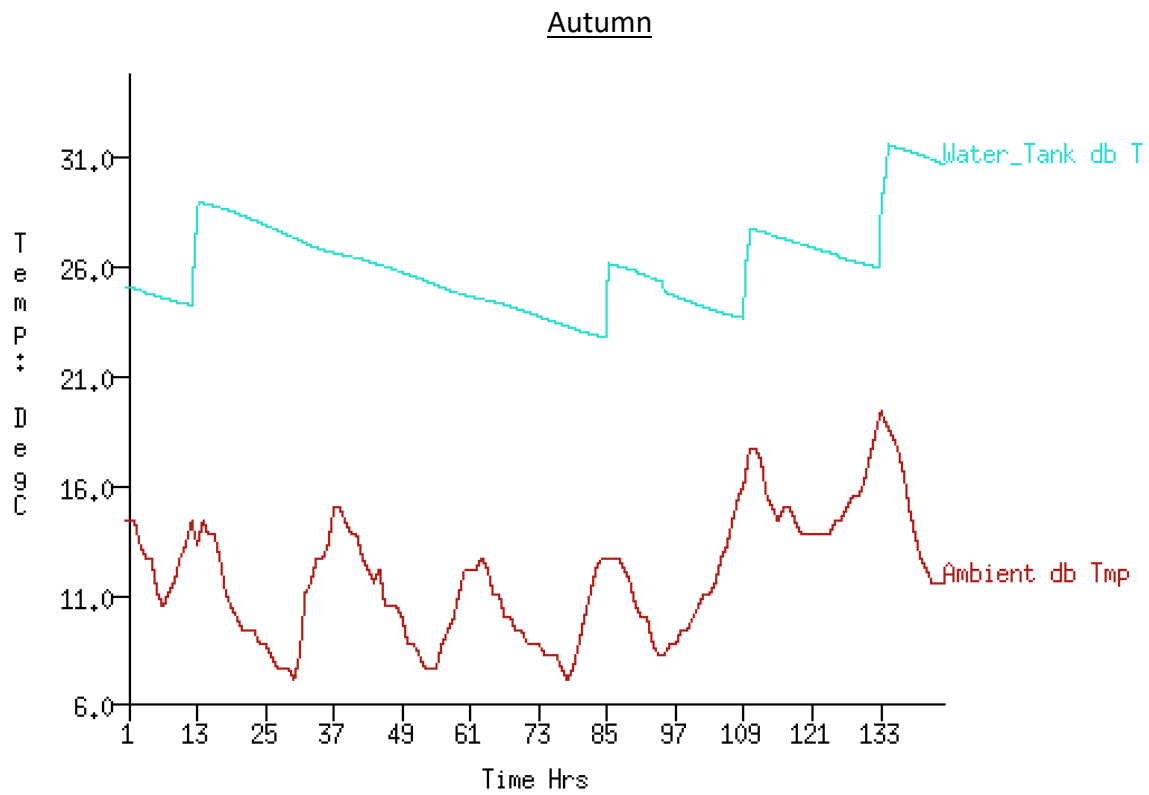


Figure 16 - Arbitrary 5 day period in Autumn (Glasgow)

It can be deduced from Figure 13 and 16 that the FAC is unsuitable for use in Winter and Autumn in Glasgow based on initial design. The maximum temperature gained in winter does not surpass 13°C as ambient temperatures are sub 10°C. In Autumn (Figure 16), although water tank temperature gain is higher, it is still not high enough to reach the low temperature application boundary.

In the Spring time period the water temperature reaches the lower bound of acceptable water temperature, although cannot sustain the temperatures long enough to be classed as suitable for low temperature application.

However, in the Spring, the ambient temperatures range from 2°C to 20°C which is averagely less than that of the Autumn water temperatures (7°C – 19°C). In the spring the temperatures can be maintained in the plates and therefore heat the water better than in Autumn. This is due to the fact the convective radiation provided by the sun in Autumn is of lower strength than in Spring due to the position of the sun. The total convection absorbed by the glazing in Autumn obtains a maximum at just over 40W while in Spring the total convection absorbed surpasses 60W (This is illustrated in Appendix: A, Figure 32 and 34). This also proves the fact that the temperature of the water achieved does not solely depend on the ambient temperature.

The Summer month the water temperature achieved by the FAC fits the low temperature application boundaries of 40°C – 60°C. This is the result of careful design procedure followed from many research papers. The max water temperature obtained is 56°C and minimum temperature obtained 41°C. These temperatures are achieved with large amount of shortwave radiation from the sun, alongside higher ambient temperatures.

As a result of this analysis, it was concluded that the FAC in Scottish climates, without drastic design changes, would be suitable for application in the summer months. The following results section focuses on the performance of the FAC and if any improvements could be made.

## 6.2 Modifications to Base Model

The base case design of the FAC was based off of various papers, detailing the design considerations for the FPC due to the fact there are no previous designs of a FAC. Therefore, the design may have features which could be improved upon. In this section, various aspects of the FAC will be altered and simulated in ESP-r to find the design with best thermal performance. The aspects that will be focused on include:

- Absorber plate spacing
- Glazing
- Pump flowrate
- Thermal tank size
- Insulation

## 6.3 Design Objective

The main design objectives are as follows:

- For low temperature application, water is required at 60°C with a minimum of 40°C (Sö zen & Menlik, 2008). Therefore, the design must average a water temperature of 50°C, to ensure hot water is accessible. The optimal design shall provide water no hotter than 60°C and no colder than 40°C.
- A large factor that hinders the production of the FPC is design complexity. Simplicity of design is of high priority and where possible will be simplified.

## 6.4 Base Model

### 6.4.1 Temperature Distribution

The temperature distribution across the flooded absorber is important for efficiency as uneven temperature distribution can result in lower water temperature gain. As previously mentioned, this is a real problem experienced by the conventional parallel tube FPC. Below is a graph of lower, mid and upper absorber plates:

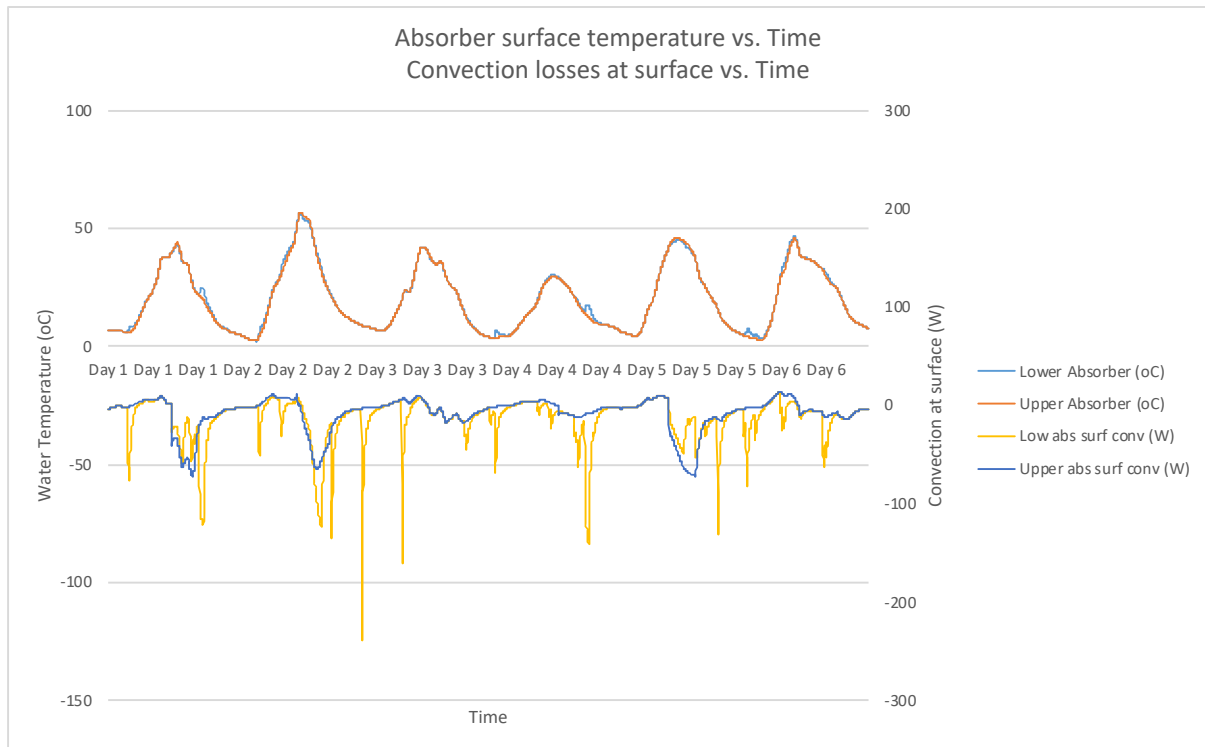


Figure 17 - Temperature distribution across absorber plate with varying surface convection

The lower and upper absorber surface temperature, in the positive sector of Figure 17 follows similar paths. The convective heat losses can be seen to deviate from lower absorber plate to upper absorber plate. The distribution of heat along the collector from lower to upper absorber is at a constant, increasing heat transfer efficiency as energy is not expended traveling to areas in the plate where water is present. Also, as the water is in contact with the whole absorber face, instead of just parallel pipes, the plates heat up evenly meaning heat spots do not occur increasing convective losses.

This is a problem that is found with the parallel tube configuration of FPC designs, although not with the FAC design.

#### 6.4.2 Stagnation Temperature

The stagnation temperature is the temperature of the absorber system when there is no thermal fluid present in the collector area. The simulation obtains these results by disconnecting the flow network and disconnecting the control scheme from the simulation.

Below are the results of the absorber temperatures obtained. Due to the fact each absorber surface experienced the same heat flux, only the mid absorber temperature is shown:

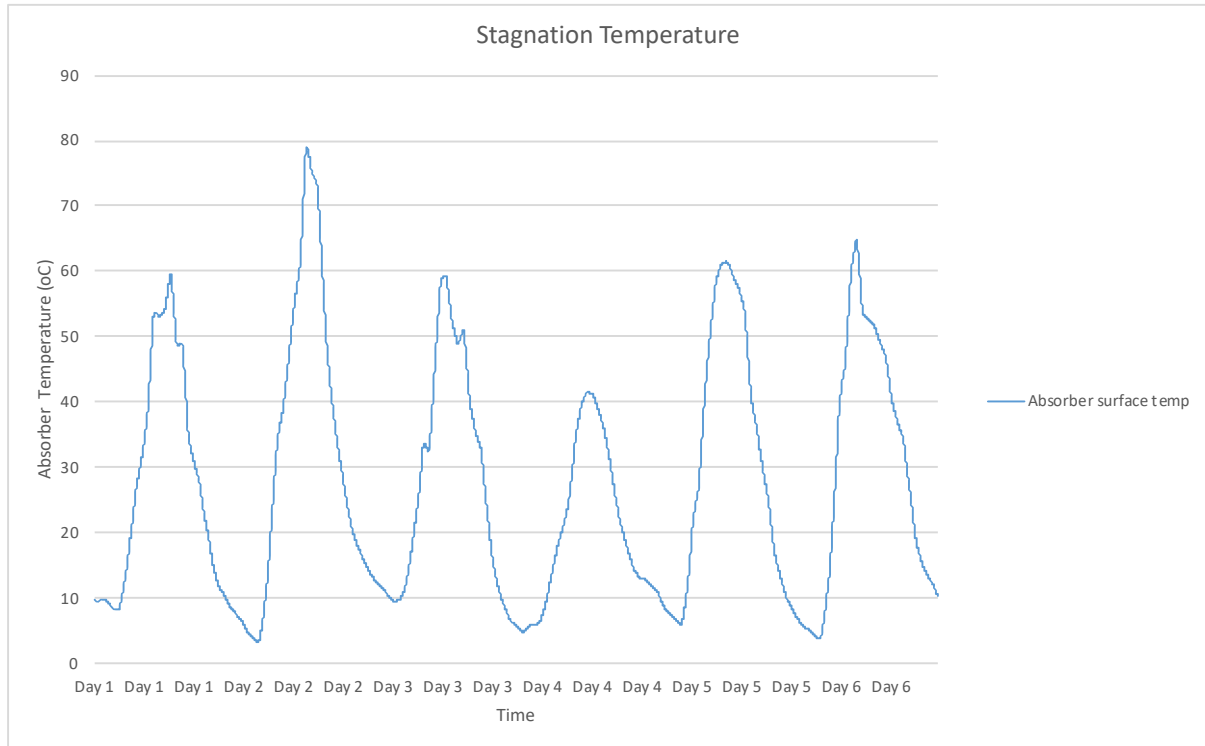


Figure 18 - Stagnation temperature of mid absorber

Stagnation temperatures of the FAC hit a maximum at day 2 of the simulation. However, the maximum temperature achieved is below 80°C which is well below acceptable temperatures for Copper. The surface of the absorber does not heat up to temperatures that would be detrimental to the system, therefore pump failure would not be an issue with the FAC.

## 6.5 Modifications to Base Model

### 6.5.1 Flowrate and Tank Size

To understand the effect that flowrate had on the temperature gain of the water tank, three different sizes of water were simulated with 5 increasing flowrates, individually. Tank sizes of 0.152m<sup>3</sup> (152L), 0.206m<sup>3</sup> (206L) and 0.369m<sup>3</sup> (369L) were assessed. Flowrates of water provided by the constant mass flowrate pump were provided ranging from 0.01kg/s to 1.5kg/s. The results are plotted on Figure 19 – 21.

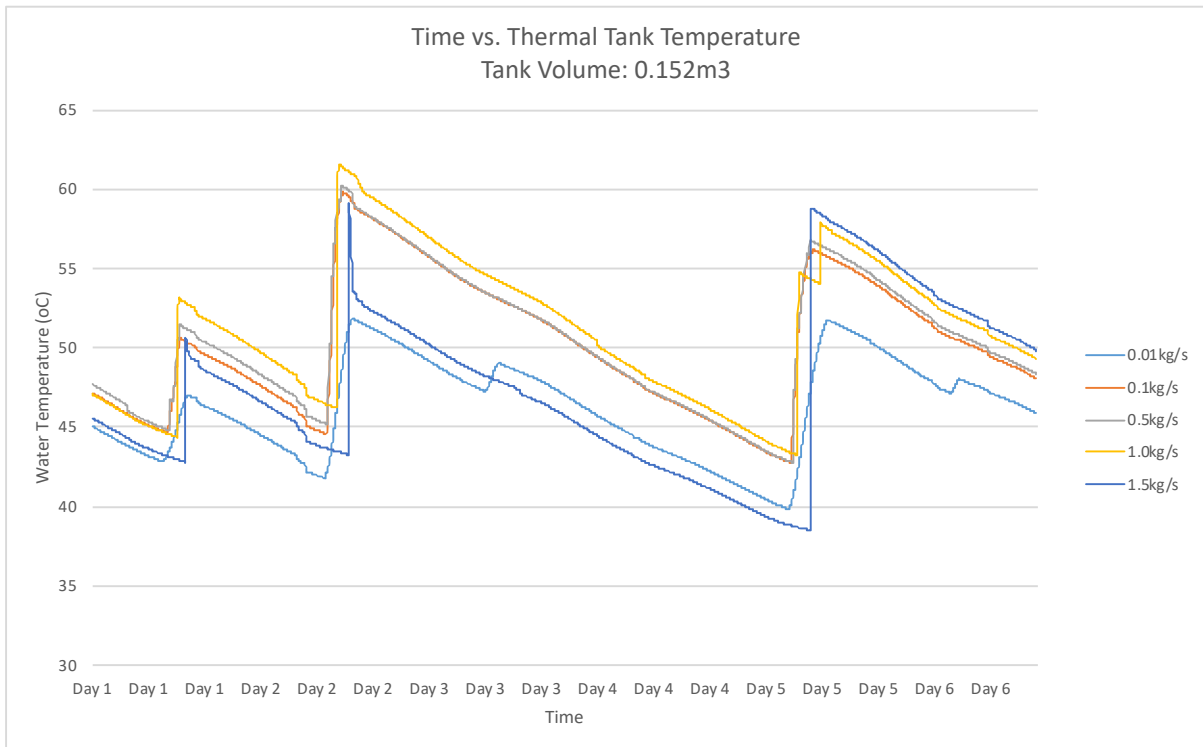


Figure 19 - Water temperature gain for various flowrates (152L)

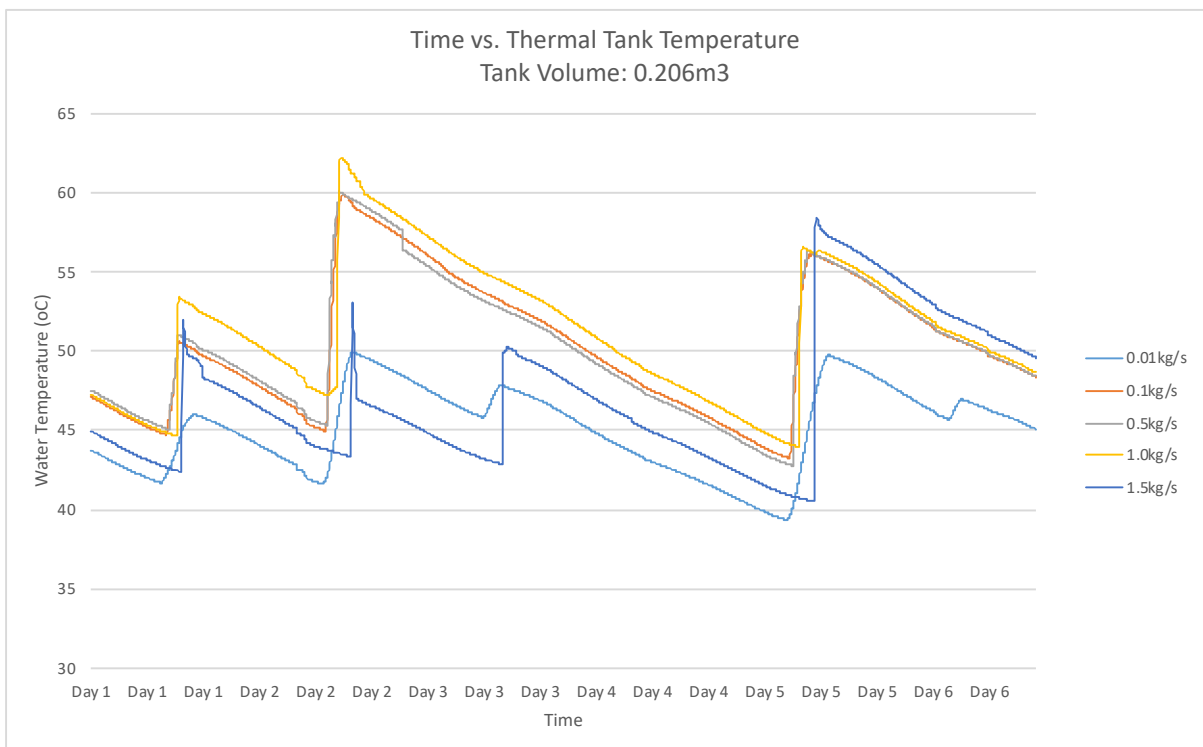


Figure 20 - Water temperature gain for various flowrates (206L)

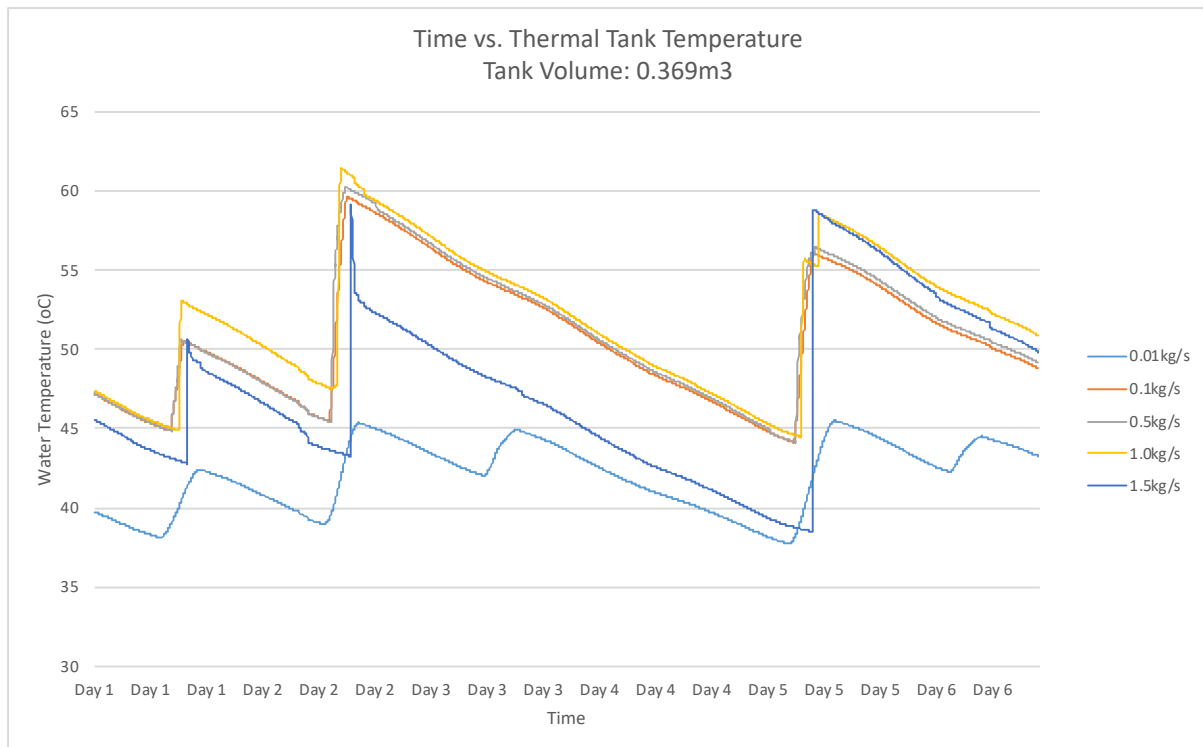


Figure 21 - Water temperature gain for various flowrates (369L)

The initial findings show that the flowrate that achieves maximum temperature for any size of water tank is 1kg/s. 1 kg of water occupies 1 litre and the total volume of the combined absorber plates is 0.066L (2mm spacing). This means that 1L passes through the 3m length of absorber plate each second. This is an indicator of the high thermal efficiency of the transfer of heat due to the entire face being in contact with the water at all times.

For each tank volume, it is observed that 1.5kg/s is too high a flowrate to be classed as a satisfactory. The temperature achieved (dark blue data series) quickly increases but then falls again soon after, dramatically reducing the water tank temperature. This is due to the fact the pump cannot react quick enough to the control system in place (at 30ts/h – control updates every 2 minutes). The temperature also does not stabilise much above 50°C for any run with 1.5kg/s flowrate. This is due to the fact water passes through the absorber system at too fast a rate to heat up significantly. Although the temperature would eventually reach acceptable limits, the solar flux produced by the sun is time dependant.

A similar but opposite situation results from a flowrate of 0.01kg/s. For increasing tank size, the average temperature can be seen to drop from 46.2°C in the 152l tank to 45.1°C in the 206L tank and then 42.0°C in the large 369L tank. This can be explained due to the increasing amount of water in the tank that the low flowrate needs to heat. As the tank size increases, the heated water begins to have less effect on the bulk temperature. The lower flowrate also means the temperature increase is slower.

In section 2.4.2, according to (DEFRA, 2013), the average household uses 349 litres of water each day in the UK. Therefore, if the system was to be used in a common household, a tank size of 369 litres would provide sufficient hot water coupled to the FAC, with a 20-litre safety margin.

When determining optimum flowrate, a low flowrate is desirable due to less energy being needed by the pumping system. In Figure 21 (369L), for the 5 day period, 0.1kg/s, 0.5kg/s and 1.0kg/s all achieve similar results, however at two events in graph (day 1 & day 5) the temperature can be seen to gain 3-4°C by the 1kg/s. However, all three flowrates stay in the acceptable bounds for low temperature application 40-60°C. Therefore, for a 369L tank size, a 0.1kg/s flowrate is chosen.

The flowrate of 0.1kg/s and the effect on the 369L water tank temperature can be observed in Figure 22. The pump is only activated for short periods of time as the water is heated rapidly through the FAC.

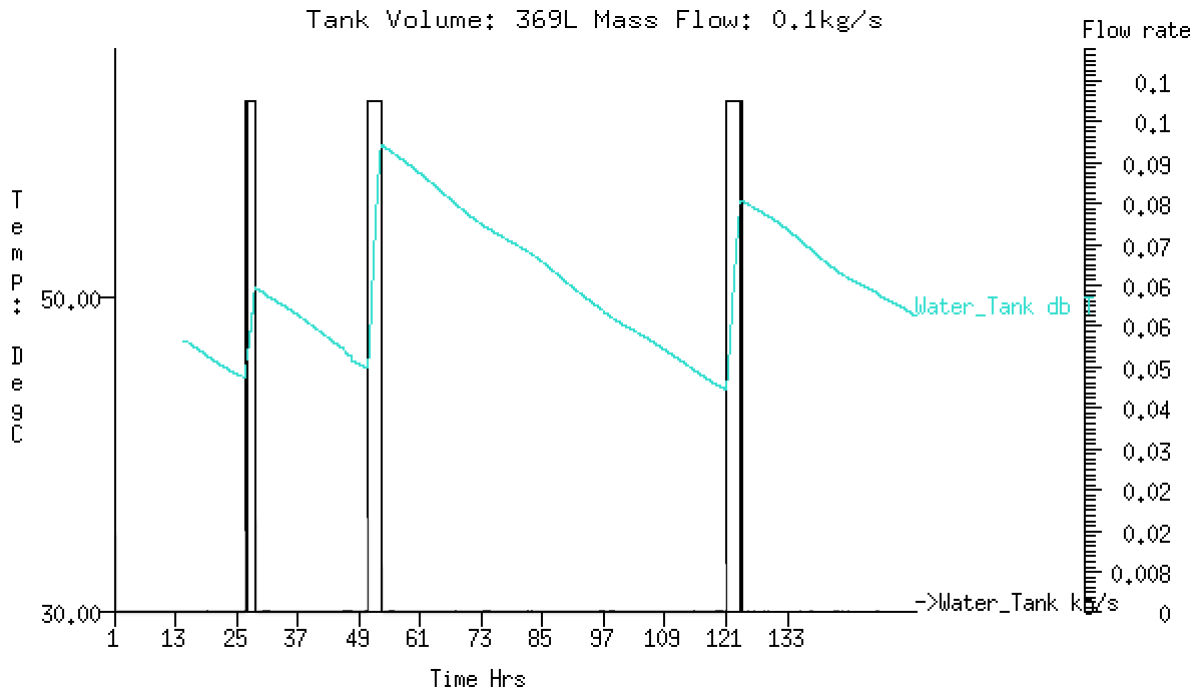


Figure 22 - Mass flow: 0.1kg/s Tank volume: 369L

### 6.5.2 Glazing

The material in the base case model for the glazing cover is detailed in section 6.3.3. A single layer of float glass with continuous R values of 0.17 W/m<sup>2</sup>K is used as the cover.

Research shows (Kalidasan & Srinivas, 2014; Köhl, 2012) that multiple layers of glazing can increase the temperature of the absorber plate. To assess this, a single layer, two layers and three layers of glazing are tested individually. Table 10 below describes the constituent dimensions and materials used in the three simulations. The glass used in the simulation is common float glass. Float glass achieves an emissivity of 0.83, compared to low iron tempered glass with emissivity upwards of 0.9 (Köhl, 2012).

Table 10 - Construction details of glazing materials

Construction	Layer	Description	Thickness	Conductivity	Density	Specific Heat	Emmissivity	Absorptivity	R
			(mm)	(W/mK)	(kg/m <sup>3</sup> )	(J/kgK)			(m <sup>2</sup> K/W)
single_glaz	1	Clear Float Glass	6	1.05	2500	750	0.83	0.05	0.01
dbl_glaz	External	Clear Float Glass	6	1.05	2500	750	0.83	0.05	0.01
	2	Air Gap	12	0	>0	0	0.99	0.99	0.17
	Internal	Clear Float Glass	6	1.05	2500	750	0.83	0.05	0.01
triplglz_1.8	External	Clear Float Glass	6	1.05	2500	750	0.83	0.05	0.01
	2	Air Gap	12	0	>0	0	0.99	0.99	0.17
	3	Clear Float Glass	6	1.05	2500	750	0.83	0.05	0.01
	5	Air Gap	12	0	>0	0	0.99	0.99	0.17
	Internal	Clear Float Glass	6	1.05	2500	750	0.83	0.05	0.01

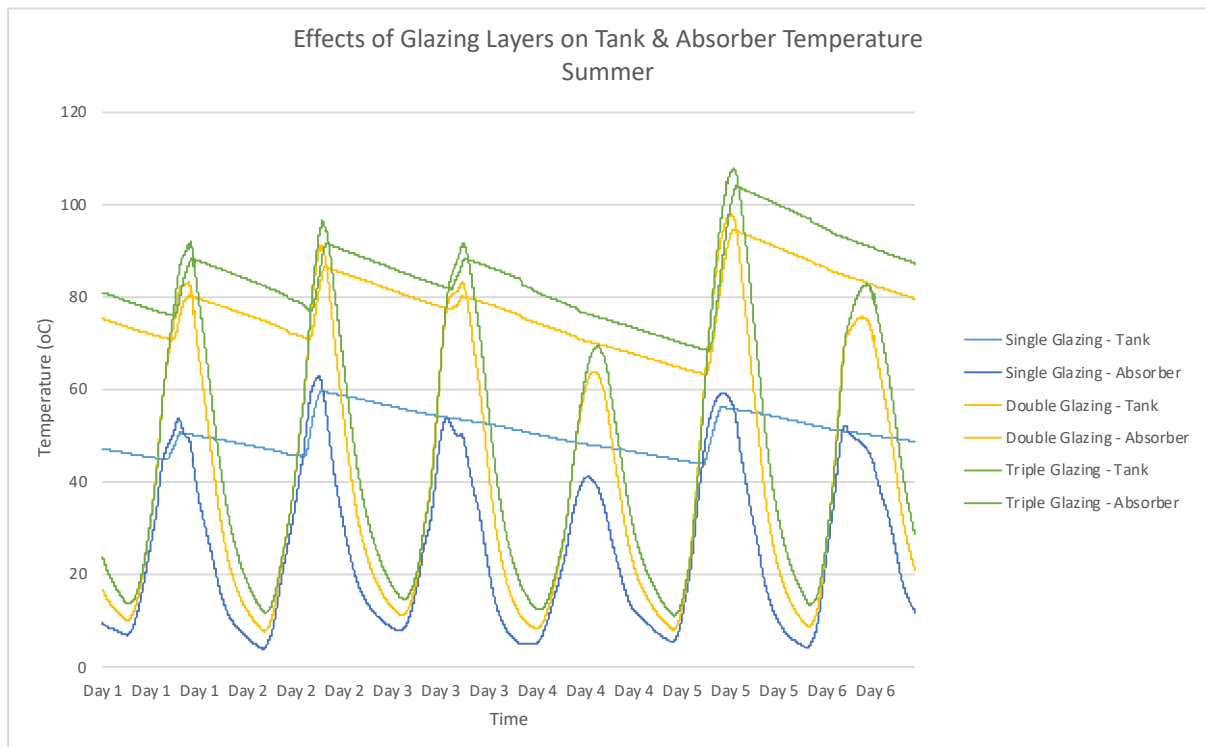


Figure 23 - Effects of Glazing Layers on Tank & Absorber Temperature - Summer

Adding multiple layers of glazing to the solar collector increases the temperature of the water obtained drastically. Adding an extra layer (double glazing) of float glass with a 12mm airgap between increases the average water temperature obtained up to 77.8°C. Adding a third layer (triple glazing) increases the average temperature obtained to 84.3°C.

The peak temperature of the absorber plate is responsible for the water temperature gain. With an added layer of glazing, peak temperatures reach close to 100°C of the absorber. This is due to the fact the air gap in between layers is a poor conductor of heat. Shortwave radiation is allowed to pass through the glazing and then be absorbed by the black coated copper, while the heat that is produced becomes unable to pass back through the glazing. Therefore, energy is contained to a higher extent in the collector.

Due to the fact the FAC design has been aimed at low temperature application, the addition of extra layers of glazing increases the temperature of water above the predetermined maximum of 60°C. Adding extra layers of glazing also means that stagnation temperatures will increase, and this could mean that pump failures become a problem.

---

Interesting results are achieved testing the solar collector through winter months. Below is a graph various layers of glazing and the temperature effects on the water and absorber plates (Figure 24). It can be seen that adding a third layer of glazing actually reduces the temperature of the water obtained. Average temperature for single, double and triple glazing were 7.2°C, 11.8°C and 9.4°C respectively. This drop in temperature with triple glazing is a result of the extra layer blocking out useful shortwave radiation to the absorber. Two layers of glazing are optimal as they let in enough shortwave radiation, while insulating the absorber from the external environment more so than the single layer. This phenomena is backed up by (Kalidasan & Srinivas, 2014) paper on effects of additional layers of glazing.

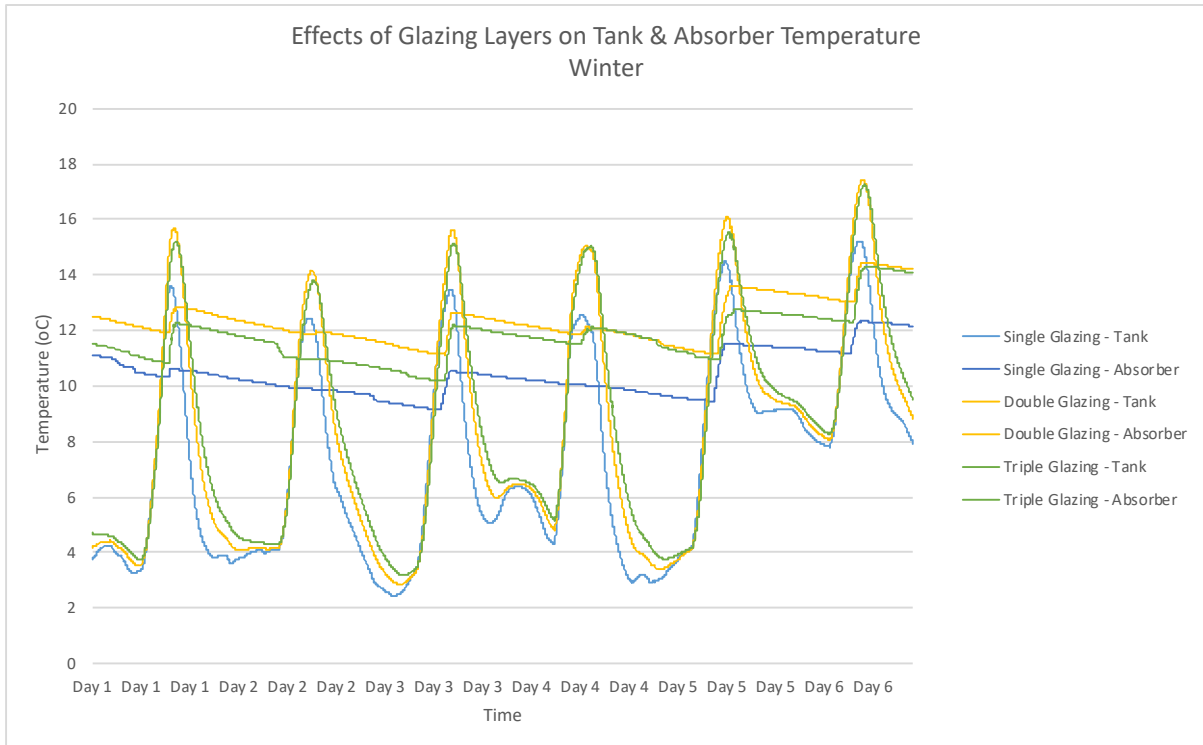


Figure 24 - Effects of Glazing Layers on Tank & Absorber Temperature – Winter

### 6.5.3 Absorber Plate Spacing

The distance between upper and lower absorber plate determines the volume of water that can flow through the collector at any one time. The larger the distance the plates are spaced, the more flowrate than can enter and absorb heat energy. However, the further spaced, the further the heat energy has to travel through to heat the entire load of passing fluid.

The base case absorber plate spacing is 2mm. Typical tubes in FPC have inner diameters of roughly 14mm (Kalidasan & Srinivas, 2014). The effects of plate spacing of 2mm, 4mm, 8mm and 20mm are presented in Figure 25 and 26.

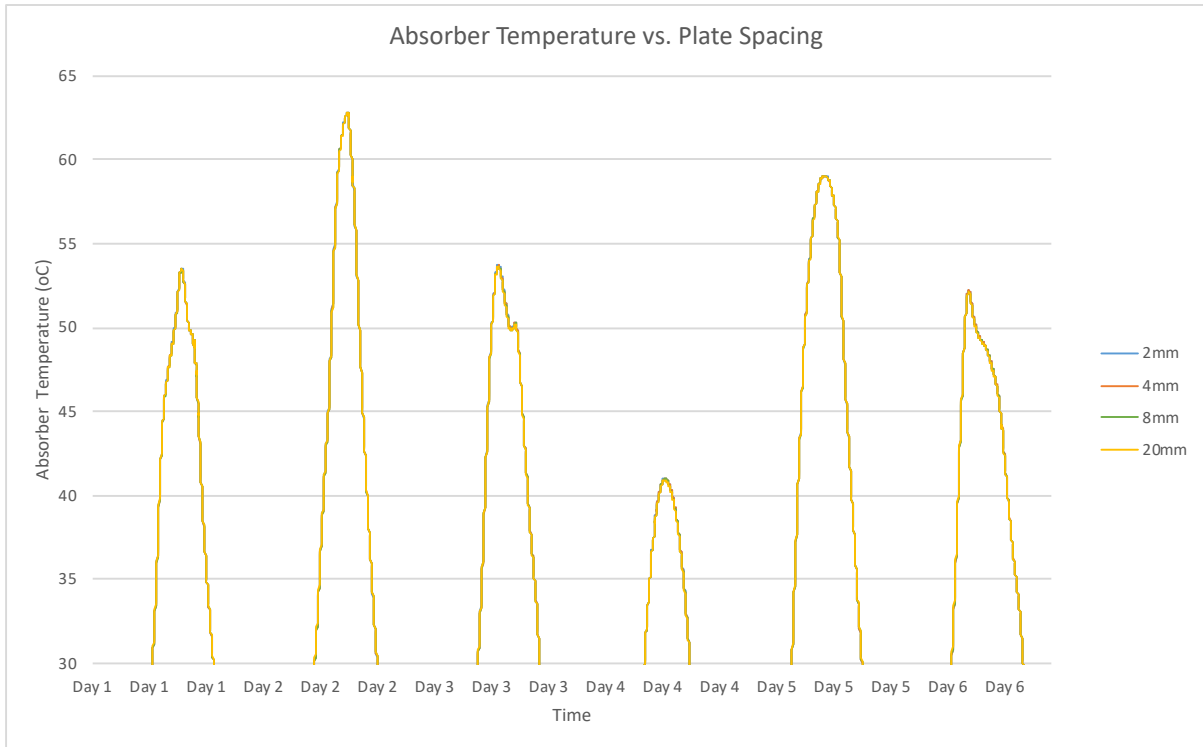


Figure 25 - Effects of plate spacing with absorber temperature

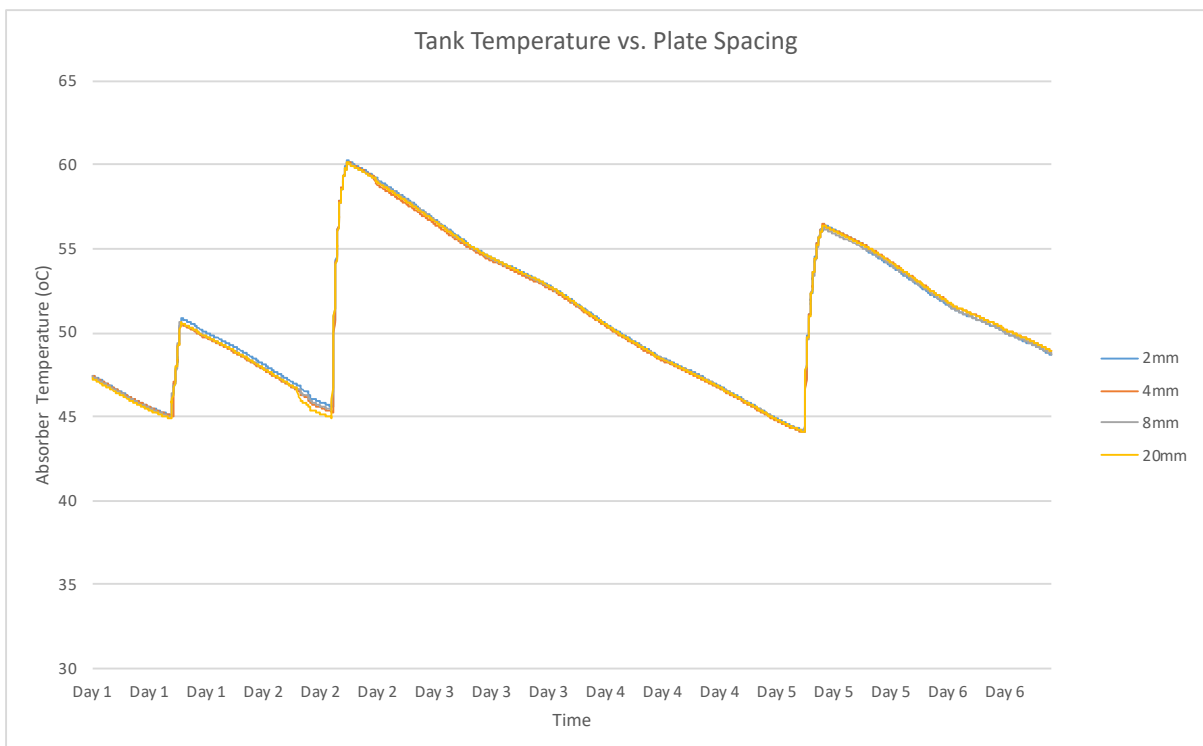


Figure 26 - Effects of water temperature gain with plate spacing

Results show no real difference to temperature gain with absorber plate spacing from 2mm – 20mm. Absorber temperatures vary almost identically while water temperature gains vary to a maximum of 1°C. It can be concluded that absorber plate spacing is not a strict variable.

This means that simplicity of design is increased. Complex measurements are not needed in order to correctly space the collector plates. Ensuring the plates are not in contact but within 20mm of each other will produce specific water temperatures for low temperature application.

#### 6.5.4 Insulation

The casing and surrounding material of the FAC is constructed from two aluminium layers, with glass fibre layer sandwiched in between. Details of the construction, termed “insul\_frame”, are displayed in Table 11

In order to assess the importance of insulation to the design and the different possibilities with insulation, 3 alternatives to the base insulation design were trialled:

- Increased thickness of insulation layer
- Glass wool (Sengar, 2004)
- Air gap – vacuum insulation (El-Sherbiny et al., 1978)

Table 11 - Insulation layers for testing

Construction	Layer	Description	Thickness	Conductivity	Density	Specific Heat	Emmissivity	Absorptivity	R
			(mm)	(W/mK)	(kg/m <sup>3</sup> )	(J/kgK)			(m <sup>2</sup> K/W)
<b>insul_frame (80mm)</b>	External	Grey Coated Aliminium	4	210	2700	880	0.82	0.72	0
	2	Glass Fibre Quilt	<b>80</b>	0.04	12	840	0.9	0.65	2
	Internal	Grey Coated Aliminium	4	210	2700	880	0.82	0.72	0
<b>insul_frame (120mm)</b>	External	Grey Coated Aliminium	4	210	2700	880	0.82	0.72	0
	2	Glass Fibre Quilt	<b>120</b>	0.04	12	840	0.9	0.65	3
	Internal	Grey Coated Aliminium	4	210	2700	880	0.82	0.72	0
<b>Glass Wool</b>	External	Grey Coated Aliminium	4	210	2700	880	0.82	0.72	0
	2	Glass wool	<b>80</b>	0.04	30	840	0.9	0.3	3
	Internal	Grey Coated Aliminium	4	210	2700	880	0.82	0.72	0
<b>Air Gap (vacuum)</b>	External	Grey Coated Aliminium	4	210	2700	880	0.82	0.72	0
	2	Air gap	<b>80</b>	0	>0	0	0.99	0.99	0.17
	Internal	Grey Coated Aliminium	4	210	2700	880	0.82	0.72	0

Figure 27 below shows the results of the variation of insulation used. It can be concluded early on that the insulation of the collector does not play a huge roll in increasing water temperatures. Increasing the glass fibre layer thickness increases temperature gain, although only very slightly. The results also show that the same thickness of glass wool performs better than glass fibre.

The most interesting result is the complete removal of the insulation layer and leaving a sealed 80mm layer of air. Temperature losses are only 3-4°C less and are still well within the low temperature application bounds (40-60°C). The air layer means design does not need complex materials for the insulation of the absorber for low temperature application. This result is also backed up in research by (Beikircher et al., 2015).

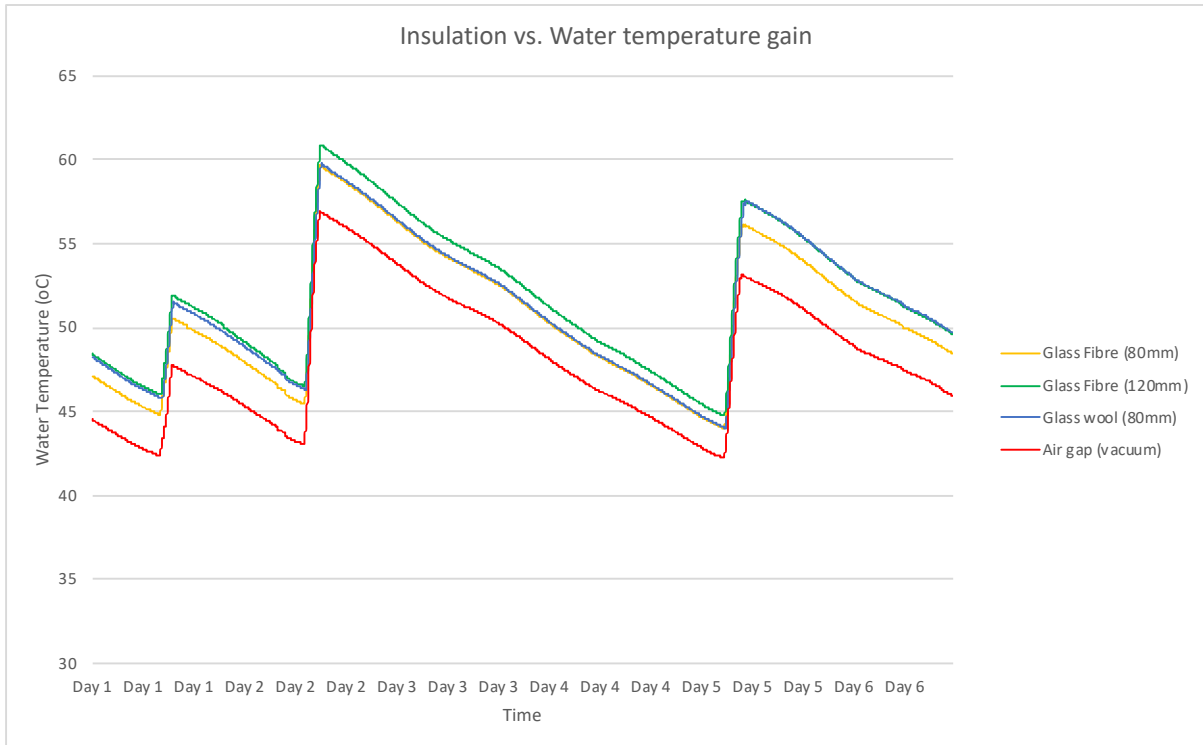


Figure 27 - Effects of Insulation on water temperature achieved

## 6.6 Final Model

As the base case model performed exceptionally well in low temperature production of water, only minor improvements were needed to improve the design. Several variables were deemed acceptable in the base after testing. These were:

- Collector absorber area of 3.318m<sup>2</sup>
- Total length of Collector 3m.
- Single layer of float glass glazing

The improvements to the base case model were:

- Increased tank size to 369L for domestic hot water use.
- Reduction in water flowrate from 0.5kg/s to 0.1kg/s.
- A realisation of increased flexibility in absorber plate spacing from 2mm – 20mm
- Removal of glass fibre insulation layer to leave vacuum insulation layer

### 6.7 System Efficiency Model

The thermal efficiency of the FAC shows the amount of solar resource the collector can utilise and turn into useful energy. In order to calculate the thermal efficiency of the model, it is important to standardize the hot water load pattern.

A model for thermal efficiency, developed by (Huang & Du, 1991) is used here (discussed in section 2.5.1).. The model describes system efficiency for daily increases in water temperature. The simulation has been run over 6 day in the Summer period. Of these 6 days, there are three distinct periods of water temperature gain. Therefore, the thermal efficiency can be used over these three days (Day 1, Day 2 and Day 5). After these efficiencies have been calculated individually, the average will be calculated to give an overall system efficiency.

Only the calculation method to Day 1 is shown here. Figures 28 – 30 show the three water heating periods over the 6 day simulation period.

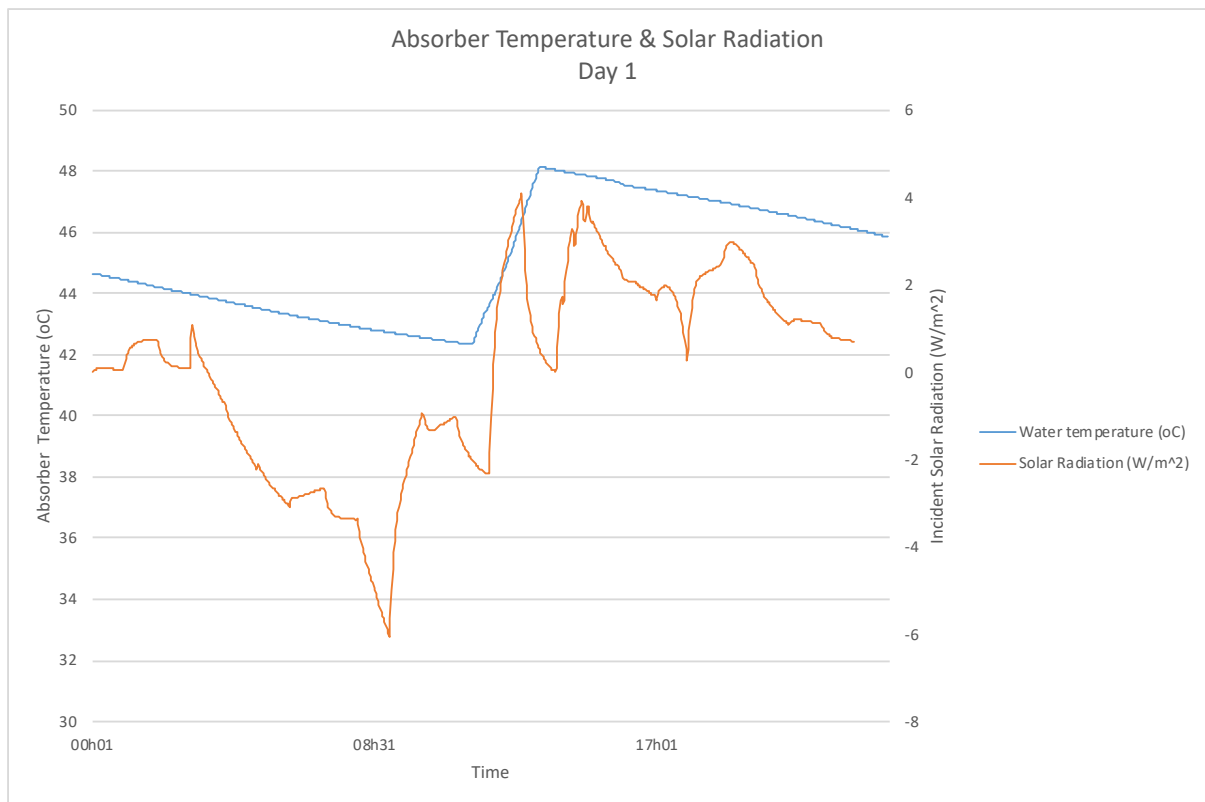


Figure 28 - Absorber temperature & Incident Solar radiation (Simulation period - day 1)

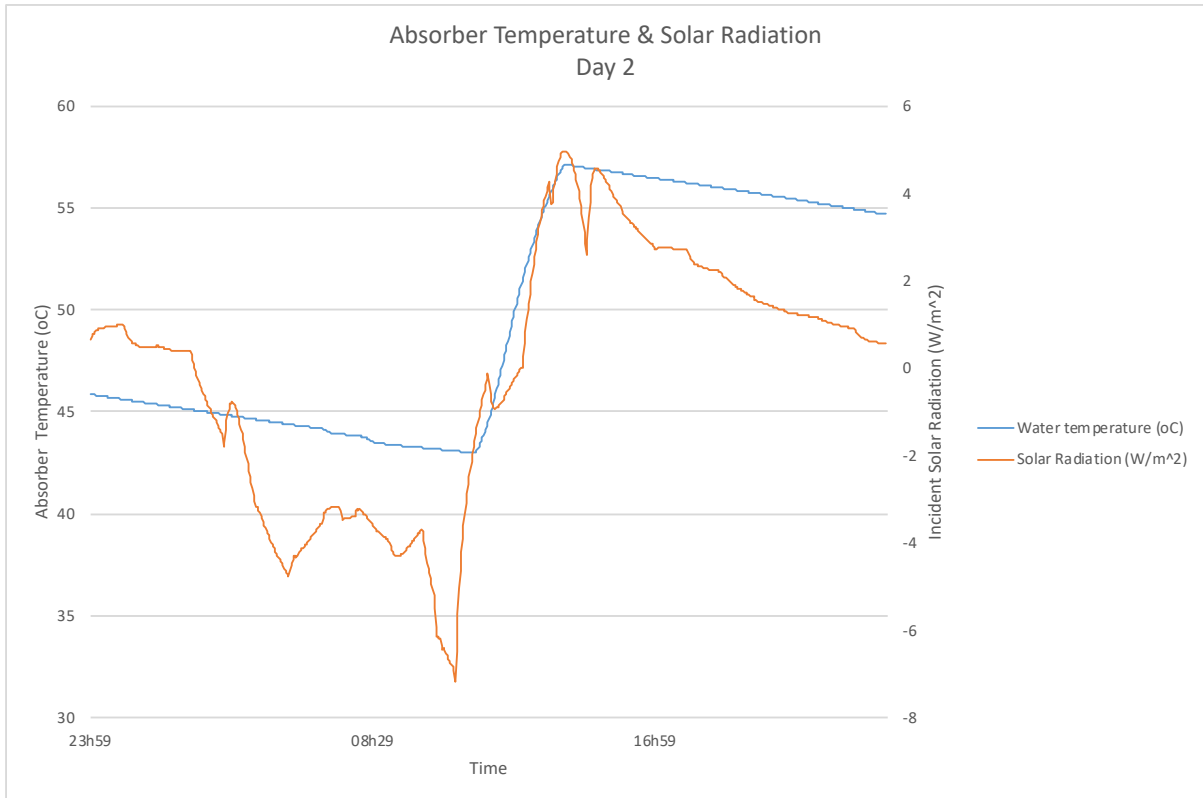


Figure 29 - Absorber temperature & Incident Solar radiation (Simulation period - day 2)

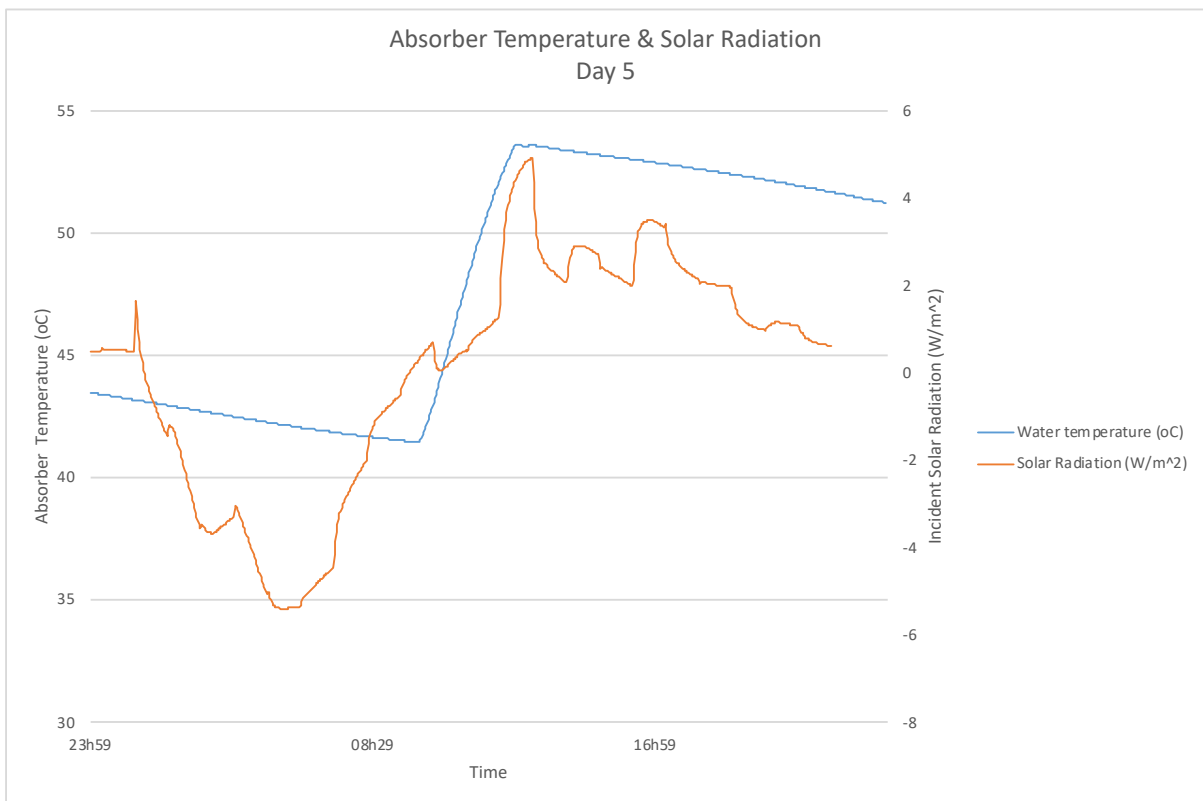


Figure 30 - Absorber temperature & Incident Solar radiation (Simulation period - day 5)

### 6.7.1 Calculation

Values needed for calculation (referring to Figure 28):

$$M = \text{Total mass of water in system} = 369 \text{ kg}$$

$$C_p = \text{heat capacity of water} = 0.004184 \frac{\text{MJ}}{\text{kg}^\circ\text{C}}$$

$$T_f = \text{final tank temperature} = 48^\circ\text{C}$$

$$T_i = \text{initial tank temperature} = 42.5^\circ\text{C}$$

$$A_c = \text{total collector area} = 3.318 \text{ m}^2$$

$$t_f = \text{final time of energy collecting phase (hour)} = 11:30 \text{ am} = 11.5 \text{ hrs}$$

$$t_i = \text{initial time of energy collecting phase (hour)} = 1:45 \text{ pm} = 13.75 \text{ hrs}$$

$$I_T = \text{incident solar radiation on collector surface} = 3.93 \frac{\text{W}}{\text{m}^2}$$

Calculation of daily total solar absorption:

$$Q_{net} = MC_p(T_f - T_i)$$

$$Q_{net} = 369 * 0.004184 (48 - 42.5)$$

$$Q_{net} = 8.49 \frac{\text{MJ}}{\text{day}}$$

Calculation of daily total net energy absorption per unit area of collector surface:

$$q_{net} = \frac{Q_{net}}{A_c}$$

$$q_{net} = \frac{8.5}{3.318}$$

$$q_{net} = 2.56 \frac{\text{MJ}}{\text{m}^2 \text{ day}}$$

Calculation of daily total solar irradiation incident on collector surface (11:30am – 1:45pm):

$$H_t = \int_{t_i}^{t_f} I_t dt$$

$$H_t = \int_{11.5}^{13.75} 3.39 dt$$

$$H_t = [3.39t]_{11.5}^{13.75}$$

$$H_t = (3.39 * 13.75) - (3.39 * 11.5)$$

$$H_t = 7.63$$

Calculation of system efficiency for day 1 of the simulation period:

$$\eta_s = \frac{q_{net}}{H_t}$$

$$\eta_s = \frac{2.56}{7.6275}$$

$$\eta_s = 0.336$$

$$\eta_{s,1} = 33.6\%$$

Table 12 and 13 displays the values needed for input to the calculation along with the system efficiency and global system efficiency.

Table 12 - Variables for efficiency calculation

Heating Period	M	Cp	Ti	Tf	Ac	ti	tf	It
	(kg)	(MJ/kgC)	(oC)	(oC)	(m2)	(hr)	(hr)	(W/m2)
Day 1	369	0.004184	42.5	48	3.318	11:30	13:45	3.39
Day 2	369	0.004184	43	57	3.318	11:30	14:45	4.95
Day 6	369	0.004184	41.5	53.5	3.318	09:45	13:00	4.9

Table 13 - Calculated system energy & efficiency

Heating Period	Qnet	qnet	Ht	System Efficiency
	MJ/day	MJ/m2day		(%)
Day 1	8.49	2.56	7.63	33.6
Day 2	21.61	6.51	14.85	43.8
Day 5	18.53	5.58	15.93	35.0

Therefore, the total average system efficiency of the FAC is calculated as:

$$\eta_T = \frac{\eta_{s,1} + \eta_{s,2} + \eta_{s,5}}{3}$$

$$\eta_T = \frac{0.336 + 0.438 + 0.350}{3}$$

$$\eta_T = 0.375$$

$$\eta_T = 37.5\%$$

The overall FAC in the summer simulation period makes use of on average 37.5% of the total energy provided by the sun. It is noticed that for the greatest water temperature increase in day 2 (14°C), the largest daily system efficiency is produced at 43.8%. Referring to Appendix B: Figure 36, maximum efficiency occurs when the direct normal solar radiation is at a maximum for day 5 (108hrs). The FAC performs best when large temperature changes in the water occur, therefore the systems thermal efficiency increases when there is large amounts of solar radiation.

## 7. Final Discussion

A solar water heating system for low temperature application has been developed. The base model designed performed very well in the Scottish summer environment, producing water within the low temperature application bounds ( $40^{\circ}\text{C} - 60^{\circ}\text{C}$ ). However, the system could not produce water temperatures in the Spring, Autumn and Winter months that was satisfactory for low temperature bounds.

Temperature distribution through the typical parallel tube absorber configuration has been noted as unsatisfactory although this problem is abated with the design of the FAC. Figure 17 shows that the temperature distributed over the absorber surface is uniform, aiding the transfer of heat to the water. As a result of this, it is shown that the FAC design performs well with a broad range of water flowrates, from  $0.01\text{kg/s}$  up to  $1\text{kg/s}$  (Figure 21 – 23). This is due to the fact the water is always in complete contact with the absorber surface. Again, this shows that water flowrate does not need to be a fixed value, aiding in the simplicity of performance. A water tank of 369L was chosen in order to meet the demands of a typical dwelling.

Design simplicity was a secondary aim of this project. The design of an FAC consists of simply two absorber sheets which do not need to be welded in any place. After simulation, it was also found that absorber spacing was not a strict variable therefore complex measurements were not essential in design procedures. Figure 25 and 26 show that spacings from  $2\text{mm} - 20\text{mm}$  obtain similar results, well within the bounds of low temperature application.

The effects of adding layers of glazing in the Summer simulation period showed that water temperature gain was dramatically increased. Adding one layer of glazing produced a max temperature of just under  $100^{\circ}\text{C}$ , while a third layer produced steam. As a temperature bound of  $40^{\circ}\text{C} - 60^{\circ}\text{C}$  was set, extra glazing was not required. However, in the interest of latent heat systems, the FAC would perform well. This effect was reversed in the Winter months, as can be seen in Figure 24, as the third layer of glazing reduced water temperature gain. This is caused by the extra layer blocking out useful shortwave radiation to the absorber. In winter,

the collector relies on shortwave radiation for temperature gain as the ambient temperature is much lower.

The glazing material was also chosen to be float glass. Float glass is used in a broader range of applications compared to commonly used low iron glass. This means that it is far more likely to be available in less developed areas.

The tilt angle of the FAC was kept horizontal. After reviewing the literature, it is found the values of optimum tilt are disparate. However, in Summer months, collector tilt is relatively close to horizontal. The optimum tilt completely depends on the location the collector is set up in. Achieving appropriate water temperatures with a  $0^\circ$  tilt means that azimuth angle also becomes irrelevant. This means the collector can be deployed with little knowledge of angles and orientation, aiding to the simplicity.

Within the construction of the collector, it was also found that removing the layer of glass fibre had a very small effect on water temperature gain (Figure 27). Using an air gap instead of insulation material only reduced the temperature of water obtained by a few degrees. The lowest temperature achieved was still above the lower bound of  $40^\circ\text{C}$ . Removing the need for specific insulation materials again meets the secondary aim of simple design.

The FAC design was simulated in a Scottish climate to test the performance in a low solar radiation environment. It was assumed that if the collector could perform well in a Scottish environment, it would be absolutely applicable in a solar rich climate. If the FAC was simulated in a solar rich environment, it could not be concluded that it could work in a less solar rich environment.

Even with the simplicity of design, thermal efficiency of the FAC still reached an average of 37.5%, in low solar conditions (Glasgow). As the design was aimed at meeting low temperature requirements and ideally being simple, high efficiency was not expected or necessary. However, it was found that when temperature gain of water was large, system efficiency increased. For a temperature gain of  $5.5^\circ\text{C}$ , a system efficiency was calculated as

33.6%. When water temperature gain rose to 14°C, an efficiency 43.8% was obtained. In light of this, the FAC could be very efficient for high water temperature gain. However, in order to get a better understanding of overall system efficiency, a larger simulation period would need to be completed.

The main findings of the FAC compared to the FPC design were as follows:

- The FAC can handle high flowrates compared to FPC. This is due to the fact the absorber is in constant contact with the fluid instead of just being in pipes.
- Simple design
  - No insulation material required for low temperature application
  - Can be laid flat, no complex procedure to ensure collector tilt
  - Flexibility of spacing of absorber plates up to 20mm.

## 8. Conclusion

To sum up the major components of the final model developed:

- Collector absorber area of 3.318m<sup>2</sup>
- Total length of Collector 3m.
- Single layer of float glass glazing
- Tank size to 369L for domestic hot water use.
- Water flowrate: 0.1kg/s.
- Absorber spacing between 2mm – 20mm
- Vacuum insulation layer

The main design objectives have been met by the designed FAC. Water is produced between temperatures of 40 – 60°C which was the initial aim of the system. Then through testing in ESP-r simulation environment, the base design was proven to work well with only minor adjustments needed. A system overall efficiency of 37.5% was found which is lower than standard solar thermal collectors. However, system design was proven to be simple and therefore has the possibility of being widely deployable.

## 9. Future Work

The areas in which the work completed in this thesis could be furthered are as follows:

- To obtain a more accurate understanding of system efficiency, the FAC should be simulated and tested under standard EN-12975. The EN-12975 provides the European standard for performance testing of solar collectors. This would give a realistic efficiency value that could be truly compared to other solar collector designs.
- To compare the FAC with the parallel tube configuration FPC, a parallel tube FPC collector should be modelled in ESP-r. This could be done by changing the absorber geometry to pipes by cutting each thermal zone into thin strips and applying a pipe flow component link.
- To increase the accuracy of the simulation of the FAC in ESP-r, more zones could be created in order to have a smoother increase in temperature as the water flows from zone to zone.
- After adding extra layers of glazing, it was found the FAC would likely perform well even in the Spring season. The system could possibly be designed to produce water for low temperature application through the Summer and through the Spring.
- The price of the FAC system developed was not in the scope of this research. If a system price were generated, it could be used to assess the economic feasibility of the design to be deployed in LEDC's.
- Asses the possibility of the FAC design working under a thermosiphon principle. The addition of the pump means the system needs external energy in order to operate. Working under the thermosiphon principle would mean the FAC could operate anywhere, without external power requirement.

## 10. References

- Al-Beaini, S., Benhabib, M., Engelage, S., & Langton, A. (2007). *Domestic Solar Water Heater for Developing Countries*. Retrieved from <http://www.solaripedia.com/files/587.pdf>
- Al-Rawahi, N. Z., Zurigat, Y. H., & Al-Azri, N. A. (2011). Prediction of Hourly Solar Radiation on Horizontal and Inclined Surfaces for Muscat/Oman. *The Journal of Engineering Research [TJER]*, 8(2), 19. <https://doi.org/10.24200/tjer.vol8iss2pp19-31>

- Amrutkar, S. K., Ghodke, S., & Patil, K. N. (2012). Solar Flat Plate Collector Analysis, 2, 207–213. Retrieved from [www.iosrjen.org](http://www.iosrjen.org)
- Ayoub, J., & Alward, R. (1996). *Water requirements and remote arid areas: the need for small-scale desalination*. *DESALINATION ELSEVIER Desalination* (Vol. 107). Retrieved from [https://ac.els-cdn.com/S0011916496001580/1-s2.0-S0011916496001580-main.pdf?\\_tid=f0340984-3d0e-4aa2-acac-f9bb24def740&acdnat=1532531992\\_62e0a0463ccccbd7f6c1291e144bc20](https://ac.els-cdn.com/S0011916496001580/1-s2.0-S0011916496001580-main.pdf?_tid=f0340984-3d0e-4aa2-acac-f9bb24def740&acdnat=1532531992_62e0a0463ccccbd7f6c1291e144bc20)
- Bakari, R., Minja, R. J. A., & Njau, K. N. (2014). Effect of Glass Thickness on Performance of Flat Plate Solar Collectors for Fruits Drying. *Journal of Energy*, 2014, 1–8. <https://doi.org/10.1155/2014/247287>
- Beikircher, T., Berger, V., Osgyan, P., Reuß, M., & Streib, G. (2014). Low-e confined air chambers in solar flat-plate collectors as an economic new type of rear side insulation avoiding moisture problems. *Solar Energy*, 105, 280–289. <https://doi.org/10.1016/J.SOLENER.2014.03.033>
- Beikircher, T., Möckl, M., Osgyan, P., & Streib, G. (2015). Advanced solar flat plate collectors with full area absorber, front side film and rear side vacuum super insulation. *Solar Energy Materials and Solar Cells*, 141, 398–406. <https://doi.org/10.1016/J.SOLMAT.2015.06.019>
- Blaga, A. (1978). Use of plastics in solar energy applications. *Solar Energy*, 21(4), 331–338. [https://doi.org/10.1016/0038-092X\(78\)90010-5](https://doi.org/10.1016/0038-092X(78)90010-5)
- California Solar Center. (2015). Solar Thermal History. Retrieved July 23, 2018, from <http://californiasolarcenter.org/history-solarthermal/>
- Chang, T. P. (2008). Study on the Optimal Tilt Angle of Solar Collector According to Different Radiation Types. *International Journal of Applied Science and Engineering*, 6, 151. Retrieved from <https://www.cyut.edu.tw/~ijase/2008/2008/014011-6.pdf>
- Chen, X., Liu, L., Yu, P. Y., & Mao, S. S. (2011). Increasing solar absorption for photocatalysis with black hydrogenated titanium dioxide nanocrystals. *Science (New York, N.Y.)*, 331(6018), 746–50. <https://doi.org/10.1126/science.1200448>
- Chen, Z., Furbo, S., Perers, B., Fan, J., & Andersen, E. (2012). Efficiencies of Flat Plate Solar Collectors at Different Flow Rates. *Energy Procedia*, 30, 65–72. <https://doi.org/10.1016/j.egypro.2012.11.009>
- Chong, K. K., Chay, K. G., & Chin, K. H. (2012). Study of a solar water heater using stationary V-trough collector. *Renewable Energy*, 39, 207–215. <https://doi.org/10.1016/j.renene.2011.08.002>
- DEFRA. (2013). *At Home with Water - Great Britain*. Retrieved from <http://www.energysavingtrust.org.uk/sites/default/files/reports/AtHomewithWater%287%29.pdf>
- Drosou, V. N., Tsekouras, P. D., Oikonomou, T. I., Kosmopoulos, P. I., & Karytsas, C. S. (2013). The HIGH-COMBI project: High solar fraction heating and cooling systems with combination of innovative components and methods. *Renewable and Sustainable Energy Reviews*, 29, 463–472. <https://doi.org/10.1016/j.rser.2013.08.019>
- Eke, A. Ben. (2011). Prediction of optimum angle of inclination for flat plate solar collector in Zaria, Nigeria. *Agricultural Engineering International: CIGR Journal*, 13(4).
- El-Sherbiny, S. M., Hollands, K. G. T., & Raithby, G. D. (1978). Free Convection across Inclined Air Layers with One Surface V-Corrugated. *Journal of Heat Transfer*, 100(3), 410. <https://doi.org/10.1115/1.3450823>
- Elminir, H. K., Ghitas, A. E., El-Hussainy, F., Hamid, R., Beheary, M. M., & Abdel-Moneim, K.

- M. (2006). Optimum solar flat-plate collector slope: Case study for Helwan, Egypt. *Energy Conversion and Management*, 47(5), 624–637. <https://doi.org/10.1016/J.ENCONMAN.2005.05.015>
- Energy Saving Trust. (2018). Heating and Hot Water | Energy Saving Trust. Retrieved August 24, 2018, from <http://www.energysavingtrust.org.uk/home-energy-efficiency/heating-and-hot-water>
- ESRU. (n.d.). ESP-r. Retrieved July 9, 2018, from <http://www.esru.strath.ac.uk/Programs/ESP-r.htm>
- Firebird. (2011). *Guide to Solar Thermal Systems*. Retrieved from <https://firebird.uk.com/wp-content/uploads/2016/06/Guide-to-Solar-Thermal-Systems-Brochure-2012.pdf>
- Gammon, R. B. (1978). THE MEASUREMENT OF OPTICAL PROPERTIES OF SELECTIVE SURFACES USING A SOLAR CALORIMETER. *Solar Energy*, 21, 193–199. Retrieved from [https://ac.els-cdn.com/0038092X7890021X/1-s2.0-0038092X7890021X-main.pdf?\\_tid=79c05524-5041-49f5-84ba-e7ea488c5fb5&acdnat=1532006815\\_32b7b30afd43bb6a69a429fbbb4d9ed4](https://ac.els-cdn.com/0038092X7890021X/1-s2.0-0038092X7890021X-main.pdf?_tid=79c05524-5041-49f5-84ba-e7ea488c5fb5&acdnat=1532006815_32b7b30afd43bb6a69a429fbbb4d9ed4)
- Gunjo, D. G., Mahanta, P., & Robi, P. S. (2017). CFD and experimental investigation of flat plate solar water heating system under steady state condition. *Renewable Energy*, 106, 24–36. <https://doi.org/10.1016/J.RENENE.2016.12.041>
- Hirasawa, S., Tsubota, R., Kawanami, T., & Shirai, K. (2013). Reduction of heat loss from solar thermal collector by diminishing natural convection with high-porosity porous medium. *Solar Energy*, 97, 305–313. <https://doi.org/10.1016/j.solener.2013.08.035>
- Hobbi, A., & Siddiqui, K. (2009). Experimental study on the effect of heat transfer enhancement devices in flat-plate solar collectors. *International Journal of Heat and Mass Transfer*, 52(19–20), 4650–4658. <https://doi.org/10.1016/J.IJHEATMASSTRANSFER.2009.03.018>
- Huang, B. J., & Du, S. C. (1991). A Performance Test Method of Solar Thermosyphon Systems. *Journal of Solar Energy Engineering*, 113(3), 172. <https://doi.org/10.1115/1.2930489>
- Jamar, A., Majid, Z. A. A., Azmi, W. H., Norhafana, M., & Razak, A. A. (2016). A review of water heating system for solar energy applications ☆. <https://doi.org/10.1016/j.icheatmasstransfer.2016.05.028>
- Jeena, J., & Nidhi, M. J. (2015). A Review on Performance of Solar Thermal Flat Plate Collector Using Different Heat Transfer Fluids, 2(7), 204–210. Retrieved from <http://troindia.in/journal/ijcesr/vol2iss7/204-210.pdf>
- Joseph, J., Saravanan, R., & Renganarayanan, S. (2005). *Studies on a single-stage solar desalination system for domestic applications*. Retrieved from [www.elsevier.com/locate/desal](http://www.elsevier.com/locate/desal)
- Jouybari, H. J., Saedodin, S., Zamzamin, A., Nimvari, M. E., & Wongwises, S. (2017). Effects of porous material and nanoparticles on the thermal performance of a flat plate solar collector: An experimental study. *Renewable Energy*, 114, 1407–1418. <https://doi.org/10.1016/j.renene.2017.07.008>
- Kalidasan, B., & Srinivas, T. (2014). Study on Effect of Number of Transparent Covers and Refractive Index on Performance of Solar Water Heater. *Journal of Renewable Energy*, 2014, 1–11. <https://doi.org/10.1155/2014/757618>
- Kalogirou, S. (2005). Seawater desalination using renewable energy sources. *Progress in Energy and Combustion Science*, 31(3), 242–281.

- <https://doi.org/10.1016/j.pecs.2005.03.001>
- Kalogirou, S. (2014). *Solar Energy Engineering: Processes and Systems*.
- Kalogirou, S. A. (2004). Solar thermal collectors and applications. *Progress in Energy and Combustion Science*, 30(3), 231–295. <https://doi.org/10.1016/j.pecs.2004.02.001>
- Kalogirou, S. A. (2009). *Solar Energy Engineering*. Elsevier. <https://doi.org/10.1016/B978-0-12-374501-9.X0001-5>
- Karagiorgas, M., Botzios, A., & Tsoutsos, T. (2001). Industrial solar thermal applications in Greece Economic evaluation, quality requirements and case studies. *Renewable and Sustainable Energy Reviews*, 5, 157–173. Retrieved from [www.elsevier.com/locate/rser](http://www.elsevier.com/locate/rser)
- Karim, M. R., Nakoa, K. M. ., Mahmood, S. L., & Akhanda, D. M. A. R. (2012). *International journal of renewable energy research. International Journal of Renewable Energy Research (IJRER)* (Vol. 1). Gazi Univ., Fac. of Technology, Dep. of Electrical et Electronics Eng. Retrieved from <http://ijrer.com/index.php/ijrer/article/view/69>
- Kemp, C. M. (1891, April 28). Apparatus for utilizing the sun s rays for heating water. Retrieved from <https://patents.google.com/patent/US451384A/en>
- Keshavarz, S. A., Talebizadeh, P., Adalati, S., Mehrabian, M. A., & Abdolzadeh, M. (2012). *International journal of renewable energy research. International Journal of Renewable Energy Research (IJRER)* (Vol. 2). Gazi Univ., Fac. of Technology, Dep. of Electrical et Electronics Eng. Retrieved from <http://ijrer.com/index.php/ijrer/article/view/367>
- Khanna+, M. L. (1968). The Development of a Solar Water Heater and its Field Trials under Indian Tropical Conditions\*, 255–261. Retrieved from [https://ac.els-cdn.com/0038092X6890011X/1-s2.0-0038092X6890011X-main.pdf?\\_tid=53f41a28-a804-44fd-9c37-d15074c83d85&acdnat=1531911320\\_9ba0305c6e2dbb9f7f12e2d856f70839](https://ac.els-cdn.com/0038092X6890011X/1-s2.0-0038092X6890011X-main.pdf?_tid=53f41a28-a804-44fd-9c37-d15074c83d85&acdnat=1531911320_9ba0305c6e2dbb9f7f12e2d856f70839)
- Köhl, M. (2012). *Polymeric Materials for Solar Thermal Applications*. Retrieved from <http://dnb.d-nb.de>.
- Kumar Verma, S., Kumar Tiwari, A., & Singh Chauhan, D. (2017). Experimental evaluation of flat plate solar collector using nanofluids. <https://doi.org/10.1016/j.enconman.2016.12.037>
- Lampert, C. M. (1979). Coatings for enhanced photothermal energy collection II. Non-selective and energy control films. *Solar Energy Materials*, 2(1), 1–17. [https://doi.org/10.1016/0165-1633\(79\)90026-1](https://doi.org/10.1016/0165-1633(79)90026-1)
- Lenel, U. R. (1984). *A REVIEW OF MATERIALS FOR SOLAR HEATING SYSTEMS FOR DOMESTIC HOT WATER* (Vol. 32). Retrieved from [https://ac.els-cdn.com/0038092X84900549/1-s2.0-0038092X84900549-main.pdf?\\_tid=825202a5-cc78-4e29-aa57-b19f47a58112&acdnat=1534025657\\_dc42190d37629266a01fe186c06e63c1](https://ac.els-cdn.com/0038092X84900549/1-s2.0-0038092X84900549-main.pdf?_tid=825202a5-cc78-4e29-aa57-b19f47a58112&acdnat=1534025657_dc42190d37629266a01fe186c06e63c1)
- Madhukeshwara, N., & Prakash, E. S. (2012). An investigation on the performance characteristics of solar flat plate collector with different selective surface coatings. *Journal Homepage: Www.IJEE.IEEFoundation.Org ISSN*, 3(1), 2076–2909. Retrieved from [www.IJEE.IEEFoundation.org](http://www.IJEE.IEEFoundation.org)
- Mauthner, F., Weiss, W., & Spörk-Dür, M. (2014). *Solar Heat Worldwide Markets and Contribution to the Energy Supply 2014. IEA Solar Heating & Cooling Programme*. Retrieved from <https://www.iea-shc.org/data/sites/1/publications/Solar-Heat-Worldwide-2016.pdf>
- Meibodi, S. S., Kianifar, A., Niazmand, H., Mahian, O., & Wongwises, S. (2015). Experimental investigation on the thermal efficiency and performance characteristics of a flat plate solar collector using SiO<sub>2</sub> /EG-water nanofluids ☆. *International Communications in*

- Heat and Mass Transfer*, 65, 71–75.  
<https://doi.org/10.1016/j.icheatmasstransfer.2015.02.011>
- Michaelides, I. M., & Eleftheriou, P. C. (2011). An experimental investigation of the performance boundaries of a solar water heating system. *Experimental Thermal and Fluid Science*, 35(6), 1002–1009.  
<https://doi.org/10.1016/J.EXPTHERMFLUSCI.2011.02.001>
- Monterrey, T. De. (2008). Vacuum Chamber Solar Collector Development using Triz. *Solar Energy*, 2–10. Retrieved from <https://www.aitriz.org/articles/TRIZFeatures/30383131-526F76697261.pdf>
- Mordor Intelligence. (2017). *Non Concentrating Solar Collectors Market | Industry Analysis | Outlook 2022*. Retrieved from <https://www.mordorintelligence.com/industry-reports/global-non-concentrating-type-solar-collector-market-industry>
- Moss, R. W., Shire, G. S. F., Henshall, P., Eames, P. C., Arya, F., & Hyde, T. (2017). Optimal passage size for solar collector microchannel and tube-on-plate absorbers. *Solar Energy*, 153, 718–731. <https://doi.org/10.1016/j.solener.2017.05.030>
- Nikogosian, A. (2017). *FLAT PLATE SOLAR WATER HEATERS WORKING ON THERMOSYPHON PRINCIPLE IN HOT CLIMATES: CFD INVESTIGATION OF NATURAL CONVECTION FLOW*. University of Strathclyde.
- Nnamchi, S. N. (2012). *Optimum Collector Tilt Angles For Low Latitudes*. *The Open Renewable Energy Journal* (Vol. 5). Retrieved from <https://pdfs.semanticscholar.org/2b55/41a77494fe08ec545cebf3c2ff46200e20c0.pdf>
- NRC. (n.d.). Natural Resources Canada | Natural Resources Canada. Retrieved July 20, 2018, from <https://www.nrcan.gc.ca/home>
- Pandey, K. M., & Chaurasiya, R. (2016). A review on analysis and development of solar flat plate collector. *Renewable and Sustainable Energy Reviews*, 67, 641–650.  
<https://doi.org/10.1016/j.rser.2016.09.078>
- Patel, K., Pragna Patel, M., & Patel, M. J. (2012). REVIEW OF SOLAR WATER HEATING SYSTEMS. *International Journal of Advanced Engineering Technology*. Retrieved from [http://www.technicaljournalonline.com/ijeat/VOL III/IJAET VOL III ISSUE IV OCTBER DECEMBER 2012/Article 34 Vol III issue IV 2012.pdf](http://www.technicaljournalonline.com/ijeat/VOL%20III/IJAET%20VOL%20III%20ISSUE%20IV%20OCTBER%20DECEMBER%202012/Article%2034%20Vol%20III%20issue%20IV%202012.pdf)
- Raisul Islam, M., Sumathy, K., & Ullah Khan, S. (2013). Solar water heating systems and their market trends. *Renewable and Sustainable Energy Reviews*, 17, 1–25.  
<https://doi.org/10.1016/J.RSER.2012.09.011>
- Rommel, M., Köhl, M., Graf, W., Wellens, C., Brucker, F., Lustig, K., & Bahr, P. (1997). Corrosion-free collectors with selectively coated plastic absorbers. *Desalination*, 109(2), 149–155. [https://doi.org/10.1016/S0011-9164\(97\)00060-X](https://doi.org/10.1016/S0011-9164(97)00060-X)
- Russell, L. D. (2015). All-polymer Flat Plate Heating Solar Panel With Integrated Controller. Retrieved from <https://patentimages.storage.googleapis.com/b6/76/e5/8b1fa3521c717d/US20150377515A1.pdf>
- Schwarzer, K., Vieira, M. E., Müller, C., Lehmann, H., & Coutinho, L. (2003). MODULAR SOLAR THERMAL DESALINATION SYSTEM WITH FLAT PLATE COLLECTOR. Retrieved from [http://www.rio12.com/rio3/proceedings/RIO3\\_281\\_K\\_Schwarzer.pdf](http://www.rio12.com/rio3/proceedings/RIO3_281_K_Schwarzer.pdf)
- Scott, J. E. (1976). THE SOLAR WATER HEATER INDUSTRY IN SOUTH FLORIDA: HISTORY AND PROJECTIONS. *Solar Energy*, 18, 387–393. Retrieved from [https://ac.els-cdn.com/0038092X76900037/1-s2.0-0038092X76900037-main.pdf?\\_tid=70c49e48-a523-4a32-b983-](https://ac.els-cdn.com/0038092X76900037/1-s2.0-0038092X76900037-main.pdf?_tid=70c49e48-a523-4a32-b983-)

- cf9f0273cdf0&acdnat=1532369462\_cad00b6138eabbc7ba4e14221070fe1c  
Sengar, S. H. (2004). Design and Development of Composite Solar Appliances for Domestic Use. Retrieved from <http://krishikosh.egranth.ac.in/handle/1/5810019930>
- Singh, P. L., Sarviya, R. M., & Bhagoria, J. L. (2010). Heat loss study of trapezoidal cavity absorbers for linear solar concentrating collector. *Energy Conversion and Management*, 51(2), 329–337. <https://doi.org/10.1016/J.ENCONMAN.2009.09.029>
- Sö zen, A., & Menlik, T. (2008). Determination of efficiency of flat-plate solar collectors using neural network approach. <https://doi.org/10.1016/j.eswa.2007.08.080>
- Solar Energy. (2015). Low temperature thermal solar energy. Retrieved August 24, 2018, from <https://solar-energy.technology/solar-thermal/low-temperature>
- Streicher, W. (2016). Solar thermal technologies for domestic hot water preparation and space heating. *Renewable Heating and Cooling*, 9–39. <https://doi.org/10.1016/B978-1-78242-213-6.00002-3>
- TheGreenAge. (2018). Evacuated Tube Solar Thermal Hot Water Systems. Retrieved July 19, 2018, from <https://www.thegreenage.co.uk/article/how-do-evacuated-tube-solar-thermal-hot-water-systems-work/>
- U.S Department of Energy. (2002). The History of Solar. Retrieved from <http://solarcooking.org/saussure.htm>
- Ulgen, K. (2006). Optimum Tilt Angle for Solar Collectors. *Energy Sources, Part A: Recovery, Utilization, and Environmental Effects*, 28(13), 1171–1180. <https://doi.org/10.1080/00908310600584524>
- Van Niekerk, W. M. K., du Toit, C. G., & Scheffler, T. B. (1996). Performance modelling of a parallel tube polymer absorber. *Solar Energy*, 58(1–3), 39–44. [https://doi.org/10.1016/0038-092X\(96\)00052-7](https://doi.org/10.1016/0038-092X(96)00052-7)
- Wessley, G. J. J., & Mathews, P. K. (2014). Experimental Analysis of a Flat Plate Solar Collector System for Small-Scale Desalination Applications. *Advanced Materials Research*, 984–985, 800–806. <https://doi.org/10.4028/www.scientific.net/AMR.984-985.800>
- Yeh, H.-M., & Chen, L.-C. (1985). A Study on Thermosyphon Solar Water Heater With Parallel Flat-Plate Collector. Retrieved from [https://ac.els-cdn.com/0360544286901064/1-s2.0-0360544286901064-main.pdf?\\_tid=0dde640a-d681-419c-a7a5-22f8c68aed8d&acdnat=1531928027\\_1d51db7c7074a6addd16431c607dd9d8](https://ac.els-cdn.com/0360544286901064/1-s2.0-0360544286901064-main.pdf?_tid=0dde640a-d681-419c-a7a5-22f8c68aed8d&acdnat=1531928027_1d51db7c7074a6addd16431c607dd9d8)

## 11. Appendices

### Appendix A: Base Model Supplementary Data

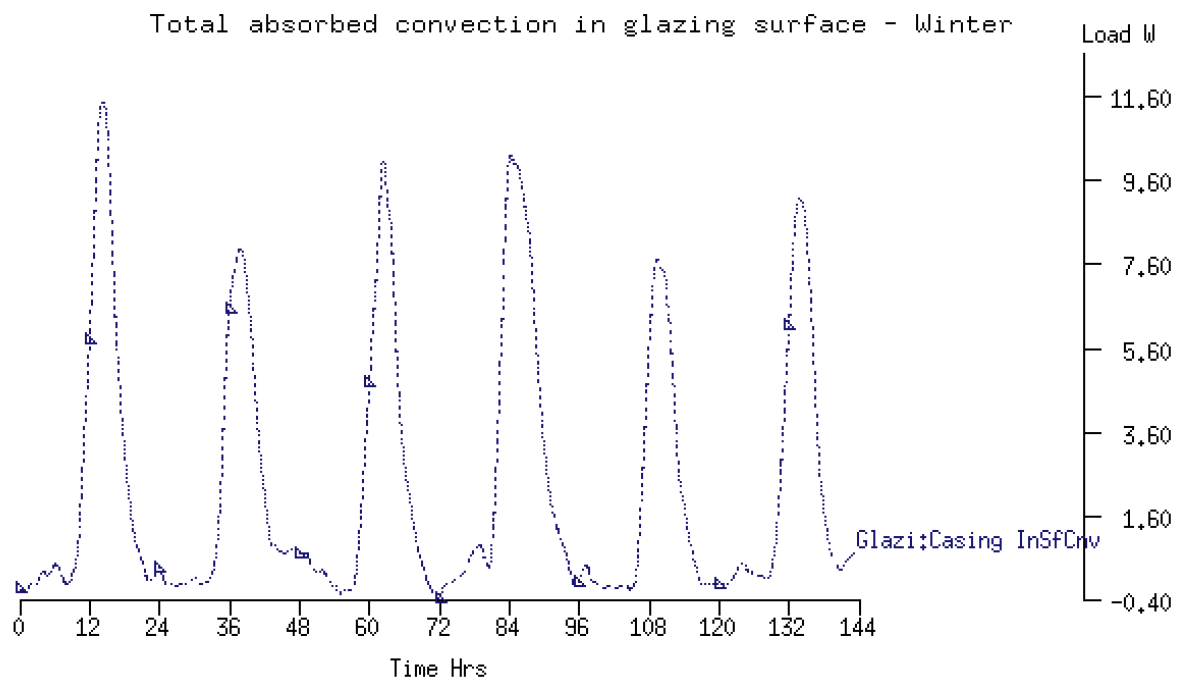


Figure 31 - Absorbed Convection in Glazing Surface (Winter0)

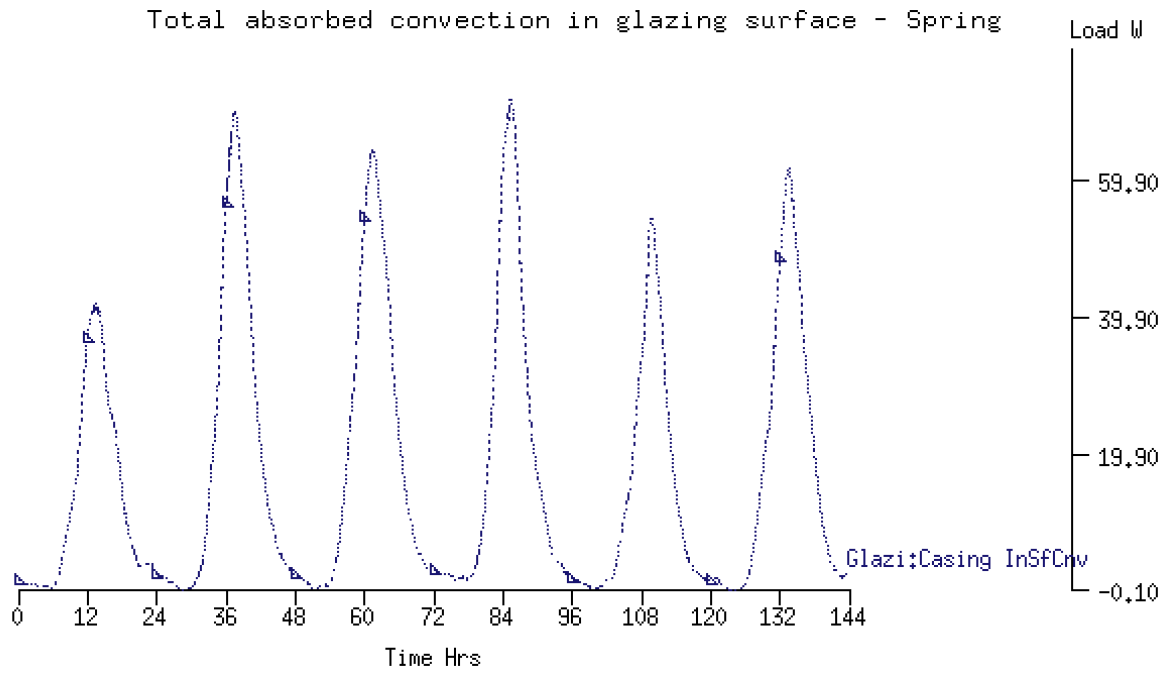


Figure 32 - Absorbed Convection in Glazing Surface (Spring)

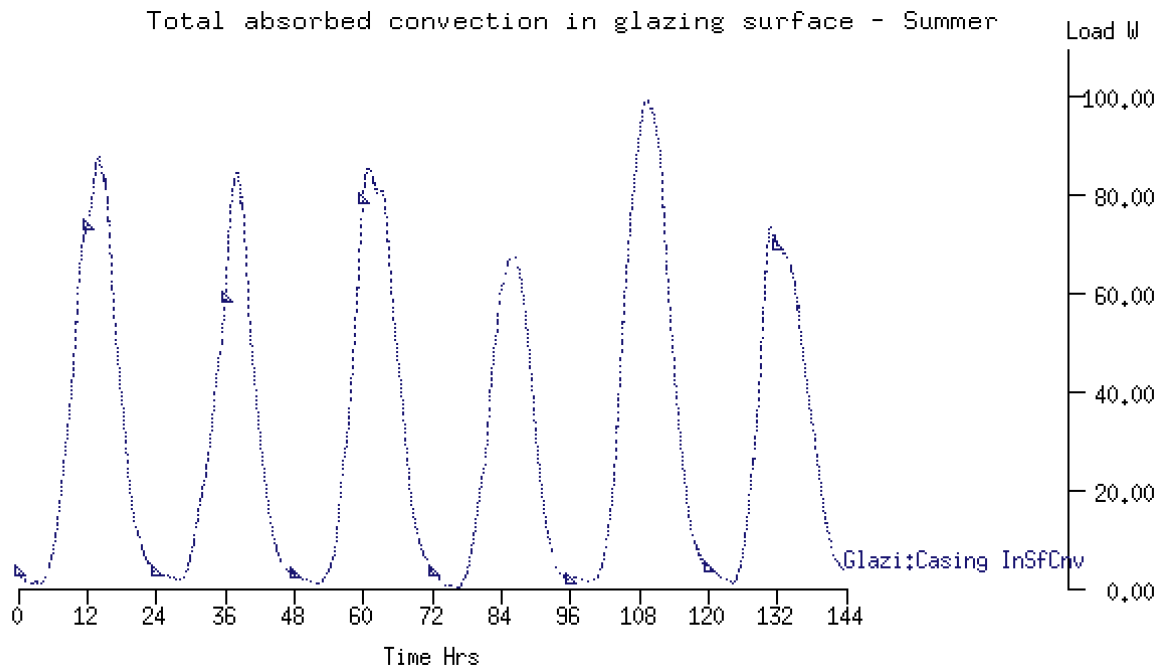


Figure 33 - Absorbed Convection in Glazing Surface (Summer)

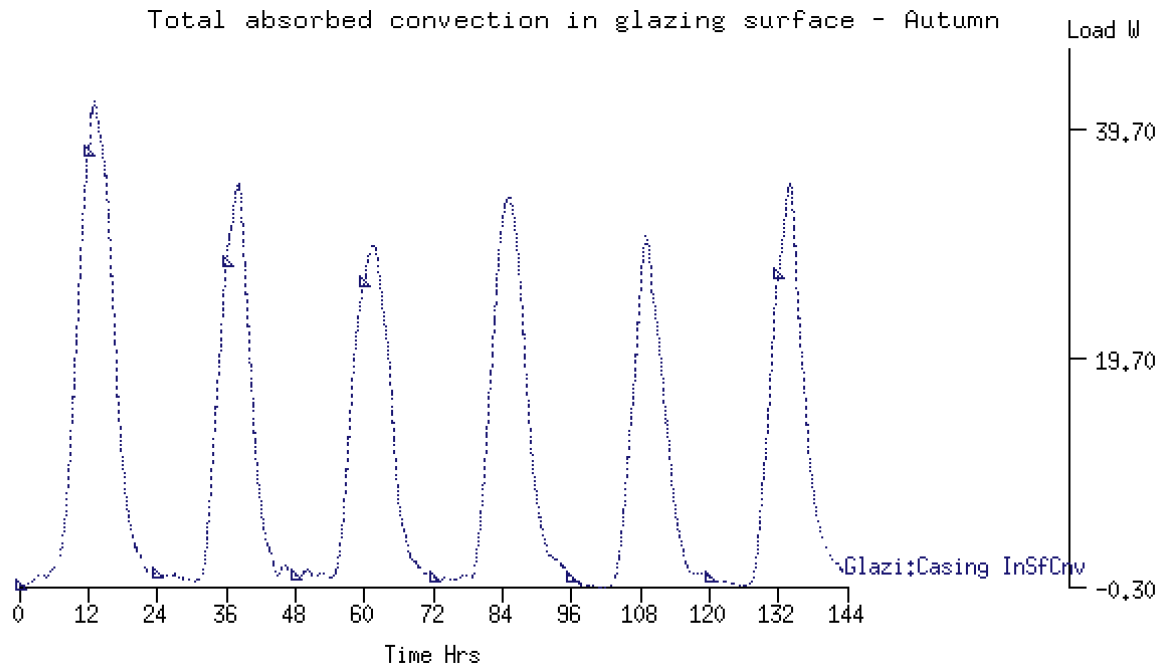


Figure 34 - Absorbed Convection in Glazing Surface (Autumn)

### Appendix B: Final Model Supplementary Data

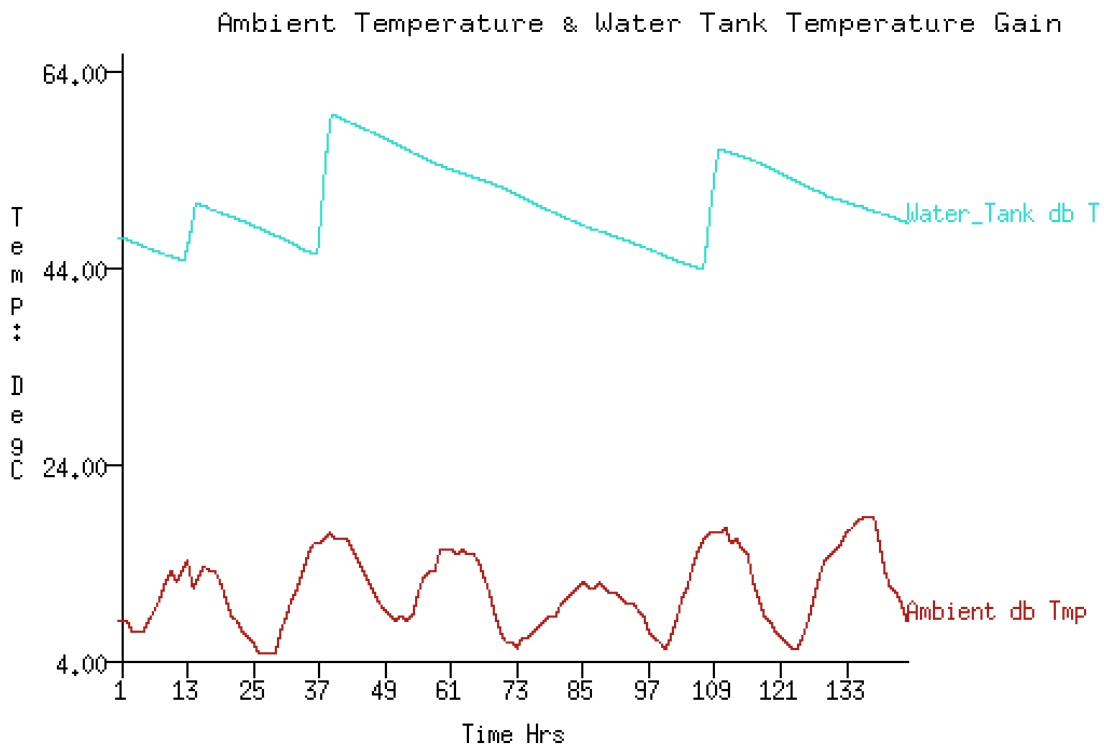


Figure 35 - Ambient Temperature and Water Tank Temperature Gain for Final Model

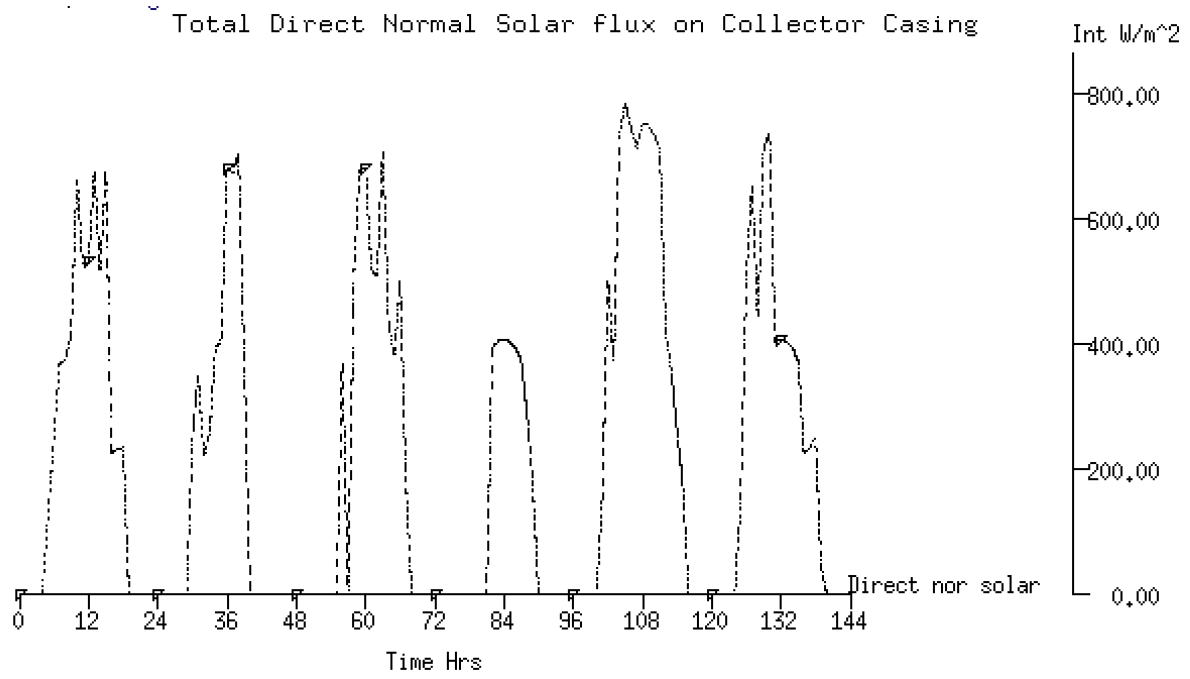


Figure 36 - Total Direct Normal Solar Flux on Collector Casing for Final Model